

POLITECNICO DI TORINO

Collegio di Ingegneria Meccanica, Aerospaziale,
dell'Autoveicolo e della Produzione

Corso di laurea magistrale in Automotive Engineering

Master Thesis

Calibration and assessment of the capability of the predictive combustion model SI-Turb



Academic Supervisors

Prof. Federico Millo

Dott. Luciano Rolando

Company Supervisor

Ing. Nick Luard

Candidate

Marco Guarnieri

Ottobre 2018

*Dedicated to
my parents, my girlfriend Sara, and my friends,
whose love, patience and understanding have helped make this thesis possible*

Ammiro tutti coloro che hanno una passione ed hanno la sapienza e la costanza di coltivarla. Sono loro il motore del mondo.

Enzo Ferrari

Acknowledgement

It is a pleasure for me to acknowledge all the people involved in this project who gave me support and strength to follow my dreams.

First of all I would like to thank my academic supervisor, Professor Federico Millo, who gave me the possibility to spend this year abroad in a big company like Jaguar Land Rover. Moreover his expertise, understanding and support have made the development of this thesis interesting and enjoyable and have helped me to grow as a professional.

A special recognition goes to my second academic supervisor, Dr. Luciano Rolando, who spent a lot of time and effort in the technical support. His advice, both from technical and personal point of view, has always been useful.

I have to thank my girlfriend, Sara, without whose love, help and patience I could not have faced this experience.

My sincere thanks goes to my manager, Efe Tunc, and all my team in Jaguar Land Rover. It has been a pleasure to start my career as an engineer with them. They always showed support, patience and willingness and thanks to them I have learned important skills for the professional life.

I would also like to thank Andrea, Francesco, Gabriele and Giorgio, the new friends I met in the UK. They made this year abroad a lovely and funny adventure.

And of course a big thank you is for the old friends in Turin. Despite the distance which has divided us during the last year, they always made me feel part of the group.

Last but not least, I want to really thank my parents who supported me in every decisions and gave me the possibility to chase my dreams.

Contents

Acknowledgement	iii
Introduction	1
1 Charge motion within the cylinder	2
1.1 Turbulence characteristics	2
1.2 In cylinder motions	8
1.2.1 Swirl	8
1.2.2 Tumble	10
1.2.3 Squish	11
2 Combustion in SI engines	13
2.1 Combustion modelling	15
2.1.1 Single-zone heat release rate analysis	16
2.1.2 0-dimensional model	18
2.2 Premixed turbulent combustion	18
3 Simulation software GT-Power	26
3.1 The software	26
3.2 Turbulence model	26
3.3 Combustion model	31
3.3.1 Predictive vs Non-Predictive combustion	33
4 Experimental set-up	39
4.1 Engine A	39
4.2 Engine B	40
5 Predictive model SI-Turb	42
5.1 Engine A calibration	44
5.2 Engine B model	50
5.3 Calibration transplant	62

5.3.1	Transplant results	63
5.4	Engine B calibration	68
5.4.1	Automatic turbulence calibration	68
5.4.2	Combustion calibration	78
5.4.3	Engine B results	82
6	Conclusions	88

List of Figures

1.1	Velocity variation as function of time in a two stroke engine	4
1.2	Turbulent flow jet through the intake valve	5
1.3	Spatial velocity autocorrelation R_x	6
1.4	Swirl motion	9
1.5	Swirl-generating inlet ports	10
1.6	Tumble motion	11
1.7	Squish generation	12
2.1	Pressure versus crank angle (a) and relative torque versus spark advance (b)	14
2.2	Combustion development angles	16
2.3	Open system boundary	17
2.4	Wiebe function	18
2.5	Borghgi plot for premixed turbulent combustion	20
2.6	Kinematic interaction between the flame front and an eddy of the size of Gibson scale	22
2.7	Gibson scale within the inertial range	23
2.8	Transport of preheated material by an eddy of size l_m	24
2.9	Mixing scale within the inertial range	25
3.1	Turbulence parameters effect on TKE	31
3.2	Turbulence parameters effect on Geometric Length Scale	32
4.1	Engine A map	40
4.2	Engine B map	41
5.1	SI-Turb calibration procedure	43
5.2	Ideal experimental setup	44
5.3	Engine A Turbulent Kinetic Energy 1500 rpm 28% bmep	47
5.4	Engine A Turbulent Kinetic Energy 5500 rpm 100% bmep	47
5.5	Fixed combustion parameters for Engine A	48
5.6	Variable combustion parameter for Engine A	48

5.7	Engine A pressure trend comparison	49
5.8	Engine A burn rate trend comparison	49
5.9	Non-Predictive combustion calibration	50
5.10	CPOA single cylinder model (left) and inputs (right)	51
5.11	Intake valve lift	52
5.12	Blowdown and exhaust valve lift	53
5.13	Engine B map	54
5.14	Compressor inlet pressure	55
5.15	Volumetric efficiency comparison	56
5.16	CPOA pressure when blowby is considered	57
5.17	<i>Engine B</i> Detailed model cylinder pressure	59
5.18	<i>Engine B</i> Detailed model burn rates	59
5.19	<i>Engine B</i> Detailed model performance (1)	60
5.20	<i>Engine B</i> Detailed model performance (2)	60
5.21	Errors of the detailed model compared to the experimental results	61
5.22	Flow and Combustion objects of the cylinder template	62
5.23	<i>Engine B</i> SI-Turb transplant model pressure	65
5.24	<i>Engine B</i> SI-Turb transplant model burn rates	65
5.25	<i>Engine B</i> SI-Turb transplant model performance (1)	66
5.26	<i>Engine B</i> SI-Turb transplant model performance (2)	66
5.27	Errors of the SI-Turb transplant compared to the experimental results	67
5.28	Boundary conditions location in 1D model of <i>Engine B</i>	69
5.29	Crank angle interval for turbulence calibration	70
5.30	<i>Engine B</i> Turbulent Kinetic Energy 1500 rpm 92% load	74
5.31	<i>Engine B</i> Turbulent Kinetic Energy 1500 rpm 92% load, zoom in the crank angle of interest	74
5.32	<i>Engine B</i> Turbulent Kinetic Energy 5000 rpm 100% load	75
5.33	<i>Engine B</i> Turbulent Kinetic Energy 5000 rpm 100% load, zoom in the crank angle of interest	75
5.34	<i>Engine B</i> Turbulent Kinetic Energy 1750 rpm 100% load	76
5.35	<i>Engine B</i> Turbulent Kinetic Energy 1750 rpm 100% load, zoom in the crank angle of interest	76
5.36	<i>Engine B</i> Turbulent Kinetic Energy 4500 rpm 100% load	77
5.37	<i>Engine B</i> Turbulent Kinetic Energy 4500 rpm 100% load, zoom in the crank angle of interest	77
5.38	Measured + Predicted model and initialisation	78
5.39	EngCylCombSITurb setup: Main tab	79

5.40 EngCylCombSITurb setup: LamSpeed tab	79
5.41 EngCylCombSITurb setup: TrbSpeed tab	80
5.42 Advanced Direct Optimiser setup	81
5.43 Optimisation parameters setup	82
5.44 <i>Engine B</i> SI-Turb final model pressure	84
5.45 <i>Engine B</i> SI-Turb final model burn rates	84
5.46 <i>Engine B</i> SI-Turb final model performance (1)	85
5.47 <i>Engine B</i> SI-Turb final model performance (2)	85
5.48 Errors of the SI-Turb final model compared to the experimental results . .	86
5.49 Burn rate RMSE comparison	87

List of Tables

1.1	Turbulence parameters in single cylinder engine	8
3.1	Turbulence parameters	30
3.2	Combustion multipliers	38
4.1	Engine A characteristics	39
4.2	Engine B characteristics	41
5.1	Detail model errors summary	58
5.2	SI-Turb transplant model errors summary	64
5.3	Population size typical values	72
5.4	Genetic algorithm settings	80
5.5	Typical ranges of the combustion multipliers	81
5.6	Combustion multipliers results from ADO	82
5.7	SI-Turb final model errors summary	86

MSc thesis in Automotive Engineering

Marco Guarnieri

October 16, 2018

Introduction

In the automotive field, the aim of these days is to reduce CO₂ emissions of vehicles: the most promising solution for what concerns Internal Combustion Engines (ICE) and in particular Spark Ignition (SI) engines is the adoption of downsized turbocharged petrol engines. However this technology together with the continuously increasing levels of boost to achieve the desired performance requires a precise description of the combustion process so that the effects of parameters such as spark timing, EGR rate, compression ratio changes or knock level can be well evaluated. The development and the validation of reliable methods able to describe the condition inside the cylinders and the evolution of the combustion process have therefore acquired great importance in the most recent times. The common practice to properly evaluate the flow motion in the cylinder and the combustion process is to run 3D Computation Fluid Dynamics (CFD) simulations which are accurate but also very time-consuming. As a consequence, the CFD analysis cannot always be used during the design and calibration phases of a new engine development. Since during these steps fast and reliable answers are necessary, innovative 0/1 Dimensional (0/1D) methods for the prediction of in-cylinder flow conditions and the combustion evolution have been investigated. One of these approaches is the 0D phenomenological turbulence model, built inside the commercial code GT-Suite, which will be used and calibrated in this project to evaluate the flow conditions inside the cylinder. Then the turbulence model will be coupled with the predictive combustion model from GT-Suite and its predictive capability will be assessed. An interesting analysis about the potential benefits of the use of this predictive tool when moving to a new engine will be carried out: the goal is to evaluate what happens and which are the results when using the turbulence and combustion calibration from a previous engine for a new one, which presents a slightly changed geometry. As final step, a predictive model will be calibrated from scratch and the comparison with the calibration of the previous engine will be evaluated.

Chapter 1

Charge motion within the cylinder

Gas motion condition within the engine cylinder is one of the most influencing factors for what concerns the combustion process (both the start and the development of it), the fuel-air mixing, the heat transfer and the pollutant formation. The initial in-cylinder motion conditions are set up in the intake stroke and are influenced by the valves and ports design and then they might be modified during the compression stroke. The charge motion represents therefore a really complex topic that plays an essential role in the definition of the engine performance. As a consequence, in the last years a lot of time and effort have been spent to develop the knowledge about the phenomenon and to investigate the possibility to predict the characteristics as a function of engine operating conditions. This chapter will therefore focus on description of the charge conditions when it enters the cylinder and especially it will review all the mathematical models used. A more complete description of the topic can be found in [1] and [2].

1.1 Turbulence characteristics

The engine cylinders are characterised by turbulent flow, which guarantees higher rates of transfer and mixing if compared with the rates typical of molecular diffusion. The local fluctuations in the turbulent flow field are responsible for the higher rates of momentum, heat and mass transfer, which in the end are beneficial for the operation of internal combustion engines, both spark-ignition and diesel ones. The turbulent flow is dissipative and rotational:

- The fluid kinetic energy is dissipated via viscous effect due to the shear stresses which perform deformation work on the fluid. The shear in the mean flow represents therefore the source of energy for turbulent velocity fluctuations, without which the turbulence decays.

- Turbulence is made of high fluctuating vorticity, which can be maintained only if the velocity fluctuations are three dimensional.

The turbulent flow is strictly influenced by the environment in which it develops. The velocity fields in an internal combustion engines are time dependent because the processes that generate them are periodic and the flow motion is turbulent, due to the velocities and dimensions involved. As a consequence, the flow is unsteady, irregular (it may present high cycle-to-cycle variations) and random; all these feature make the description of such a field very difficult. Statistical models must be therefore used. They rely on several quantities, the most important of which are the mean velocity, the fluctuating velocity about the mean and different length and time scales.

If a steady turbulent flow is considered, the instantaneous local fluid velocity in a specific direction is:

$$U(t) = \bar{U} + u(t)$$

While the mean velocity \bar{U} is the time average of $U(t)$:

$$\bar{U} = \lim_{\tau \rightarrow \infty} \frac{1}{\tau} \int_{t_0}^{t_0+\tau} U(t) dt$$

the fluctuating velocity u is defined by its root mean square value, i.e. the turbulent intensity u' :

$$u' = \lim_{\tau \rightarrow \infty} \sqrt{\frac{1}{\tau} \int_{t_0}^{t_0+\tau} u^2 dt} = \lim_{\tau \rightarrow \infty} \sqrt{\frac{1}{\tau} \int_{t_0}^{t_0+\tau} (U^2 - \bar{U}^2) dt}$$

The problem is represented by the quantities involved in internal combustion engines. They are not steady, i.e. they are not independent from time: since the flow conditions can vary significantly from one engine cycle to the other, the results are both cycle-to-cycle variations in the mean flow as well as turbulent fluctuations about that particular cycle's mean value. In order to solve this issue, the *ensemble-averaging* or *phase-averaging* approach can be adopted, since in the cylinder the flow can be considered as quasi-periodic. The instantaneous velocity, as a function of the crank angle position θ and considering the i -th cycle, can be written as:

$$U(\theta, i) = \bar{U}(\theta, i) + u(\theta, i)$$

The ensemble-average (or phase-average) is the average, over a large number of measurements at the position, of the quantity at a specific crank angle during the cycle:

$$\bar{U}_{EA}(\theta) = \frac{1}{N_c} \sum_{i=1}^{N_c} U(\theta, i)$$

with N_c equal to the number of test performed. If this procedure is performed for all the crank angle positions, the final profile of the ensemble-averaged velocity is obtained.

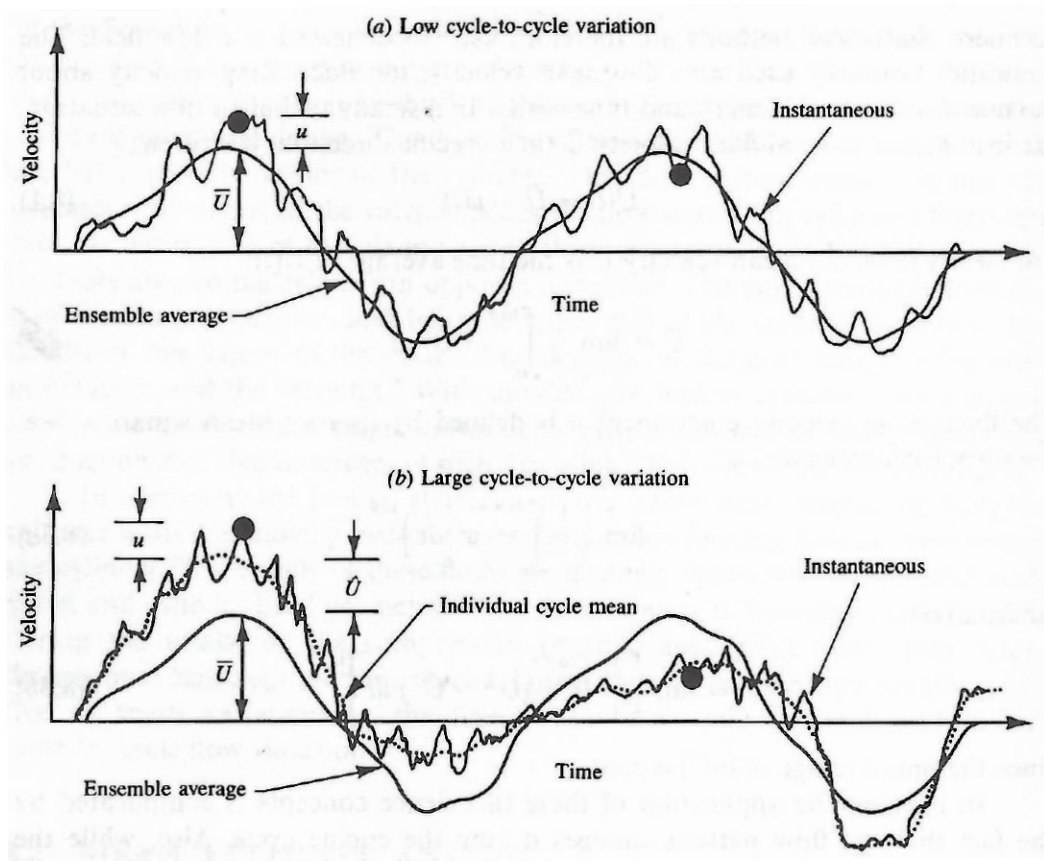


Figure 1.1: Velocity variation as function of time in a two stroke engine

Figure 1.1 shows the velocity variation with time at a fixed location in the cylinder during two consecutive cycles of a two stroke engine. Dots represent the measurements of instantaneous velocity at the same crank angle. The ensemble-average is the solid smooth line. In case of low cycle-to-cycle variations (top graph) the cycle mean velocity and the ensemble-averaged velocity can be overlapped; while if large cycle-to-cycle variations are present (bottom graph), these two quantities are separated by the quantity \hat{U} , i.e. the cycle-by-cycle variation in the mean velocity. It is defined as the difference between the mean velocity in a particular cycle and the ensemble-averaged mean velocity over many cycles:

$$\hat{U}(\theta, i) = \bar{U}(\theta, i) - \bar{U}_{EA}(\theta)$$

As a conclusion, the instantaneous velocity equation can be re-written as:

$$U(\theta, i) = \bar{U}_{EA}(\theta) + \hat{U}(\theta, i) + u(\theta, i)$$

The main issues which this statistical approach shows are:

- The engine periodicity is not rigid; significant cycle-to-cycle variations can in fact be present.
- The mean charge motion as a consequence varies from cycle to cycle.

- The description in terms of ensemble-averaged quantities loses the information about the individual cycles on behalf of a mean cycle. This mean cycle is more significant compared to a random cycle (which could be very far from the average one) but it doesn't have a particular physical meaning.

In order to fully describe the charge motion within the cylinder, in addition to the mean and the turbulent velocities, some time and length scales must to be introduced. In figure 1.2 the largest eddies in the flow generated by the fluid jet entering the cylinder are represented; they then deteriorate into smaller and smaller eddies, in which the kinetic energy is dissipated due to viscous effects. This process is described with the three length and time scales listed below:

- Integral length scale l_i and time τ_i
- Taylor micro length scale l_m and time τ_m
- Kolmogorov length scale l_k and time τ_k

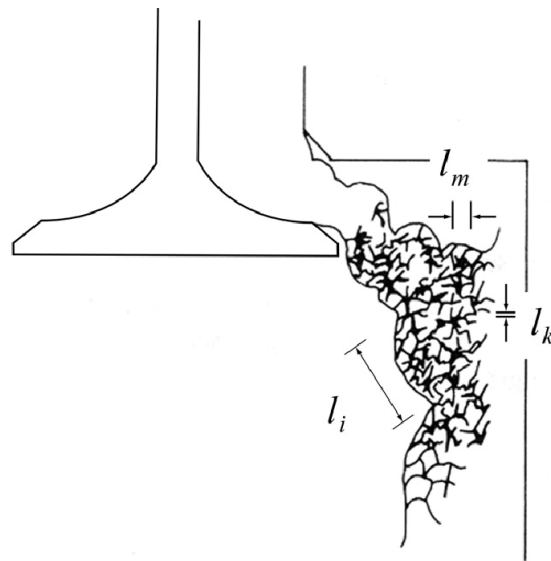


Figure 1.2: Turbulent flow jet through the intake valve

The integral length scale l_i gives information about the dimension of the largest eddies, which are comparable with valve lift during intake or with the gap between the piston and the head at the end of the compression stroke. Velocity measurements taken in two points separated by a distance x (significantly smaller than l_i) will correlate with each other for distance greater than the integral length scale, no correlation will exist. The length scale l_i is defined as the integral of the autocorrelation coefficient of the velocity of two adjacent points in the flow with respect to the distance x between them:

$$l_i = \int_{t_0}^{\infty} R_x dx$$

where

$$R_x = \frac{1}{N_m - 1} \sum_{i=1}^{N_m} \frac{u(x_0)u(x_0 + x)}{u'(x_0)u'(x_0 + x)}$$

The trend of the spatial velocity autocorrelation R_x as function of distance x is represented in the figure 1.3.

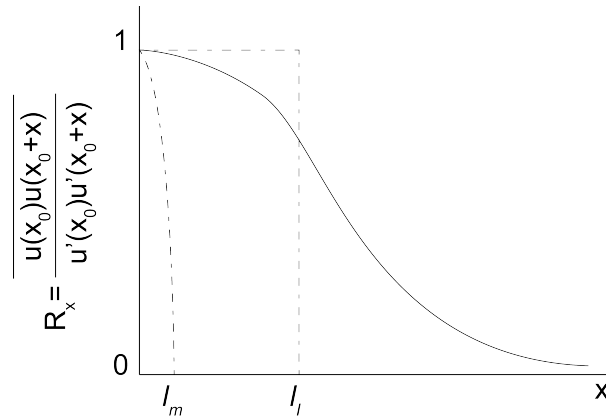


Figure 1.3: Spatial velocity autocorrelation R_x

If a fixed point in space and two different time instants t_0 and $t_0 + t$ are considered, the integral time scale τ_i can be evaluated as:

$$\tau_i = \int_{t_0}^{\infty} R_t dt$$

where

$$R_t = \frac{1}{N_m - 1} \sum_{i=1}^{N_m} \frac{u(t_0)u(t_0 + t)}{u'(t_0)u'(t_0 + t)}$$

and N_m is the number of measurements. The integral time scale τ_i gives the information about the time needed by a large eddy to pass the observation point or, in case of a flow without mean motion, about the lifetime of the eddy itself.

The largest eddies are unstable, because they produce velocity gradients in the flow and, as a consequence, viscous shear stresses. Because of these stresses, the kinetic energy is dissipated to heat due to viscous effects and eddies of smaller and smaller size originate. These are more likely to be isotropic (have no preferred direction) than are the large eddies. In order to describe this process, two new scales need to be introduced. The Taylor micro length scale l_m is defined as the value for which the Taylor series of the spatial autocorrelation function R_x intersects the x-axis, in the point x_0 , as shown in figure 1.3:

$$l_m = -\frac{2}{(\partial^2 R_x / \partial x^2)_{x=x_0}}$$

It represents the spacing between the small eddies or the intensity of the local gradient of the turbulent fluctuation, thanks to the relation below:

$$\frac{\partial u}{\partial x} \approx \frac{u'}{l_m}$$

In a similar way, the micro time scale τ_m is obtained from the temporal autocorrelation function R_t :

$$\tau_m = -\frac{2}{(\partial^2 R_t / \partial t^2)_{t=t_0}}$$

This scale represents the inverse of the frequency of appearance of the small dissipation eddies. Since the time scales are much easier to measure, there are some relations which link time and length scales. These expressions are valid under certain conditions (not typical in internal combustion engines): isotropic and quasi-steady flow and low level of turbulence $u'/u \ll 1$.

$$l_i = \bar{U} \tau_i \qquad l_m = \bar{U} \tau_m$$

The last scale to be introduced is the Kolmogorov one. The dissipation of turbulence takes place in the smallest eddies. At this smallest scale of the turbulent motion the molecular viscosity dissipates small-eddies kinetic energy into heat. Both Kolmogorov length and time scale can be described as follows:

$$l_k = \left(\frac{\nu^3}{\epsilon} \right)^{1/4} \qquad \tau_k = \left(\frac{\nu}{\epsilon} \right)^{1/2}$$

where ν is the kinematic viscosity of the fluid and ϵ is the dissipation rate of the kinetic energy.

The order of magnitude of the length and time scales described so far are listed in the table 1.1. These measurements have been taken from a single cylinder engine running at $n = 33 \text{ rps}$. The ratio between the integral and the micro length scales is around 4, while the absolute values are comparable with the valve lift and the space between piston and head (around 10 mm). The same ratio is held if time scales are considered. Moreover, since τ_i is close to $2 \div 3 \%$ of the time of one single stroke (equal to 15 ms), this means that the lifetime of the largest eddies is lower than the time that these eddies spend in the cylinder. The values of the Kolmogorov scales show that the molecular dissipation processes happen in really small regions and for a lower time, if compared to larger eddies.

	u'	u_p	l_i	l_m	l_k	τ_i	τ_m	τ_k
	[m/s]	[m/s]	[mm]	[mm]	[mm]	[ms]	[ms]	[ms]
Half Intake	5	20	4	1	0.02	0.4	0.07	0.04
End Compression	1.5	10	4	1	0.03	0.8	0.2	0.12

Table 1.1: Turbulence parameters in single cylinder engine

1.2 In cylinder motions

Usually, when the fresh charge enters the cylinder, rotational movements both in planes normal to cylinder axis and in planes through this axis arise. These motion play an important role in the combustion process because the last in time and promote the fuel and air mixing, thus increasing combustion speed. In the next sections, the main three charge motions, i.e. swirl, squish and tumble, will be analysed.

1.2.1 Swirl

Swirl is usually defined as the organised rotation of the charge about the cylinder axis, as depicted in Figure 1.4. It is created by bringing the intake flow into the cylinder with an initial angular momentum. While some decay in swirl due to friction occurs during the engine cycle, intake generated swirl usually persists through the compression, combustion and expansion processes. In engine designs with bowl-in-piston combustion chambers, the rotational motion set up during intake is substantially modified during compression. Swirl is used in diesels and some stratified-charge engine concepts to promote more rapid mixing between the inducted air charge and the injected fuel. Swirl is also used to-speed up the combustion process in spark-ignition engines. In two-stroke engines it is used to improve scavenging.

The swirl motion can be measured with an impulse swirl meter. Air is blown steadily through the inlet port and valve assembly in the cylinder head into an appropriately located equivalent of the cylinder. A honeycomb flow straightener is pivoted on the cylinder centerline (with low friction bearings) and is mounted between 1 and 1.5 bore diameters down the cylinder. Its diameter is close to the cylinder bore. It provides information about the total torque exerted by the swirling flow. This torque equals the flux of angular momentum through the plane coinciding with the flow-straightener upstream face. The dimensionless swirl parameter which can be defines is

$$C_s = \frac{8T}{\dot{m}v_0B}$$

where T is the torque, \dot{m} is the air mass flow rate, B is the cylinder bore used to obtain

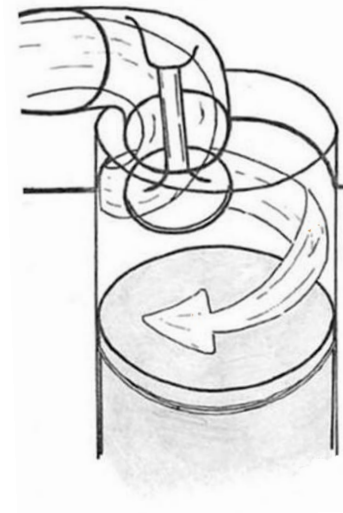


Figure 1.4: Swirl motion

a dimensionless coefficient, while v_0 is the characteristic velocity, which is obtained from the pressure drop across the valve using the incompressible flow equation:

$$v_0 = \left[\frac{2\Delta p}{\rho} \right]^{1/2}$$

Swirl motion is generated during the intake stroke, following two general approaches. In one, the flow is discharged into the cylinder tangentially toward the cylinder wall, where it is deflected sideways and downward in a swirling motion. In the other, the swirl is largely generated within the inlet port: the flow is forced to rotate about the valve axis before it enters the cylinder. The former type of motion is achieved by forcing the flow distribution around the circumference of the inlet valve to be nonuniform, so that the inlet flow has a substantial net angular momentum about the cylinder axis. The directed port and deflector wall port in Figure 1.5a and 1.5b are two common ways of achieving this result. The directed port brings the flow toward the valve opening in the desired tangential direction. Its passage is straight, which due to other cylinder head requirements restricts the flow area and results in a relatively low discharge coefficient. The deflector wall port uses the port inner side wall to force the flow preferentially through the outer periphery of the valve opening, in a tangential direction. Since only one wall is used to obtain a directional effect, the port areas are less restrictive.

The second approach is to generate swirl within the port, about the valve axis, prior to the flow entering the cylinder. Two examples of such helical ports are shown in Figure 1.5c and 1.5d. Usually, with helical ports, a higher flow discharge coefficient at equivalent levels of swirl is obtained, since the whole periphery or the valve open area can be fully utilised. A higher volumetric efficiency is the consequence. Also, helical ports are less sensitive to position displacements, such as can occur in casting, since the swirl generated

depends mainly on the port geometry above the valve and not the position of the port relative to the cylinder axis.

Flow rotation about the cylinder axis can also be generated by masking off or shrouding part of the peripheral inlet valve open area. Mask or shroud on the valve in research engines is chosen because changes can easily be made. In production engines however, the added cost and weight, the problems of distortion, the need to prevent valve rotation, and the reduced volumetric efficiency make masking the valve an unattractive approach.

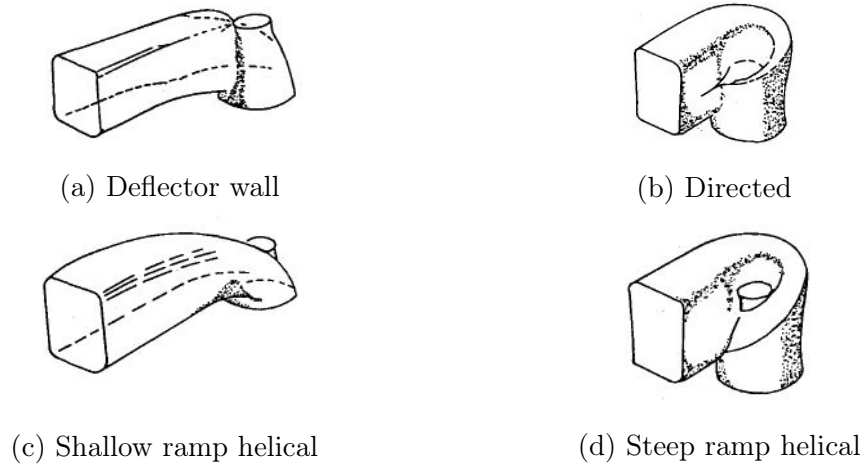


Figure 1.5: Swirl-generating inlet ports

1.2.2 Tumble

With the term tumble, we refer to the rotational motion in a plane through the cylinder axis, as represented in Figure 1.6. This charge motion originates during the induction and then it is amplified at the end of the compression stroke.

If a traditional intake port is used, during the intake a tumble vortex is generated in the area below the valve face. This is the consequence of the interaction of the incoming flow with the cylinder wall and the piston, on exhaust side. In this case, its lifetime is short because of the low intensity and the presence of a possible opposite vortex on intake side. Therefore, if the goal is to promote the tumble, the intake port design should increase the velocity of the incoming flow (from $50 \div 60$ m/s of traditional design to $90 \div 120$ m/s) and point the flow in the area below the exhaust valve. Once the high speed flow enters the cylinder, it interacts with the walls and the piston top surface and the tumble vortex is generated. Then, when the piston moves upwards during the compression stroke, the vortex is squashed and, in order to obey to the momentum conservation equation, the velocity increases, since the radius is decreased. An other possibility to increase the tumble level is the usage of a shield in the intake valve: in this case, the incoming flow

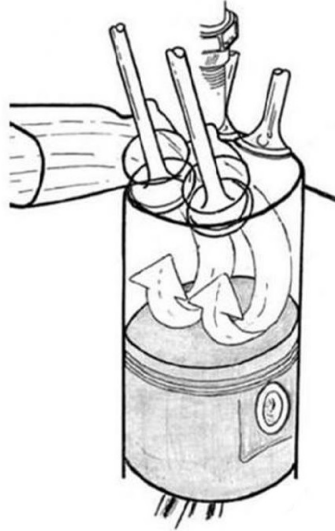


Figure 1.6: Tumble motion

can not enter the cylinder along the intake side, thus increasing the momentum of the initial vortex.

Similar measurement systems to the one used for the definition of the swirl parameter can be used in the case of tumble. The torque T applied by the air flow to the impulse meter in steady-state condition is measured and the dimensionless tumble number C_T is obtained as follows:

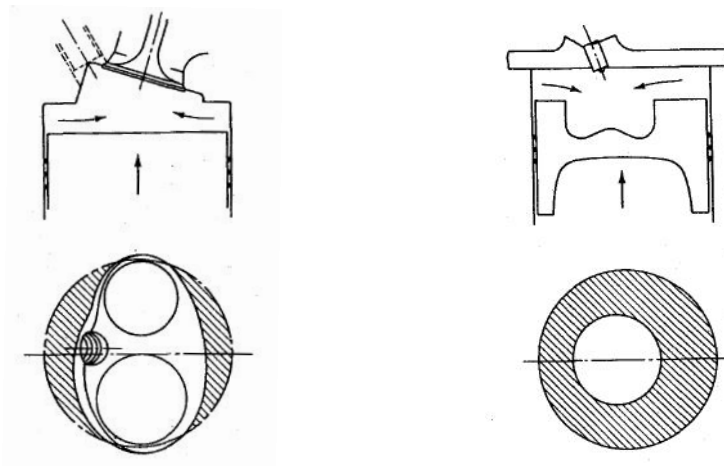
$$C_T = \frac{8T}{\dot{m}v_0B}$$

where \dot{m} is the air mass flow rate, v_0 the velocity and B the cylinder bore as in the swirl formula.

1.2.3 Squish

Squish is represented by the radially inward or transverse gas motion which occurs toward the end of the compression stroke when a portion of the piston face and cylinder head approach each other closely, as shown in Figure. This particular charge motion plays therefore an essential role in the start of the combustion process, since it strictly influences its development. Figure 1.7 shows squish originates from piston motion. Figure 1.7a refers to a typical wedge-shaped SI engine combustion chamber while Figure 1.7b to a bowl-in-piston diesel combustion chamber. The amount of squish can be quantified by means of the percentage squish area, i.e. the percentage of the piston area, $\pi B^2/4$, which closely approaches the cylinder head (the shaded areas in Figure 1.7).

An important remark has to be highlighted at this point: while swirl and tumble motion (which are produced by the system geometry) are produced also in stationary conditions, squish originates only when the piston is moving. Therefore, for the case of the



(a) Wedge-shaped SI engine

(b) Bowl-in-piston DI diesel engine

Figure 1.7: Squish generation

squish, it is not possible to define a global parameter from measurement of the stationary flow. As a consequence, it is necessary to measure the velocities under dynamic conditions or to predict these values with fluid dynamics models.

Chapter 2

Combustion in SI engines

This chapter is focused on the description of the development and the modelling of the combustion process in a Spark Ignition (SI) engine; complete details can be found in [1], [2] and [3]. In SI engine, the mixture of air and fuel is inducted through the intake valves into the cylinder, it mixes with residual gases, then it is compressed and under normal operating conditions the combustion is triggered towards the end of the compression stroke by the electric discharge of the spark-plug. As a consequence of the combustion start, a turbulent flame front, whose shape is very irregular, develops and then propagates through the combustion chamber till it reaches the cylinder walls where it extinguishes. At the first stage of the spark discharge, the energy release from the developing flame is too small to have a considerable pressure rise but as the flame continues to propagate inside the combustion chamber, the pressure suddenly rises above the value it would have in absence of the combustion. Then the maximum in-cylinder pressure is achieved after the Top Dead Centre (TDC), but before the charge is fully burned; then it decreases as the cylinder volume increases, because of the descending motion of the piston. Following this description it is possible to divide the combustion process into four steps:

- spark ignition
- early flame development
- flame propagation
- flame termination

Since the flame growth and propagation depend on local mixture motion and composition, the pressure and the mass fraction burned vary from cycle-to-cycle and also from cylinder-to-cylinder, due to uneven mixing or induced quantities among cylinders. Mixture motion and composition close to the spark-plug at the time of the electric discharge play an essential role, because they are responsible for the early stages of the flame development.

Therefore, cycle-to-cycle and cylinder-to-cylinder variations are really important for Internal Combustion Engines (ICE), because the extreme cycles limit the engine operating regime.

An other important parameter of the combustion is the timing: by properly locate the combustion process relative to the TDC, it is possible to obtain the maximum power or torque. The combustion usually starts before the end of the compression stroke, continues in the early stages of the power stroke and ends after the peak pressure has been reached. The main parameter involved is therefore the spark timing: if the start of combustion is advanced before TDC the compression work transfer (from the piston to the cylinder gases) increases, while if the spark timing is retarded, the peak pressure is lower and the expansion work transfer (from the gases to the piston) reduces. The optimum timing which gives the maximum achievable torque is called Maximum Brake Torque timing or MBT timing and it occurs when the opposite trends of the two work transfers offset each other. This optimum timing is strictly influenced by engine design, operating conditions and properties of fuel,air and burned gas mixture. In the Figure 2.1, it is possible to see the effect of the spark timing on the cylinder pressure (on the left) and on the torque (on the right).

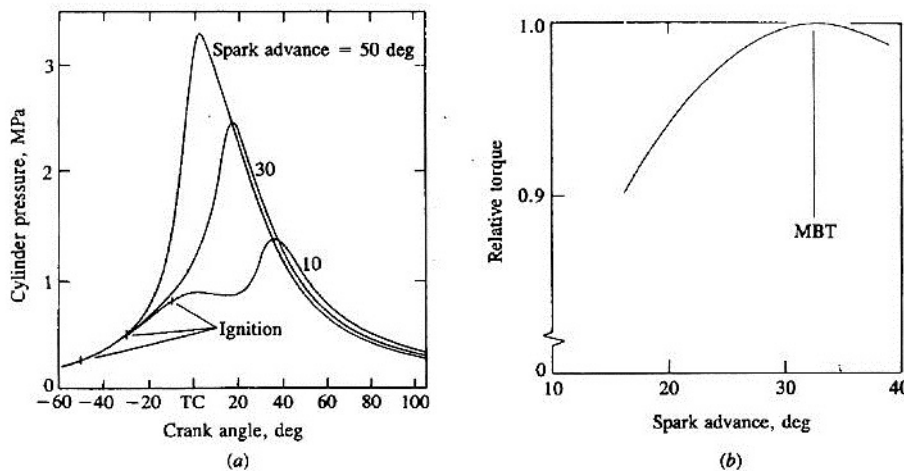


Figure 2.1: Pressure versus crank angle (a) and relative torque versus spark advance (b)

So far the description of the combustion was focus on the normal combustion process, i.e. the one in which the flame moves steadily in the chamber and all the charge is fully burned. However, the fuel composition, the engine design or operating points and other factors may lead to the so-called abnormal combustion phenomena. Among these, two main types of abnormal combustion can be identified:

- *Knock* is the autoignition of the end-gas (i.e.the portion of fuel, air and residual gas mixture ahead of the flame front), which as the flame propagates through the

chamber is compressed, thus leading to pressure, temperature and density raise. Therefore in a portion of the end-gas, some chemical reaction may start spontaneously, releasing energy at very high rate. The consequences are high-frequency pressure oscillations and the typical sharp metallic noise, called knock.

- *Surface ignition* is the ignition of the air and fuel mixture by any hot spot in the combustion chamber, like overheated valves or spark plugs. It can be divided into *preignition*, if the ignition occurs before the spark plug ignites the charge, and *postignition*, if it happens after the normal combustion.

2.1 Combustion modelling

Combustion modelling is based on the evaluation of the mass of fuel burned in time during the engine cycle (also called mass fraction burned), which is defined as the ratio between the mass of fuel burned at the angle θ and the total mass of fuel injected:

$$x_b = \frac{m_{f,b(\theta)}}{m_{f,inj,TOT}}$$

This function provides information related to the development of the combustion process itself. The amount of fuel burned is in fact correlated to the amount of energy released during the combustion, i.e. to the heat release rate. The rate at which fuel and air mixture burns increases immediately following the spark discharge till reaching its maximum halfway through the burning process and then it decreases to almost zero at the end of the combustion. As a results of this, the mass fraction burned has its typical S-shape. This curve is useful to identify and describe the stages of the combustion process. Typically, some characteristic values are considered which are the values of the crank angle when the mass fraction burned is equal to 10%, 50% and 90%. These values are usually indicated as MFB10, MFB50, MFB90 and expressed in crank angle degrees. The start of combustion (SOC) may be also identified starting from the $x_b(\theta)$ curve, as the first point where the value of the fraction becomes higher than zero. The end of combustion (EOC) could also be identified as the crank angle for which it is equal to 1, so that the combustion duration can be calculated as the angular difference between EOC and SOC. In some cases, where EOC cannot be easily defined, an indication of the combustion duration can be expressed as the difference between MFB90 and MFB10, the so called MFB10-90.

The evolution of the combustion process in a SI engine can be described using three main crank angle interval:

- *Flame development angle* $\Delta\theta_d$. The crank angle interval between the spark discharge and the time when a small but significant fraction of the cylinder mass has burned or fuel chemical energy has been released. Usually this corresponds to MFB10.

- *Rapid burning angle* $\Delta\theta_b$. The crank angle interval required to burn the bulk of the charge. It is defined as the interval between the end of the flame-development stage (MFB10) and the end of the flame-propagation process (MFB90).
- *Overall burning angle* $\Delta\theta_0$. The duration of the overall burning process. It is the sum of the previous quantities.

These three combustion angles are shown in the Figure 2.2 below. In the graph, both the in-cylinder (blue curve) and the motored pressure (red dotted curve) are present; the green dotted line represents instead the mass fraction burned, used to identify $\Delta\theta_d$, $\Delta\theta_b$ and $\Delta\theta_0$ angles. As a consequences of these, the start of combustion and the mass fraction burned 10% and 90% are also represented.

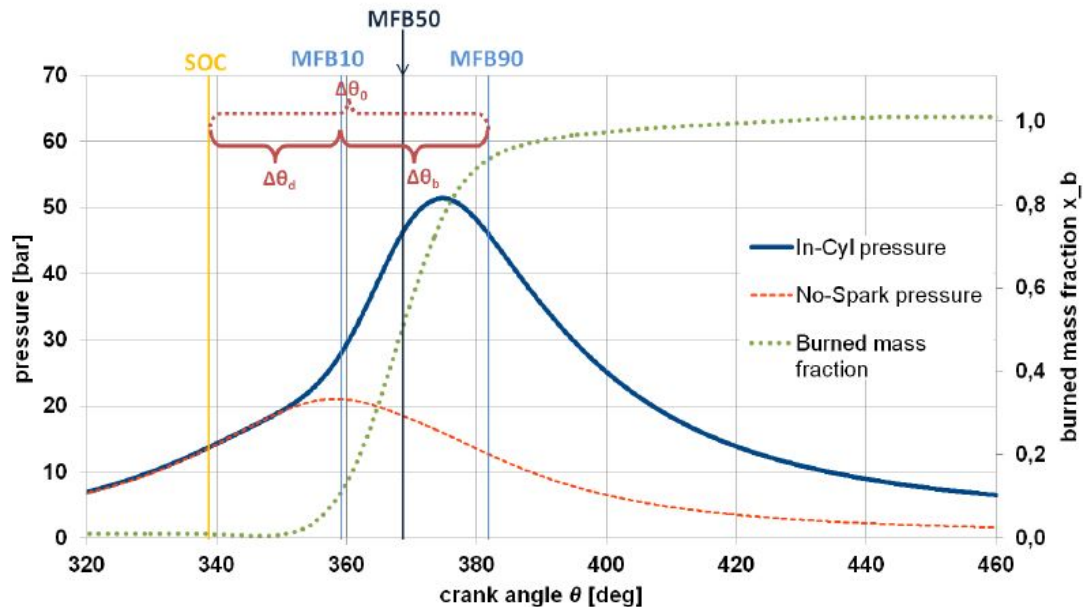


Figure 2.2: Combustion development angles

2.1.1 Single-zone heat release rate analysis

With the first method to model combustion it is possible to account for the effect of heat transfer and leakages. The basic hypothesis behind the single-zone model is that the gas inside the chamber can be considered homogeneous. Therefore, by studying the “average” thermodynamic state of the cylinder charge starting from the measured pressure and volume change, it is possible to determine the *Net Heat Release Rate* (also called apparent HRR). The system under study has open boundaries to account for mass flows inside and outside the control volume (leakages, fuel injection in direct injection engines), as it is shown in Figure 2.3.

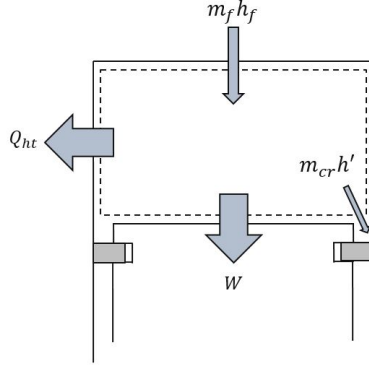


Figure 2.3: Open system boundary

The first law of thermodynamics is applied to this open system:

$$\delta Q_{ch} = dU_s + \delta Q_{ht} + \delta W + \sum h_i dm_i$$

The change in sensible energy of the charge dU_s , is separated from that due to change in composition: the term δQ_{ch} represents the chemical energy released by combustion. The work term is piston work and equal to $p dV$. δQ_{ht} is heat transfer to the chamber walls. The mass flux term represents flow across the system boundary; so in the absence of fuel injection, it represents the flow into and out of the crevice regions.

The sensible energy of the charge can be written as

$$dU_s = mc_v(T)dT + u(t)dm$$

where m is the mass within the system, T is the mean charge temperature and c_v is the specific heat of the gas. Considering the equation above for the energy dU_s and that $dm_i = dm_{cr} = -dm$, the first law becomes

$$\delta Q_{ch} - \delta Q_{ht} = mc_v dT + (h' - u)dm_{cr} + p dV$$

where $dm_{cr} > 0$ when flow is out of the cylinder into the crevice, $dm_{cr} < 0$ when flow is from the crevice to the cylinder and h' is evaluated at cylinder conditions when $dm_{cr} > 0$ and at crevice conditions when $dm_{cr} < 0$. The term on the left hand side of the equation above represents the apparent heat release AHRR.

From the knowledge of the chemical power \dot{Q}_{ch} , it is possible then to calculate the mass fraction burned as the ratio between the instantaneous chemical energy at time instant t and the total amount of energy available, which is obtained from the total injected fuel mass $m_{f,inj,TOT}$ and the lower heating value of the fuel H_{IL} .

$$x_b(t) = \frac{\int_{SOI}^t \dot{Q}_{ch} dt}{m_{f,inj,TOT} H_{IL}}$$

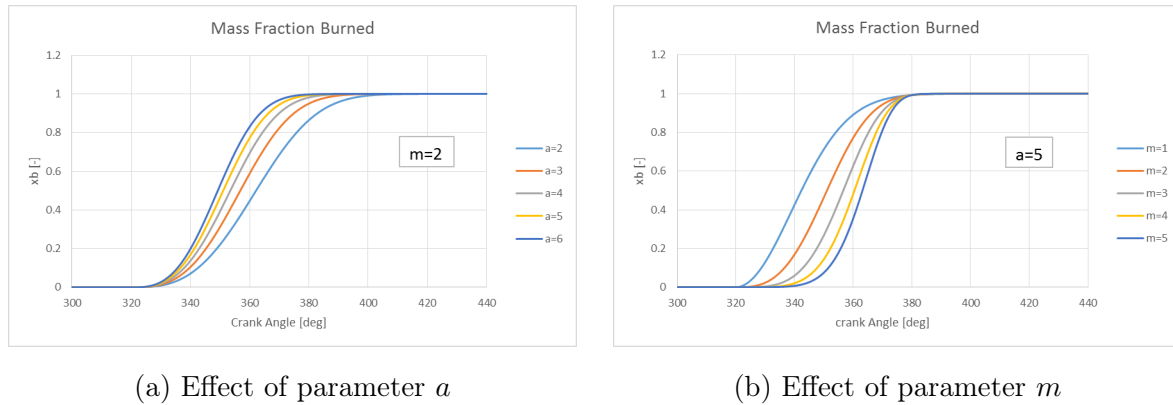


Figure 2.4: Wiebe function

2.1.2 0-dimensional model

The second approach to model the combustion process is to approximate the mass fraction burned curve through the usage of the so called Wiebe function, which has been originally developed for SI engines:

$$x_b = 1 - \exp \left[-a \left(\frac{\theta - \theta_0}{\Delta\theta} \right)^{m+1} \right]$$

where θ is the generic crank angle and θ_0 is the crank angle at the start of combustion (SOC), $\Delta\theta$ is the combustion duration. The coefficients a and m are two tuning factors which modify the shape of the curve and are called respectively rate factor and shape factor. The effects of these is visible in Figure 2.4a and 2.4b.

Although this approach may result very simple in terms of calculations and therefore may provide benefits in terms of computational power, it misses any physical relation. Moreover, in order to obtain good results, a tuning procedure for parameters a and m should be performed to match experimental data.

2.2 Premixed turbulent combustion

In the spark-ignition engine the fuel and air mixing is promoted by turbulence during a sufficiently long time down to the molecular level before combustion is initiated by a spark. As a consequence of the spark released energy, a flame kernel generates and grows at first by laminar, then by turbulent flame propagation. The turbulent burning velocity is therefore plays a very important role in premixed turbulent combustion. Laminar flames in premixed fuel, air, residual gas mixtures are characterised by a laminar flame speed s_L and a laminar flame thickness δ_L . The laminar flame speed is the velocity at which the flame propagates into quiescent premixed unburned mixture ahead of the flame. The

laminar flame thickness is defined from the molecular diffusivity D_L , with the formula:

$$\delta_L = \frac{D_L}{s_L}$$

Turbulent flames are characterised by the root mean square velocity fluctuation, the turbulence intensity u' and the various length scales of the turbulent flow ahead of the flame. The integral length scale l_i is a measure of the size of the large energy-containing structures of the flow. The Kolmogorov scale l_k defines the smallest structures of the flow where small-scale kinetic energy is dissipated via molecular viscosity.

In order to characterise the turbulent premixed flames, three dimensionless parameters are used: the Reynolds number Re , the Dammköler number Da and the Karlovitz number Ka . The first of these numbers is obtained with the formula:

$$Re = \frac{u'l_i}{\nu} = \frac{u'l_i}{s_L\delta_L}$$

where the kinematic viscosity ν can be written as the laminar burning speed s_L times the flame thickness δ_L , if the Schmidt number $Sc = \nu/D$ is assumed to be equal to the unity. The characteristic turbulent eddy turnover time τ_T can be defined as:

$$\tau_T = \frac{l_i}{u'}$$

while the characteristic chemical reaction time, which is the residence time in laminar flame, can be written as:

$$\tau_L = \frac{\delta_L}{s_L}$$

From the knowledge of these two times, the Dammköler number Da can be identified as the ratio of the eddy turnover time and the laminar burning time:

$$Da = \frac{\tau_T}{\tau_L} = \frac{l_i s_L}{\delta_L u'}$$

In the end, the Karlovitz number is equal to the inverse of a Dammköler number defined with the Kolmogorov time scale rather than with the integral time scale, as in the formula below:

$$Ka = \frac{\tau_L}{\tau_k} = \frac{\delta_L^2}{l_k^2} = \frac{u_k^2}{s_L^2}$$

Since the flame thickness δ_L includes the preheat, the inner and the oxidation layers, a second Karlovitz number can be introduced to describe the width of the inner layer l_δ only, which is $l_\delta = \delta\delta_L$:

$$Ka_\delta = \frac{l_\delta^2}{l_k^2} = \delta^2 \frac{\delta_L^2}{l_k^2} = \delta^2 Ka$$

Using all the numbers defined above and referring to regime diagram (the so-called Borghi plot) in Figure 2.5, where the logarithm of u'/s_L is plotted versus the logarithm of l_i/δ_L ,

all the possible conditions of the flame front in a premixed turbulent combustion can be identified. In the following definitions, the inequality $Re > 1$ separates the turbulent from the laminar regime, while the inequality $Ka < 1$ represents the split between fast and slow chemistry. All the flame regimes in the Borghi plot are:

- *Laminar Flames*: $Re < 1$
- *Wrinkled Flamelets*: $Re > 1$ and $u'/s_L < 1$
- *Corrugated Flamelets*: $Re > 1$, $u'/s_L > 1$ and $Ka < 1$
- *Thin Reaction Zones*: $Re > 1$, $u'/s_L > 1$, $Ka > 1$ and $Ka_\delta < 1$
- *Broken Reaction Zones*: $Re > 1$, $u'/s_L > 1$, $Ka > 1$ and $Ka_\delta > 1$

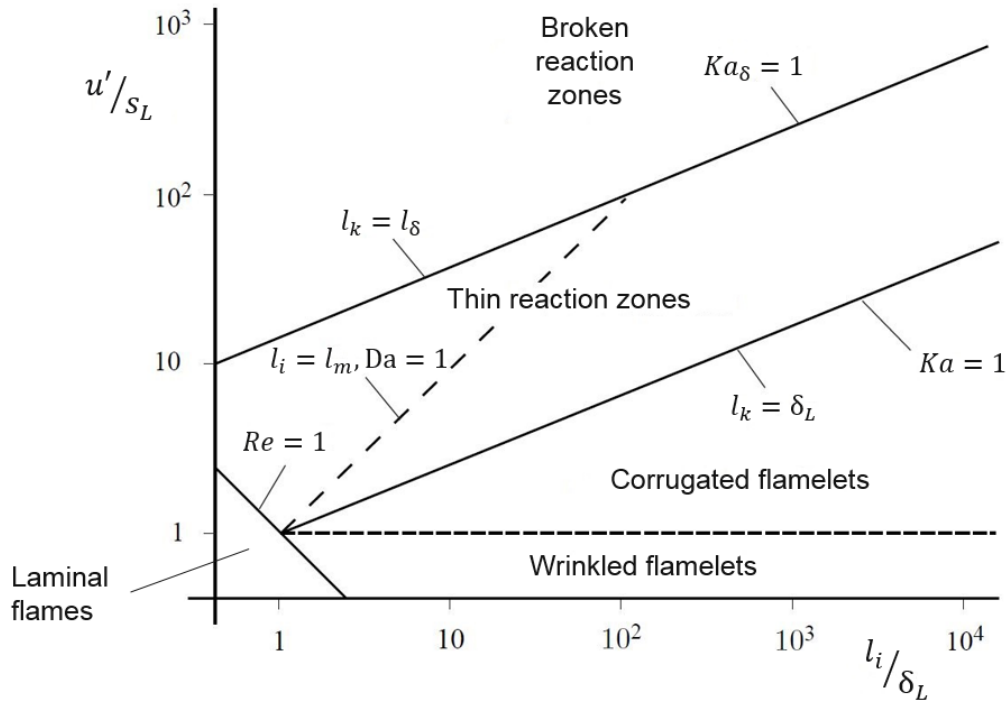


Figure 2.5: Borghi plot for premixed turbulent combustion

At this point, all the flame regimes will be analysed, one by one. The first region, i.e. the *laminar flames*, corresponds to the lower-left corner of the plot and it describes the flame conditions in absence of turbulence. This zone has no practical interest, since, as described in the previous sections, the development of the flame front in internal combustion engine is characterised by turbulent conditions.

In the case of *wrinkled flamelets* regime, the inequality $u'/s_L < 1$ is true. Since u' may be interpreted as the turnover velocity of the large eddies, it means that even those eddies cannot convolute the flame front enough to form multiple connected reaction sheets.

Laminar flame propagation is dominating over turbulent flame propagation in this regime. Internal combustion engines never work under this regime.

When the *corrugated flamelets* zone is considered, there is an interaction between turbulent and laminar flame propagation. Since in this region $Ka < 1$, the following inequality holds:

$$u' \geq s_L \geq u_k$$

This means that since the velocity u' of large eddies is larger than the burning velocity s_L , these eddies will push the flame front around, causing a substantial corrugation. Conversely, the smallest eddies, having a turnover velocity u_k less than the burning velocity, will not wrinkle the flame front.

In order to identify the size of the eddy able to interact locally with the flame front, a brief recap about the Kolmogorov's 1941 theory on the universal range of turbulence has to be made. According to this hypothesis, there is a transfer from the energy containing eddies of the characteristic size of the integral length scale l_i to smaller and smaller eddies. This energy transfer per unit turnover time of the large eddies is equal to the viscous dissipation of energy ε at Kolmogorov scale and can be defined as the ratio between the kinetic energy of the turbulent flow at integral scale and the integral time scale τ_i :

$$\varepsilon = \frac{k}{\tau_i}$$

Since the kinetic energy and the velocity vector are

$$k = \frac{1}{2} \vec{u}^2$$

$$\vec{u} = u\vec{i} + v\vec{j} + w\vec{k}$$

but under the assumption of homogeneous and isotropic flow $u = v = w$, the kinetic energy can be written as

$$k = \frac{3}{2} u'^2.$$

Considering that the relation between integral time and length scale is

$$\tau_i = \frac{l_i}{u'},$$

the energy transfer rate is defined as

$$\varepsilon = \frac{u'^3}{l_i}.$$

In between the largest integral scale and the smallest Kolmogorov scale, there is the inertial range. In this range the energy transfer rate is constant and therefore the turnover time τ_n , the eddy length scale l_n and the velocity u_n are related as follows:

$$\varepsilon = \frac{u_n^2}{\tau_n} = \frac{u_n^3}{l_n} = \frac{l_n^2}{\tau_n^3}.$$

Coming back to the definition of the size of the eddy which interacts locally with the flame front, the Gibson scale has to be introduced. It is defined inside the inertial range when the turnover velocity u_n is set equal to the laminar burning speed s_L , as in the formula below:

$$l_G = \frac{s_L^3}{\varepsilon}$$

The Gibson scale is the size of burned pockets which move into the unburned mixture with velocity s_L . These pockets try to grow there due to the advance of the flame front normal to itself, but they are reduced in size again by the arriving eddies of size l_G with turnover velocity $u_n = s_L$, which penetrate into the burnt gas and are consumed by flame advancement. Therefore, the result is a kinematic equilibrium in the formation of these pockets. This mechanism is depicted in Figure 2.6. It is also possible to have a graphical

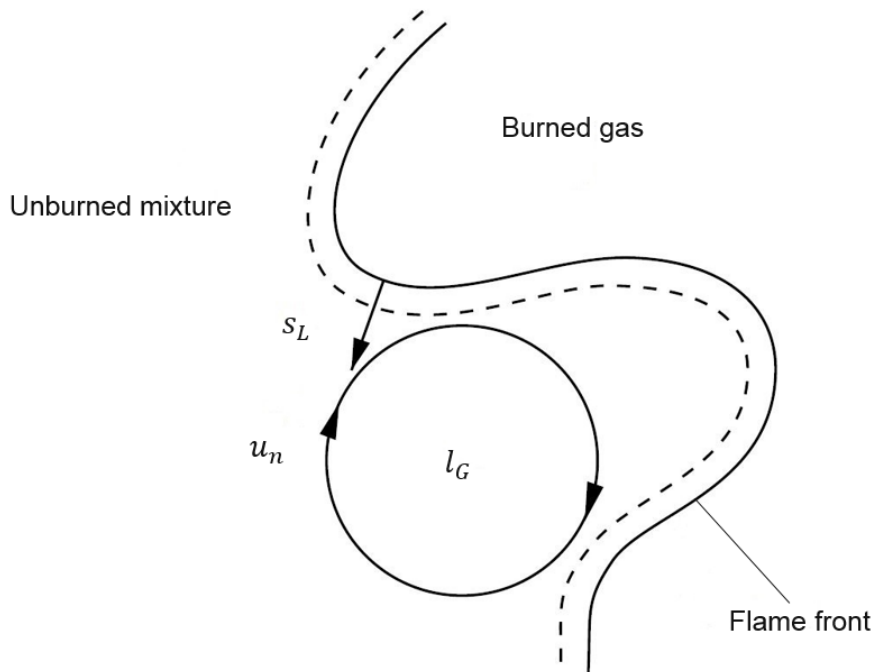


Figure 2.6: Kinematic interaction between the flame front and an eddy of the size of Gibson scale

representation of the Gibson scale l_G within the inertial range, thanks to the graph in Figure 2.7. In this picture, the logarithm of the velocity u_n is plotted versus the logarithm of the length scale l_n . Since the turnover velocity can be written as $u_n^3 = \varepsilon l_n$, the slope of the line is $1/3$ and the equation in logarithmic scale is

$$\log u_n = \frac{1}{3} \log l_n + \frac{1}{3} \log \varepsilon.$$

To proceed in the analysis, the assumptions of keeping constant u' , l_i , ε , u_k and l_k have to be made. If one enters on the vertical axis of the graph with equal to the burning

velocity s_L , one obtains l_G as the corresponding length scale on the horizontal axis. The laminar flame thickness δ_L is smaller than l_k in the corrugated flamelet regime. From this diagram the limits of the Gibson scale are highlighted. If the laminar burning velocity is equal to u' , l_G is equal to the integral length scale l_i ; this case corresponds to the borderline between corrugated and wrinkled flamelets in Figure 2.5. If s_L is equal to the Kolmogorov velocity u_k , l_G is equal to the Kolmogorov length scale l_k ; this corresponds to the line $Ka = 1$ in Figure 2.5. As a result, the Gibson length scale may vary between the Kolmogorov and the integral length scales in the corrugated flamelet regime.

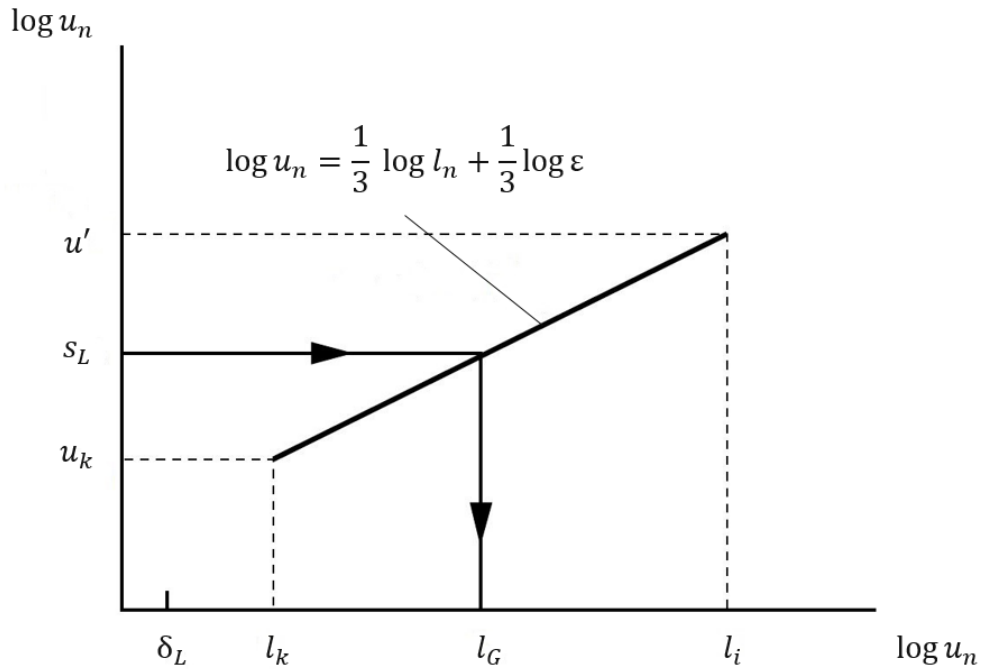


Figure 2.7: Gibson scale within the inertial range

The third regime of interest is the *thin reaction zones*. This regime corresponds to the area in between $Ka > 1$ and $Ka_\delta < 1$ in the Borghi plot of Figure 2.5. Using the definition of these two number, the thin reaction zone corresponds to the area where $l_k < \delta_L$, which means that the small eddies can enter the preheat layer and increase the scalar mixing, but since $l_k > l_\delta$ these eddies can not penetrate the inner layer. Moreover, in this regime the burning velocity is smaller than the Kolmogorov velocity which would lead to a Gibson scale that is smaller than l_k . Therefore the Gibson scale has no meaning within this regime.

In the case of laminar flames, the characteristic time is defines as the time that a flame needs to propagate across its own thickness

$$\tau_L = \frac{\delta_L}{s_L}.$$

In order to describe the interaction of the eddies with the reaction front, the mixing length

scale has to be introduced. It is obtained by setting $\tau_L = \tau_n$ in the equation of the energy transfer rate:

$$\varepsilon = \frac{u_n^2}{\tau_n} = \frac{u_n^3}{l_n} = \frac{l_n^2}{\tau_n^3}.$$

The results is the mixing length scale

$$l_M = \sqrt{\varepsilon \tau_L^3}.$$

This scale is defined as the size of an eddy within the inertial range which has a turnover time equal to the time needed to diffuse heat over a distance equal to the thickness δ_L . During half its turnover time an eddy of size l_M interacts with the advancing reaction front and transports preheated fluid from a region of thickness δ_L away from the reaction zone over a distance corresponding to its own size. This is what the Figure 2.8 shows. Much smaller eddies will also do this but since their size is smaller, their action will be masked by eddies of size l_M . Much larger eddies have a longer turn-over time and would therefore be able to transport thicker structures than those of thickness δ_L , namely of the thickness l_M across their own width. They will therefore corrugate the broadened flame structure at scales larger than l_M . The physical interpretation of the mixing length scale is therefore that of the maximum distance that preheated fluid can be transported ahead of the flame.

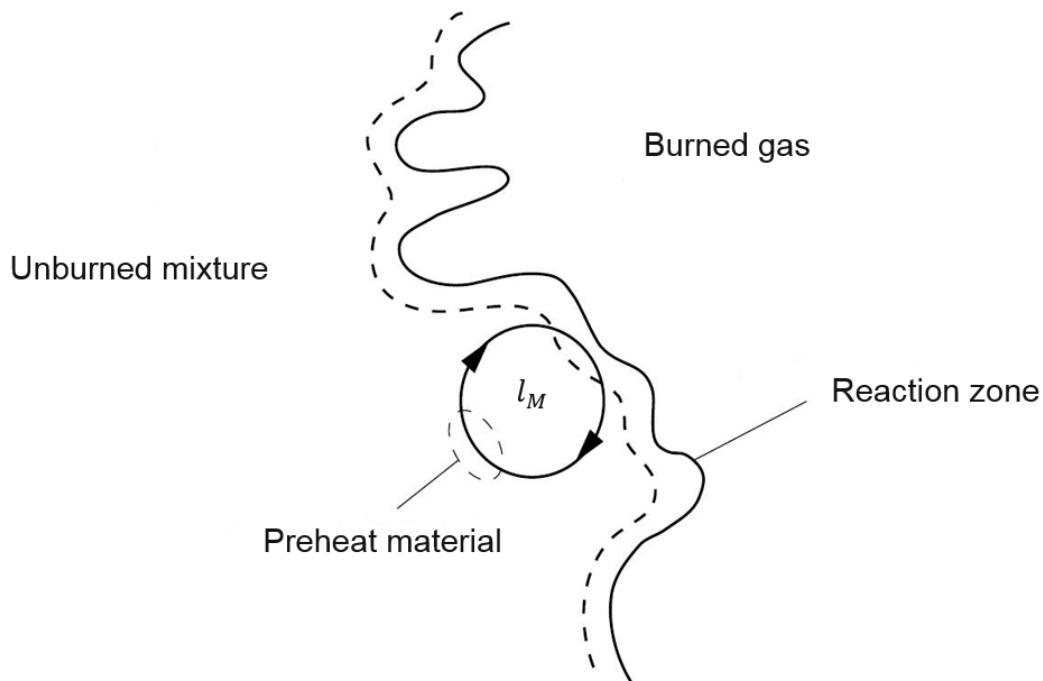


Figure 2.8: Transport of preheated material by an eddy of size l_m

Again, it is possible to evaluate the mixing length scale with the log-log graph in Figure 2.9, where the time scale is plotted versus the length scale. Since the length scale

can be written as $l_n^2 = \varepsilon \tau_n^3$, the slope of the line is $2/3$ and the equation in logarithmic scale is

$$\log \tau_n = \frac{2}{3} \log l_n - \frac{1}{3} \log \varepsilon.$$

If one enters the y-axis at $\tau_L = \tau_n$, the scale l_M on the length scale axis is obtained. It should be noted that all eddies having a size between l_k and l_M have a shorter turnover time than l_M and therefore are able to mix the scalar fields (like the temperature) in front of the thin reaction zones more rapidly. If τ_L is equal to the Kolmogorov time τ_k , l_M is equal to the Kolmogorov scale l_k . In this case, the result is $l_M = \delta_L$ which corresponds to the border between the thin reaction zones regime and the corrugated flamelet regime. Similarly, if the flame time τ_L is equal to the integral time τ_i , l_M is equal to the integral length scale l_i . This corresponds to $Da = 1$ which is also shown in Figure 2.5.

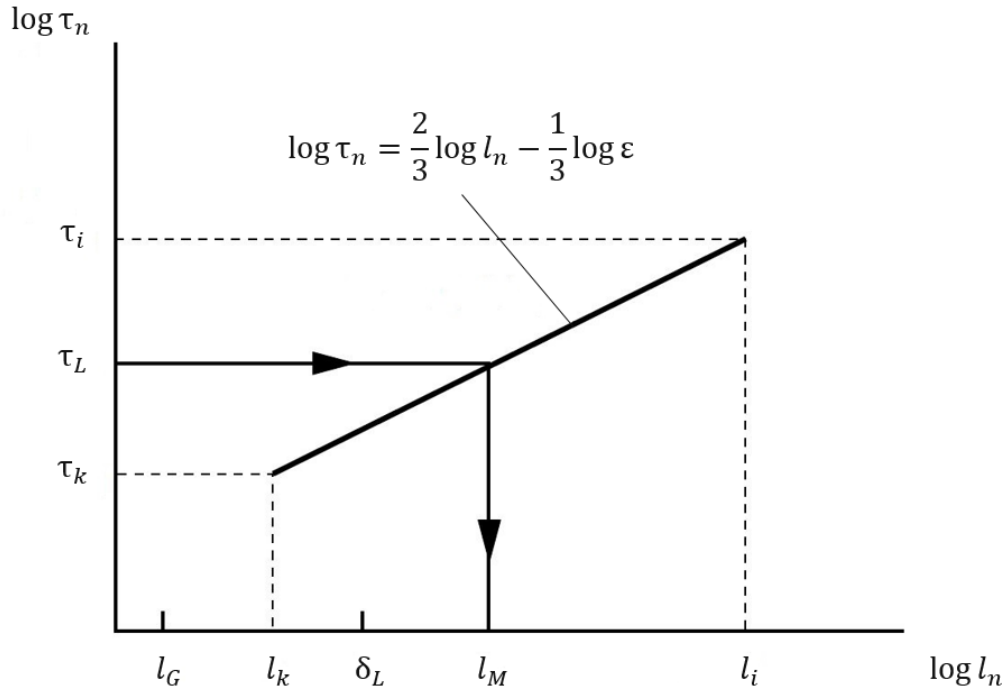


Figure 2.9: Mixing scale within the inertial range

The last turbulent regime to be analysed is the *broken reaction zones*. This area is characterised by $Ka_\delta > 1$, which means that the smallest eddies (at Kolmogorov scale) are smaller than the reaction zone thickness l_δ . As a consequence, they are able to enter the inner layer and perturb these zones until the reactions break down due to loss of radicals, thus leading to combustion extinguishment. The broken reaction zone corresponds to the slow chemistry condition.

Chapter 3

Simulation software GT-Power

3.1 The software

GT-SUITE, which includes the GT-POWER Engine Library, is the leading engine and vehicle simulation tool used by engine makers and suppliers. It is suitable for analysis of vehicle and engine performance, cooling, injection, lubrication, valvetrain, cranktrain and more. It is based on a 1-D fluid dynamics solver in which the three fluid dynamics equations (mass, momentum and energy conservation) are solved following a finite-differences method, i.e. a numerical method for solving differential equations by approximating them with difference equations, in which finite differences approximate the derivatives.

The software's aim is to generate an engine model representative of the real one. This task is performed using predefined templates for objects like the cylinder, the crankshaft, the valves, the turbocharger and the aftertreatment devices, while the geometry of the intake and exhaust systems is modelled with pipes and flowsplits. Thermal models are also used to impose temperatures for the head, piston and cylinder walls and to calculate the heat exchange; chemical models instead are helpful if the user want to add the reactions occurring in the cylinders during combustion or in the catalytic converters or DPFs.

3.2 Turbulence model

Turbulence inside the cylinder is an important flow condition which is generated via high shear flows that occur during the intake process, via high velocity injection sprays and by the destruction of macro-scale motions produced by tumbling and/or swirling structures close to top dead centre (TDC). Moreover, the turbulence level is responsible for different phenomena, such as the early flame kernel development, flame propagation and gas-to-wall heat transfer, which in the end are responsible for the engine output performance. Therefore a lot of effort, time and money have been spent (in the form of 3-D CFD

simulations) in order to properly describe what happens inside the cylinder: unfortunately the problem that the CFD approach shows is represented by the high computational power required. The solution has been found in zero dimensional (0D) phenomenological sub-models able to simulate the in-cylinder conditions in a faster and accurate way, even if calibration is required. In a 0D field, the in-cylinder flow models in the literature follow either a K-k energy cascade approach or a k- ϵ approach (where K is the mean kinetic energy, k represents the turbulent kinetic energy and ϵ corresponds to the turbulent dissipation rate). In the energy cascade method, the mean kinetic energy and turbulent kinetic energy are modelled via two differential equations and then algebraic equations are required to model the turbulence dissipation rate and integral length scale. In the k- ϵ method instead, the turbulent kinetic energy and its dissipation are modelled via two differential equations, while the integral length scale is obtained directly from k and ϵ without requiring any additional modelling. Both these methods show some problems: in the k- ϵ approach, the contribution of the mean kinetic energy K is imposed via algebraic closure and in the K-k models the integral length scale of turbulence is approximated by either relating it to cylinder volume or functional fitting together with tuning constants, which must then be tuned using 3D-CFD. To solve all these issues, a new 0D in-cylinder flow model has been developed by Gamma Technologies. This new approach combines the K-k and the k- ϵ models into a single one, which is therefore called K-k- ϵ model. With this solution, the equation of the mean kinetic energy K handles its decay to turbulence, thus eliminating the need for an arbitrary source term, and using one equation for the turbulent kinetic energy k and one for the dissipation rate ϵ it is possible in the end to calculate the integral length scale without the need for any other modelling.

The following section deals with all the governing equations of the model, which is fully described in the original document [4]. Since the knowledge of the physics behind this new approach is mandatory to understand and properly describe each involved phenomenon, the goal of this section is to highlight and explain each parameter involved in the modelling of the turbulent field inside the commercial code GT-Power. The K-k- ϵ 0D in-cylinder flow model describes the evolution of three different quantities:

- Mean kinetic energy $K = \frac{1}{2}U^2$ where U is the mean velocity of the flow inside the cylinder
- Turbulent kinetic energy $k = \frac{3}{2}u'^2$ where u' is the intensity of the turbulent field inside the cylinder (homogeneous and isotropic)
- Turbulent dissipation rate ϵ .

thanks to the three differential equations listed below.

$$\frac{d(mK)}{dt} = C_{in}(1 - \alpha_{in})E_{in} + K\dot{m}_{out} - P_k \quad (3.1)$$

$$\frac{d(mk)}{dt} = C_{in}\alpha_{in}E_{in} + k\dot{m}_{out} + P_k + C_{Tumb}T - m\epsilon \quad (3.2)$$

$$\frac{d(m\epsilon)}{dt} = C_{in}E_{in}\frac{\sqrt{k}}{L_g} + \epsilon\dot{m}_{out} + P_\epsilon + C_{Tumb}T\frac{\sqrt{k}}{L_g} - 1.92\frac{m\epsilon^2}{k} \quad (3.3)$$

Where

α_{in} = coefficient of inflow energy

m = incylinder mass

E_{in} = energy entering the cylinder

\dot{m}_{out} = mass flow rate exiting the cylinder

P_k = production of turbulent kinetic energy

P_ϵ = production of dissipation rate

T = production of turbulence due to the decay of tumble macro-vortex

L_g = geometric length scale

In the equations (3.1), (3.2) and (3.3) it is possible to see only the effect of two model parameters, C_{in} and C_{Tumb} , but since other two are involved, a detailed look at all the sub-models is necessary. In the following each term on the right hand-side of the three model equations is analysed:

- The first term evaluates the production of the related quantity due to the flow entering the cylinder. The entering energy is calculated as

$$E_{in} = (1 - C_T)\frac{1}{2}\dot{m}_{in}v_{in}^2$$

Where the mass flow rate \dot{m}_{in} , the isentropic velocity of the flow entering the cylinder v_{in} and the valve tumble coefficient C_T are present. The tumble coefficient describes the fraction of the incoming flow energy that is converted into tumble macro-vortex and it takes values from 0 to 1. In the formula of the geometric length scale L_g , the effect of the C_{len} model parameter is also visible:

$$L_g = C_{len}min(s, 0.5B)$$

Where s and B are the instantaneous piston stroke and the cylinder bore respectively. The aim of this model parameter, $C_{len} = 0.19 \cdot C_3$, is to modulate the value of the length scale. The coefficient α_{in} represents the fraction of the inflow energy that directly enters the cylinder as turbulence and it is not generated by the cascade

process; it models the turbulence generated as soon as the valves open causing high level of shear flow. The C_{in} model parameter takes into account the actual flow velocities through the valves, which are not equal to the isentropic values. Since C_{in} can be written as $C_{in} = 0.18 \cdot C_1$, we can use the tuning constant C_1 to adjust the magnitude of the inflow source term.

- The second term describes the energy flowing out of the valves.
- The third term corresponds to the production of either the turbulent kinetic energy or the dissipation rate. The governing equations are listed below

$$P_k = C_\beta \nu_T \frac{2mK}{L_g^2} - \frac{2}{3}mk \left(\frac{\dot{\rho}}{\rho} \right) - \frac{2}{3}m\nu_T \left(\frac{\dot{\rho}}{\rho} \right)^2 \quad (3.4)$$

$$P_\epsilon = \frac{\epsilon}{k} \left[5.76C_\beta \nu_T \frac{mK}{L_g^2} - 2mk \left(\frac{\dot{\rho}}{\rho} \right) - \frac{2.64}{3}m\nu_T \left(\frac{\dot{\rho}}{\rho} \right)^2 \right] \quad (3.5)$$

Where ν_T is the turbulent viscosity (which depends on the turbulent kinetic energy and the dissipation rate), ρ is the density of the charge inside the cylinder, ρ' is its rate of change and $C_\beta = 0.38 \cdot C_2$ is the last model parameter.

- The fourth model parameter controls the intensity of the production of turbulence due to the decay of the tumble macro-vortex during the compression. In this model, the tumble is modelled as a single macro-vortex which undergoes stretching and compression during the intake and compression and it is finally destroyed into turbulence. This process is described by the time evolution equation of angular momentum and its variation in time listed here

$$L = mr_t^2 \omega$$

$$\frac{dL}{dt} = \dot{L}_{in} + \dot{L}_{out} - Lf(s/B) \frac{\sqrt{k}}{r_t}$$

Where L_{in} is the tumble production of the incoming charge, L_{out} is related to the flow going out the cylinder, r_t is the radius of the macro-vortex, and $f(s/B)$ is the tumble decay function. In particular for what concerns the K-k- ϵ approach, the contribution of the tumble decay to turbulence is modelled with term

$$T = \frac{1}{2}L\omega f(s/B) \frac{\sqrt{k}}{r_t}$$

- The fifth term represents a sink term for that respective quantity. The mean kinetic energy is converted into turbulent kinetic energy via turbulent dissipation modelled by the term P_k , the turbulent kinetic energy is converted into heat via viscous dissipation $m\epsilon$ and the dissipation of the turbulent dissipation rate is given by the term $1.92m\epsilon^2/k$.

Finally, the evolution of the integral length scale of turbulence over time can be calculated, thanks to the knowledge of the turbulent kinetic energy and the dissipation rate ($C_\mu = 0.09$ is a standard k- ϵ model constant)

$$l = C_\mu^{3/4} \frac{k^{3/2}}{\epsilon}$$

As a conclusion, since the overall goal of this method is to properly describe the turbulence level inside the cylinder, a calibration procedure is required, acting on the following tuning parameters to match the 3D-CFD outputs:

- The intake term C_1 which describes the mean and the turbulent kinetic energies during inflow into the cylinder and therefore has an impact in the crank angle interval when the intake valve is open, thus during intake and compression due to late IVC
- The production term C_2 has an impact only on the production of turbulence from the mean flow
- The geometric length scale C_3 which directly affects the geometric length scale L_g . Since this length scale appears in every terms, the C_3 term has an impact over the entire crank angle interval
- The tumble term C_{Tumb} controls the contribution of the tumble decay to turbulence production and it has an impact only during compression.

For the sake of simplicity, the turbulence tuning parameters are listed in the table below.

Name	Parameter
Intake term	C_1
Production term	C_2
Geometric Length Scale term	C_3
Tumble term	C_4

Table 3.1: Turbulence parameters

The effects of each parameter can be visually represented using the plots of the turbulent kinetic energy and the normalised (with respect to teh cylinder bore) turbulent length scale, as function of the crank angle. The baseline configuration shown in the following graphs is represented by all the four turbulence terms set to the default value, which is equal to 1; then, for each plot, one parameter has been varied in a range from 1 to 4,

while keeping the other three equal to the default value, in order to evaluate the effect of each turbulence term separately. Moreover, each graph has been normalised with respect to the maximum overall value, so that the unit in y-axis is the fraction of the maximum, from 0 to 1.

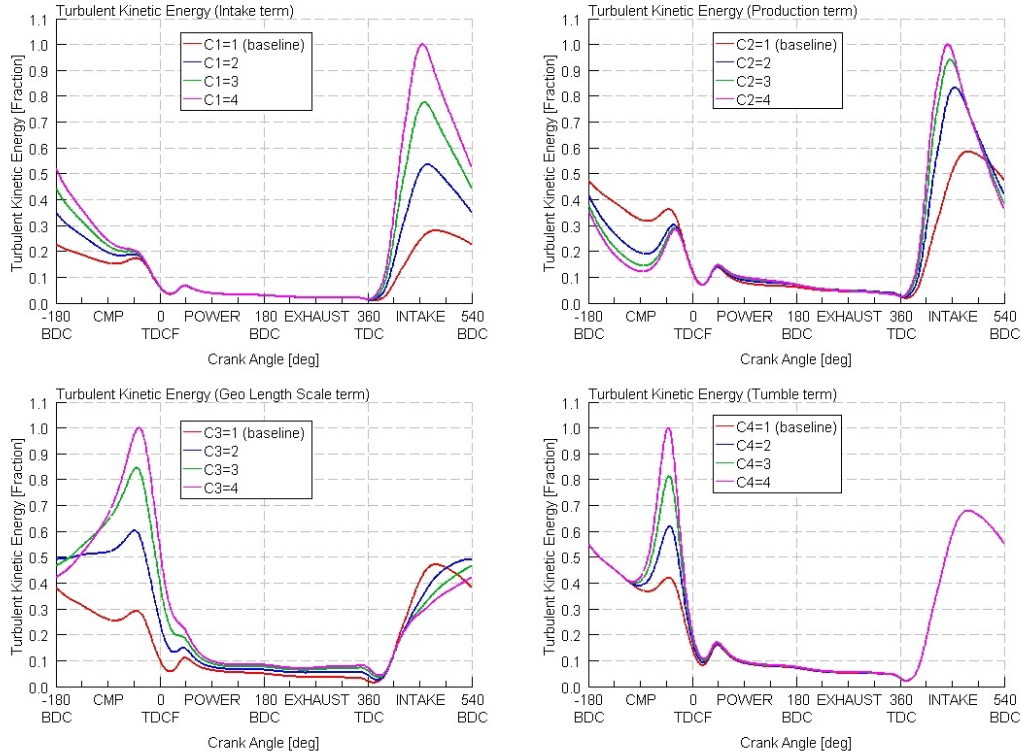


Figure 3.1: Turbulence parameters effect on TKE

3.3 Combustion model

The combustion process in GT-Power software follows the two-zone methodology, in which basically the evolution is the following:

- At the start of combustion SoC (at the spark in the SI engine), the cylinder is divided into two zones: the unburned and the burned zone. All of the contents of the cylinder at the SoC belong to the unburned zone, including residual gases from the previous cycle and EGR, if present.
- At each time step, a fuel and air mixture is transferred from the unburned zone to the burned zone. The amount of fuel-air mixture that is transferred to the burned zone is defined by the burn rate, which is imposed or calculated by the combustion model.

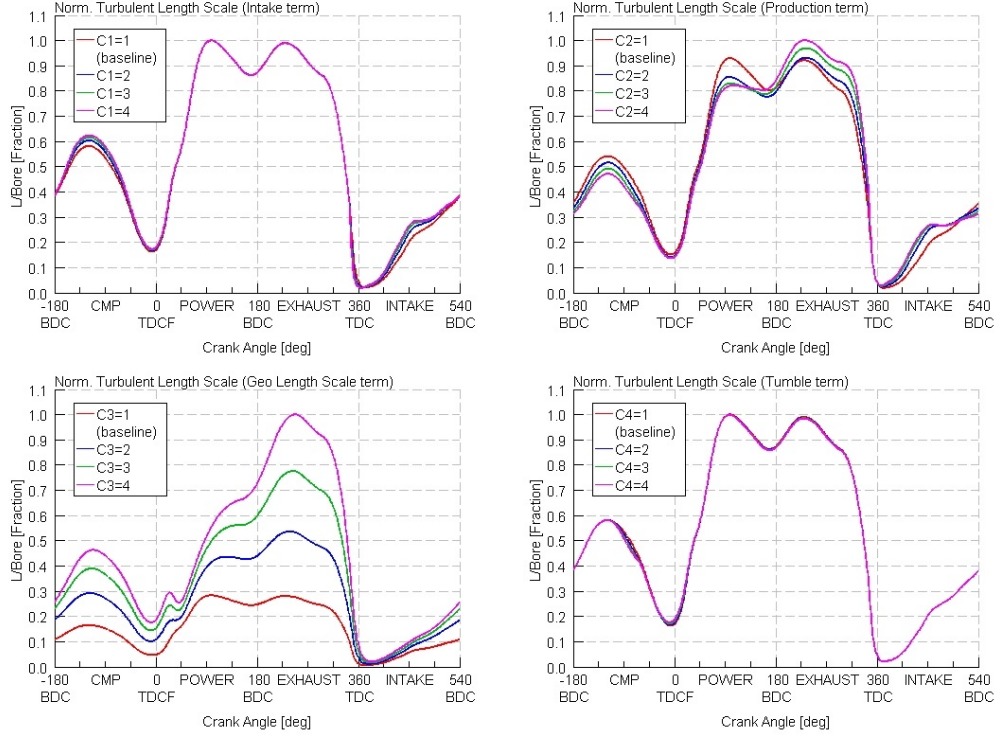


Figure 3.2: Turbulence parameters effect on Geometric Length Scale

- Once this mixture has been transferred from the unburned zone to the burned zone in a given time step, a chemical equilibrium calculation is carried out for the entire "lumped" burned zone. This calculation takes into account all of the atoms of each species (C, H, O, N, S, Ar) present in the burned zone at that time, and obtains from these an equilibrium concentration of the 13 products of combustion species (N_2 , O_2 , H_2O , CO_2 , CO , H_2 , N , O , H , NO , OH , SO_2 , Ar). The equilibrium concentrations of the species depend strongly on the current burned zone temperature and to a lesser degree, the pressure.
- Once the new composition of the burned zone has been obtained, the internal energy of each species is calculated. Then, the energy of the whole burned zone is obtained by summation over all of the species. Applying the principle of the conservation of energy, the new unburned and burned zone temperatures and cylinder pressure are obtained.

In the two zone model, the following energy equations are solved in each time step:

$$\frac{d(m_u e_u)}{dt} = -p \frac{dV_u}{dt} - Q_u + \left(\frac{dm_f}{dt} h_f + \frac{dm_a}{dt} h_a \right) + \frac{dm_{f,i}}{dt} h_{f,i} \quad (3.6)$$

$$\frac{d(m_b e_b)}{dt} = -p \frac{dV_b}{dt} - Q_b - \left(\frac{dm_f}{dt} h_f + \frac{dm_a}{dt} h_a \right) \quad (3.7)$$

Where

m_u = unburned zone mass

m_b = burned zone mass

m_f = fuel mass

m_a = air mass

$m_{f,i}$ = injected fuel mass

e_u = unburned zone energy

e_b = burned zone energy

p = cylinder pressure

V_u = unburned zone volume

V_b = burned zone volume

Q_u = unburned zone heat transfer rate

Q_b = burned zone heat transfer rate

h_f = enthalpy of fuel mass

h_a = enthalpy of air mass

$h_{f,i}$ = enthalpy of injected fuel mass

Equation 3.6 refers to the unburned zone while equation 3.7 to the burned one. On the right hand side of these equations, three terms related to pressure work, heat transfer and combustion are present, while only the unburned zone equation contains the fourth term about the addition of enthalpy from injected fuel.

3.3.1 Predictive vs Non-Predictive combustion

All the combustion models in GT-Power, except some cases, follow the two-zone approach but an important distinction has to be made between predictive, non-predictive and semi-predictive models, because the choice depends on simulation intent. A non-predictive combustion model simply imposes a burn rate as a function of crank angle regardless of the conditions in the cylinder, assuming that there is sufficient fuel available in the cylinder to support the burn rate. With the term “burn rate” we refer to the rate at which fuel and air molecules are transferred from the unburned to the burned gas region and begin to participate in the chemical reactions. Non-predictive models show the advantage that the calculation time is low but they are useful only when the variable to be studied has no impact on burn rate; for instance, this represents a huge drawback when the influence of the injection timing has to be assessed. Therefore when the variable to be studied has a real impact on burn rate, the most adequate solution is the adoption of predictive models: they are able to predict the burn rate, automatically adjusting to different conditions (rpm, EGR, etc.) with no changes required in the model inputs. However the drawbacks

that come with this type of models are represented by the increased calculation time and complexity and the need for a precise calibration. A semi-predictive combustion model may be a good substitute for a predictive model in some cases. This model is sensitive to the significant variables that influence combustion rate and responds appropriately to changes in those variables, but does not use any physical models to predict that response. Instead, these models utilize a non-predictive (Wiebe) methodology where the combustion burn rate is imposed, with lookups or other methods to calculate the proper Wiebe parameters based on the significant input variables.

Non-Predictive models

Inside the software GT-Power, there are a lot of possibilities to implement a non-predictive combustion model. The first option is to impose a burn rate profile directly as a function of crank angle: this task is performed with the "EngCylCombProfile" template. It is particularly useful if the cylinder pressure from the engine has been measured in the test bench because the burn rate can be calculated from the cylinder pressure. Calculating a burn rate from measured cylinder pressure is sometimes referred to as a "reverse run", because the inputs and outputs of the calculation are reversed from the typical combustion calculations in engine simulation. In a "forward run", the burn rate is the input and the cylinder pressure is the result. In a reverse run, the cylinder pressure is the input and the burn rate is the result. They both perform the calculation using the same equations of the Two-Zone Combustion model, described in Section 3.3.

The burn rate calculation can be performed directly in the software following one of the two proposed methods. The first method, called 'Stand-Alone Burn Rate Calculation', can be performed with only the measured cylinder pressure (from a single cycle or an assemble average), a few basic cycle average results (volumetric efficiency, cylinder trapping ratio and residual fraction etc.) and engine cylinder geometry. A very simple model should be built that need only include the EngCylinder and EngineCrankTrain (and an injector for DI diesel or GDI applications). The cylinder pressure is used as an input in the EngCylinder Object and the Cylinder Pressure Analysis Mode is set to "Measured CylP only". The simulation will run as follows: at beginning of a cycle, a rough calculation of combustion burn rate is done making some assumptions about heat transfer (Woschni model); the resulting burn rate is applied during the forward simulation cycle and the true heat transfer rate is stored; a final burn rate calculation is done with the true heat transfer from the simulation and all results stored; the final burn rate is applied during the forward simulation cycle in order to provide a comparison of measurement versus simulation. The advantage of this method is represented by the low calculation time and by the single input required (cylinder pressure); however, it shows the disadvantage of

requiring the estimation of certain input parameters that are difficult or impossible to measure in the test like the cylinder trapping ratio or the residual fraction.

The second approach is called Three Pressure Analysis Burn Rate Calculation (TPA), because as the name suggests three input pressures are necessary: intake, cylinder and exhaust. For this analysis, no estimation of the residual fraction and trapping ratio are needed as inputs. This approach requires an engine model including valves and ports at a minimum. The simulation is run for multiple cycles until the model has converged (if applicable). As a result, the trapping ratio and residual fraction (and other trapped quantities) will be calculated, which is why they are not needed as inputs. As for the first method, the cylinder pressure is inserted as an input, while the Cylinder Pressure Analysis Mode is set to "TPA". The simulation methodology is the following: for the first cycle, a dummy burn rate is used and no pressure analysis is performed; for the second cycle and beyond, the forward run simulation will "pause" at the start of each cycle and calculate the apparent burn rate using the trapped conditions in the cylinder at that point (typically IVC) along with the measured pressure profile; the forward simulation run continues and the apparent burn rate calculated in the previous step is imposed during the cycle; then cycles repeat until steady state convergence is reached. The main benefit of this method is that all of the cylinder trapped quantities are predicted by the simulation. However for these quantities to be accurate, the flow characteristics of the model must be accurate. The obvious drawback is represented by the additional measurements required (instantaneous intake and exhaust pressures).

The second option available in the software to impose a burn rate profile is the use of a Wiebe function, which repeats the typical shape of an SI burn rate. This model is able to implement a reasonable burn rate if measured cylinder pressure is not available. If cylinder pressure has been measured, it is recommended to perform a reverse run calculation and to use the resulting "EngCylCombProfile" to provide a more accurate burn rate. The inputs of the Wiebe model are:

- AA = Anchor Angle (usually 50%)
- D = Duration (usually 10-90%)
- E = Wiebe Exponent
- CE = Fraction of Fuel Burned (or Combustion Efficiency)
- BM = Burned Fuel Percentage at Anchor Angle
- BS = Burned Fuel Percentage at Duration Start (usually 10%)
- BE = Burned Fuel Percentage at Duration End (usually 90%)

The governing equations of the Wiebe model are as follows: BMC is the Burned Midpoint Constant, BSC is the Burned Start Constant, BEC is the Burned End Constant, WC is the Wiebe Constant and SOC is the Start of Combustion.

$$\begin{aligned}
 BMC &= -\ln(1 - BM) \\
 BSC &= -\ln(1 - BS) \\
 BEC &= -\ln(1 - BE) \\
 WC &= \left[\frac{D}{BEC^{\frac{1}{E+1}} - BSC^{\frac{1}{E+1}}} \right]^{-(E+1)} \\
 SOC &= AA - \frac{(D)(BMC)^{\frac{1}{E+1}}}{BEC^{\frac{1}{E+1}} - BSC^{\frac{1}{E+1}}}
 \end{aligned}$$

Then the cumulative burn rate, normalised to 1, can be calculated with the formula below, where θ represents the instantaneous crank angle.

$$Combustion(\theta) = (CE) \left[1 - e^{-(WC)(\theta - SOC)^{(E+1)}} \right]$$

The combustion process starts at 0% fraction burned and continues till the values specified in the 'Fraction of Fuel Burned Attribute', typically 100%.

Predictive models

Among the different choices available in the GT-Power code, the predictive combustion model which is described and analysed in this project is the Spark-Ignition Turbulent Flame Model ('EngCylCombSITurb'). This approach predicts the burn rate for homogeneous charge, spark-ignition engines and requires the cylinder's geometry, spark locations and timing, air motion, and fuel properties as model inputs. The full details can be found in [5] and [3]. The governing equations are the following:

$$\frac{dM_e}{dt} = \rho_u A_e (S_T + S_L) \quad (3.8)$$

$$\frac{dM_b}{dt} = \frac{(M_e - M_b)}{\tau} \quad (3.9)$$

Where

M_e = entrained mass of the unburned mixture

M_b = burned mass

ρ_u = unburned density

A_e = entrainment surface area at the edge of the flame front

S_T = turbulent flame speed

S_L = laminar flame speed

τ = time constant

The first equation states that the unburned mixture of fuel and air is entrained into the flame front through the flame area at a rate proportional to the sum of the turbulent and laminar flame speeds. Since the gas entrainment is limited by the laminar flame speed during the first flame kernel development phase, the equation of the turbulent flame should be able to describe the transition between laminar and flame speed. In this equation (where R_f is the flame radius, u' the turbulent intensity and L_t the turbulent length scale)

$$S_T = C_s u' \left(1 - \frac{1}{1 + \frac{C_k R_f^2}{L_t^2}} \right)$$

the Flame Kernel Growth multiplier (C_k) in fact scales the flame front evolution from an initial smooth surface (corresponding to a complete laminar combustion) to a fully developed turbulent wrinkled flame and the Turbulent Flame Speed multiplier (C_s) is a scaling factor for the turbulent flame speed.

The second equation instead explains that the burn rate is proportional to the amount of unburned mixture behind the flame front, ($M_e - M_b$), divided by a time constant, τ . This time constant is defined as the time needed by the laminar flame speed to cover the Taylor microscale λ ; assuming isotropic turbulence, the equation of both time e length scale are listed below (C_λ is a further calibration parameter, called Taylor Length Scale multiplier)

$$\tau = \frac{\lambda}{S_L}$$

$$\lambda = \frac{C_\lambda L_t}{\sqrt{Re_t}} \quad \text{where} \quad Re_t = \frac{\rho_u u' L_t}{\mu}$$

The last effect that has to be considered is the one that the dilution (residuals and EGR) has on the laminar flame speed: this is possible thanks to the fourth combustion parameter, i.e. the Dilution Effect multiplier (DEM). The equation of the laminar flame speed becomes

$$S_L = (B_m + B_\phi (\phi - \phi_m)^2) \left(\frac{T_u}{T_0} \right)^\alpha \left(\frac{p}{p_0} \right)^\beta (1 - 2.06 Dilution^{0.77 DEM})$$

Where

B_m = maximum laminar speed

B_ϕ = laminar speed roll-off value

ϕ = in-cylinder equivalence ratio

ϕ_m = equivalence ratio at maximum speed

T_u = unburned gas temperature

$T_0 = 298$ K

$p =$ pressure

$p_0 = 101325$ Pa

$\alpha =$ temperature exponent

$\beta =$ pressure exponent

Dilution = residuals mass fraction in the unburned zone

DEM = dilution effect multiplier

As a conclusion, all the physics behind the combustion process is described in GT-Power with these four model parameters, which require a fine calibration in order to catch exactly the evolution of the physical phenomenon. They are listed in a summary Table 3.2 below.

Name	Parameter
Flame Kernel Growth multiplier	C_k
Turbulent Flame Speed multiplier	C_s
Taylor Length Scale multiplier	C_λ
Dilution Effect multiplier	<i>DEM</i>

Table 3.2: Combustion multipliers

Chapter 4

Experimental set-up

All the simulation work that will be described in this thesis has been based on the experimental tests performed on two different engines. Both of them are a 4 cylinder turbo-charged petrol engine and in particular one represents the development build of the other: from now on, we will refer to the previous engine version as *Engine A* and to the new one as *Engine B*. This chapter will focus on the description of each particular engine build and of the experimental data set available.

4.1 Engine A

The original version is a Gasoline Direct Injection (GDI) turbo-charged 2.0 litre SI engine equipped with Variable Valve Actuation (VVA), whose main characteristics are reported in Table 4.1:

N of cylinder/Layout	4/In line
Displacement	2.0 [l]
Injection	GDI
Turbocharger	Twin-scroll turbine
Intake	VVT and VVL
Exhaust	VVT
Compression ratio	9.5 : 1
Exhaust Gas Recirculation	no

Table 4.1: Engine A characteristics

For what concerns the operating conditions which have been tested in the test rig, all points at full load from 1000 rpm to 5500 rpm with 500 rpm steps have been recorded, as depicted in Figure 4.1. On the x-axis of the graph the engine speed expressed in rpm is

reported, while the y-axis shows the engine load as a percentage of the maximum value of the brake mean effective pressure (bmep).

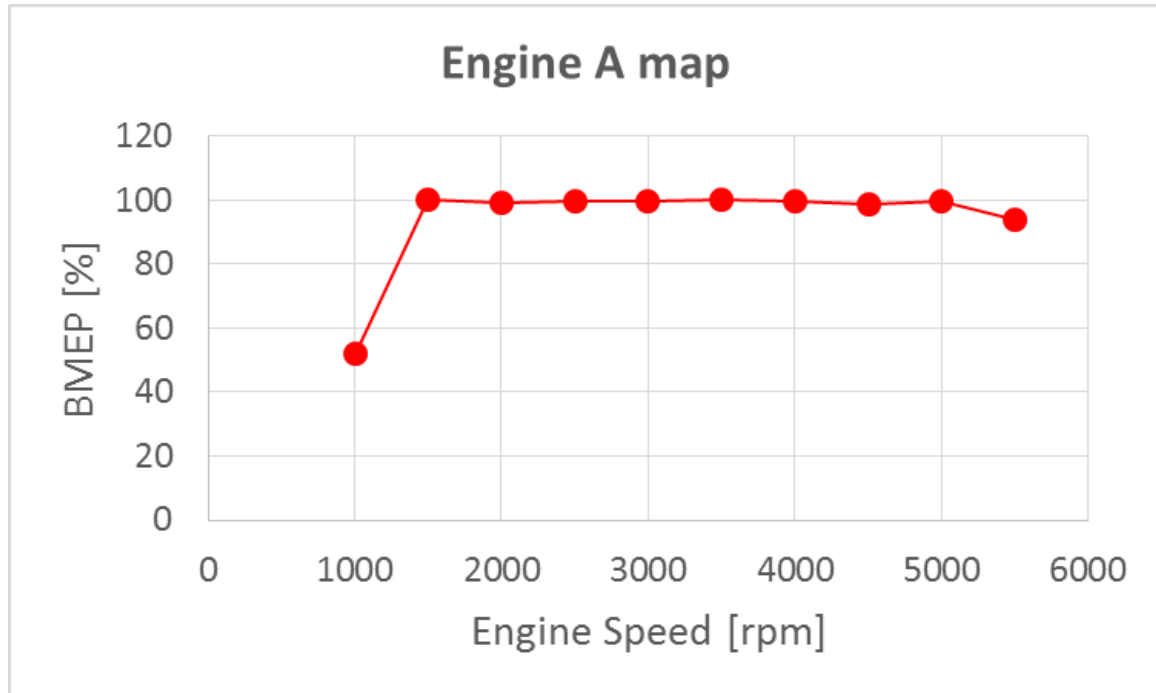


Figure 4.1: Engine A map

4.2 Engine B

The updated engine version still shows the same main characteristics of the Engine A, but some changes to the combustion, intake and boosting systems have been applied. The combustion chamber is different because new piston and head design have been used, which in the end corresponds to an higher compression ratio. Moreover, the addition of Exhaust Gas Recirculation (EGR) system is present in Engine B: the choice is a low pressure (long route) EGR combined with a EGR cooler; with this solution, combustion temperature is reduced, improving the knock limit and therefore higher CR can be adopted, thus improving engine efficiency and brake specific consumption. For what concerns the boosting system, the Engine B uses a twin-scroll turbine as the previous one but in addition it features an electrical supercharger, which is active up to the knee point at 1750 rpm. All the changes and the main characteristics of the new engine version are listed in Table 4.2.

The data set of the engine operating conditions is made of four point at full load: two test cases correspond to low engine speed and the other two to high engine speed. Figure 4.2 shows the same axes as Figure 4.1.

N of cylinder/Layout	4/In line
Displacement	2.0 [l]
Injection	GDI
Turbocharger	Twin-scroll turbine + Electrical Supercharger
Intake	VVT and VVL
Exhaust	VVT
Compression ratio	12.5 : 1
Exhaust Gas Recirculation	Low Pressure LP EGR

Table 4.2: Engine B characteristics

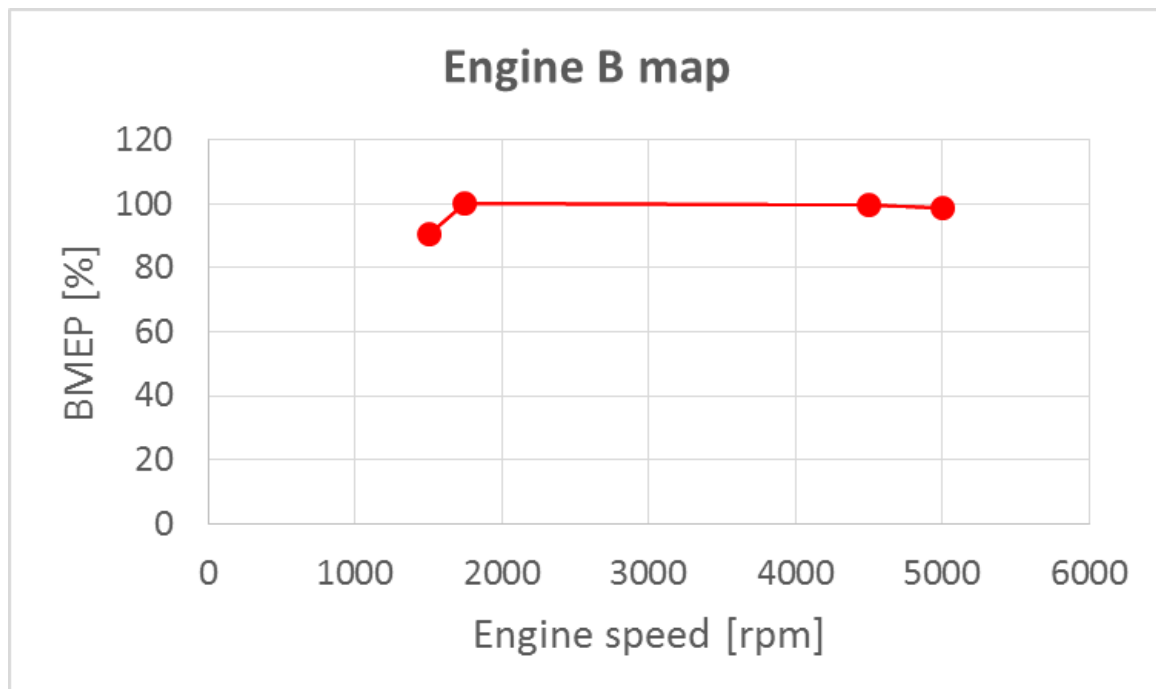


Figure 4.2: Engine B map

Chapter 5

Predictive model SI-Turb

The theoretical concepts which are the fundamentals of this project will be now applied to the two engines described in the previous chapter. The calibration of the predictive combustion had already been performed on *Engine A*, following the detailed procedure describe in the GT-Power manual [3]. It will be then followed and modified where needed to calibrate the model for the *Engine B*, in order to assess the predictive capability of this tool. The SI-Turb calibration process is made of five different steps:

- A model creation and validation, using a non-predictive combustion mode (usually Wiebe function), is required at the beginning in order to evaluate the inputs to run the CFD simulation for the turbulence level inside the cylinder. An important remark has to be highlighted here: this non-predictive model represents the starting point of the calibration process and therefore the level of fidelity required is very high; the model has to be able to fully replicate the test measurements from the gas path and engine performance point of view. In fact, the engine model with imposed combustion will be used to build the predictive one, by changing the combustion object and by adding the turbulence model.
- The calibration of the four turbulence parameters can be performed by matching the turbulent kinetic energy, normalised turbulent length scale and tumble number from GT-Power with the ones from CFD simulation. This step can be performed both with a simplified and faster single cylinder model with combustion analysis mode set to Three Pressure Analysis (TPA) or with the detailed multi-cylinder model with imposed combustion (for instance, using Wiebe function).
- The initial in-cylinder conditions evaluation is then performed using a single cylinder model and running a Three Pressure Analysis (TPA) or using the outputs from the detailed engine model with imposed combustion.

- The combustion calibration step is carried out at this point: the Advanced Direct Optimizer inside the GT-Power software makes a comparison between the burn rate from test and SITurb model and by minimising its RMSE it calculates the four optimised combustion multipliers.
- At the end, the full engine model is run with SITurb combustion model and its predictive capabilities can be assessed.

All this calibration procedure has been summarised in the Figure 5.1 below.

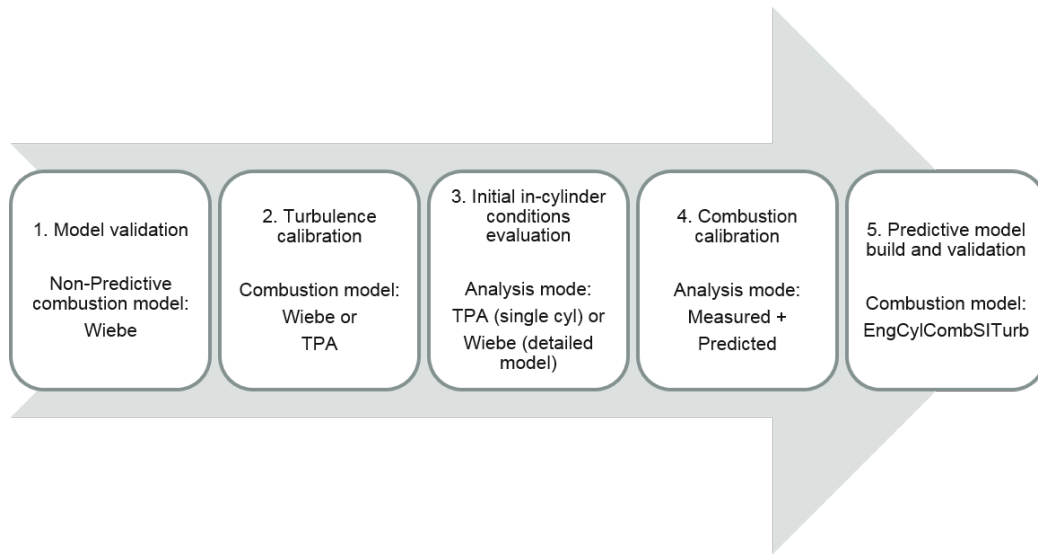


Figure 5.1: SI-Turb calibration procedure

For what concerns the model requirements, the predictive combustion model SITurb relies on measurement data, on turbulence measurements from 3D CFD and on geometrical description of the combustion chamber. The experimental set-up needed for an optimal correlation is represented in Figure 5.2, which corresponds to an ideal scenario and has no physical link with any of the engines used for this project. A minimum of 25 operating points spread over entire normal operating range (speed, load, valve timing, spark timing, internal or external EGR etc.) is needed. This set is represented in the graph by the red dots: the ones connected with the solid lines correspond to full load condition, while the others to part load. On top of these 25 calibration points, a large validation data set is required to evaluate the predictive capability of the model once it has been calibrated; the validation points are represented by the blue dots. An other important requirement is the 3D CFD analysis, whose outputs are useful to perform the turbulence calibration of the simplified 0D K-k- ϵ model inside GT-Power. In the end, the last requirement is the 3D combustion chamber description: head and piston STL files plus the spark plug location are needed to calculate convective heat transfer, in order to predict the burn rate.

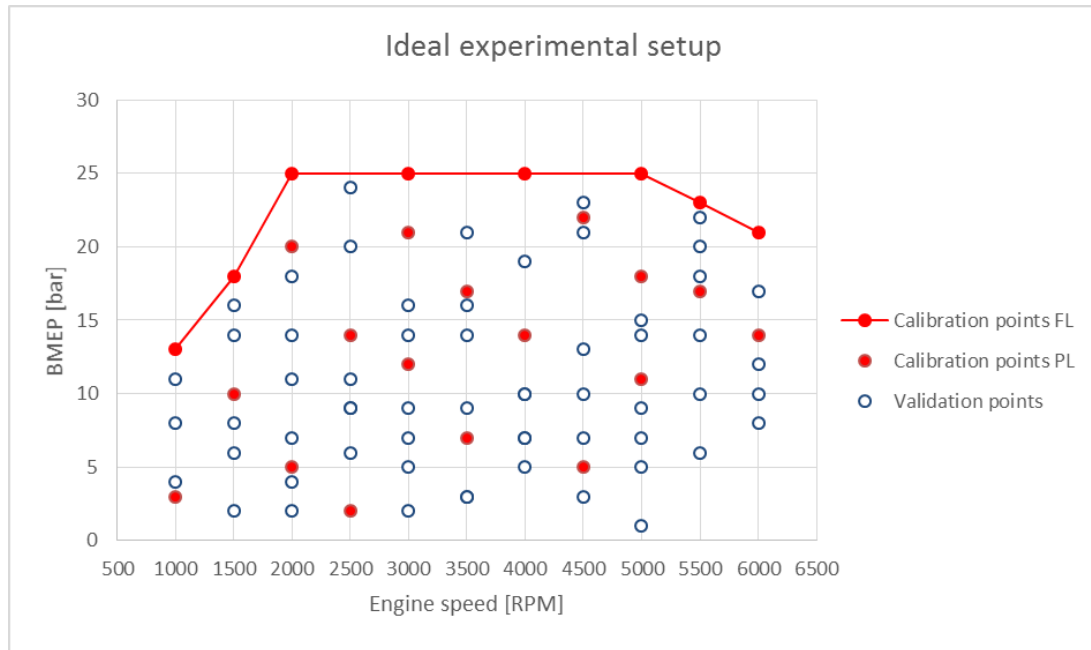


Figure 5.2: Ideal experimental setup

Since this procedure has been already applied to an existing engine version and as a consequence the turbulence and combustion calibrations are well established, the subsequent and obvious step is the evaluation of the model capability to adapt to a new engine, in which some geometrical changes have been made. The engine selected to apply the available calibration on is the *Engine B*, which represents the new model year version of the *Engine A*. From now on, the operation of applying a previous calibration on a newer engine build will be referred as "calibration transplant". As a summary, this chapter deals with the description of the project plan, following these steps:

1. Original predictive calibration on *Engine A*.
2. *Engine B* GT-Power model validation with non-predictive combustion.
3. Calibration transplant from *Engine A* to *Engine B*.
4. Calibration process for *Engine B*.

5.1 Engine A calibration

The setup of predictive combustion model SITurb has been performed for the *Engine A* following the procedure described before. In this section, all the results previously obtained will be summarised. What is described in this section represents the starting point for the assessment of the predictive capability of the SITurb tool and therefore the understanding of it is fundamental.

The turbulence calibration has been developed using the output of the CFD simulations which at that time were available. This means that the following operating points were considered:

- Low engine speed, low load case: 1500 rpm and 28% bmep.
- High engine speed, full load case: 5500 rpm and 100% bmep.

The turbulence calibration was then performed, trying to find a single set of parameters to best describe both cases. The procedure followed to find this single set was a trial and error method, which then allows the user to setup the "Flow Object" in the "Cylinder Object" of the GT-Power engine model. For sake of confidentiality, the values of the four turbulence parameters can not be shown. The results, in terms of turbulent kinetic energy, normalised turbulent length scale and tumble number plots, for both cases under study are shown in Figures 5.3 and 5.4. Also in this case, all the graphs have been normalised with respect to the maximum value, so that the y-axis shows the fraction and not the actual value. The turbulence level has the highest impact on the evolution of the combustion process in the crank angle interval immediately before the power stroke. Therefore the calibration procedure is performed in order to obtain a good match with CFD results focusing just at the end of the compression stroke. As it is possible to see from the graphs above, a single set of parameters is not able to properly describe both the low and the high rpm cases: as a consequence the high load high rpm case has been prioritised. This means that the description of the turbulent level inside the cylinder is satisfying at high rpm full load, while an overestimation at low load low rpm is obtained.

The combustion calibration step has been performed using the Direct Optimiser in GT-Power, which calculates four optimised combustion parameters by minimising the RMSE (Root Mean Square Error) between the burn rate from test and SITurb model. After some sensitivity analysis, it has been seen that the Turbulent Flame Speed multiplier (TFSm) shows the highest impact: therefore it has been chosen to vary this parameter with engine speed, while keeping all the others constant. This choice leads to a better result in terms of comparison with the measurement data, but it shows the drawback of reducing the model predictive capability: the goal of the SITurb combustion model is in fact to find a single set of parameters able to describe the entire engine map as the best trade-off, in order to be predictive in a wide area of operating points as much as possible. Moreover, the optimised combustion parameters have been maintained equal for all the cylinders, because it has been evaluated that the in-cylinder conditions are not too different from cylinder 1 to 4. The results of this calibration, in terms of the four combustion parameters described in Section 3.3, are shown in the Figure 5.5 and 5.6. In these plots the parameters have been normalised with respect to their typical value

inside the recommended range. The final achievement which is possible to obtain with the calibration of the predictive combustion model SI-Turb is shown in Figure 5.7 and 5.8. In these plots, the pressure and the burn rate trends are shown for four out of the ten operating points which have been tested. The selected conditions are: 1000 rpm and 52% bmep, 2500 rpm and 100% bmep, 4000 rpm and 100% bmep and 5500 rpm and 94% bmep. The engine load is expressed as a percentage of the maximum value the *Engine A* is able to achieve. Moreover, in each plot a comparison between the SI-Turb predictive combustion model (red curve), the imposed Wiebe combustion model (blue curve) and the measurement data (green curve) is made. As it is possible to see, the predictive model achieves a satisfying correlation with test data and it is almost able to replicate the results of the imposed Wiebe combustion model.

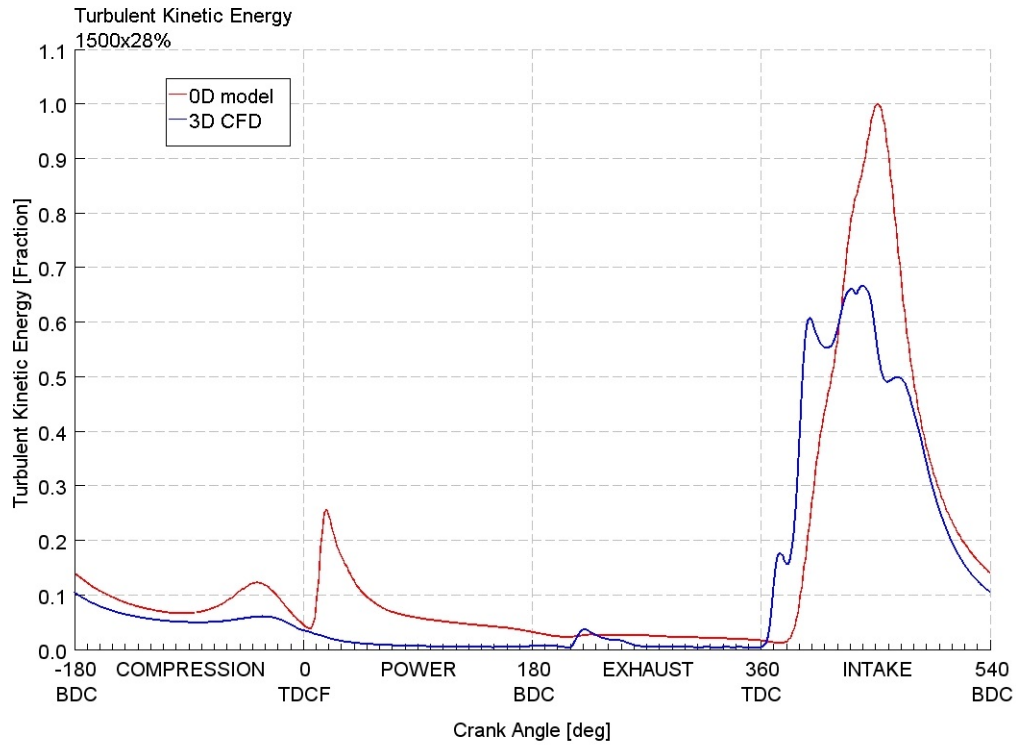


Figure 5.3: Engine A Turbulent Kinetic Energy 1500 rpm 28% bmep

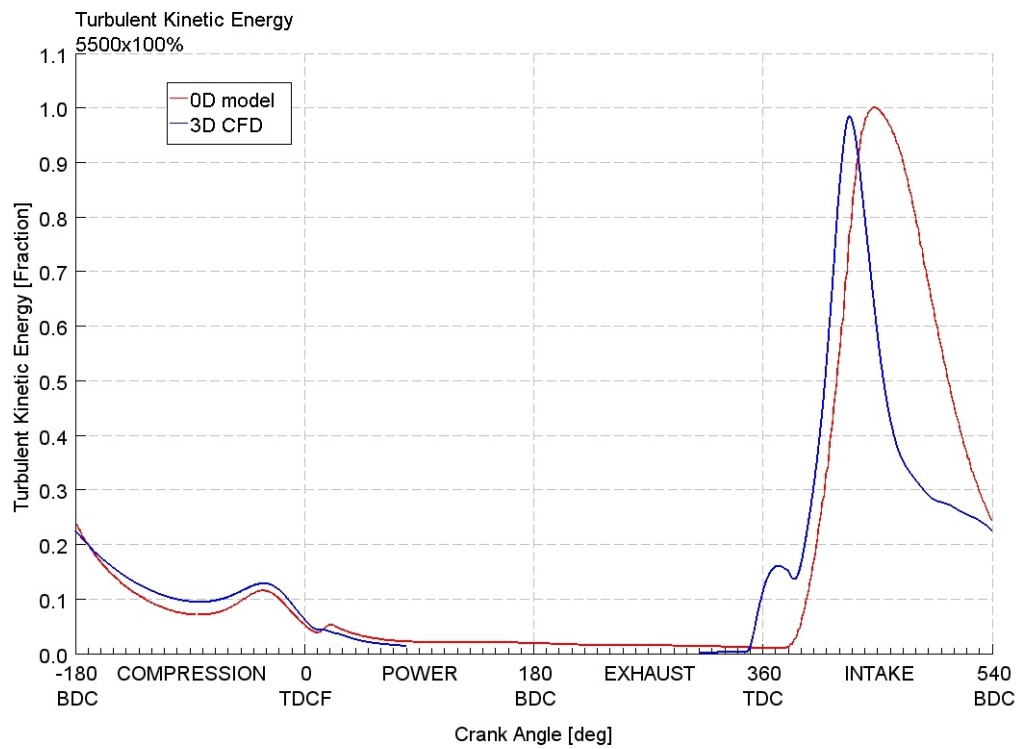


Figure 5.4: Engine A Turbulent Kinetic Energy 5500 rpm 100% bmep

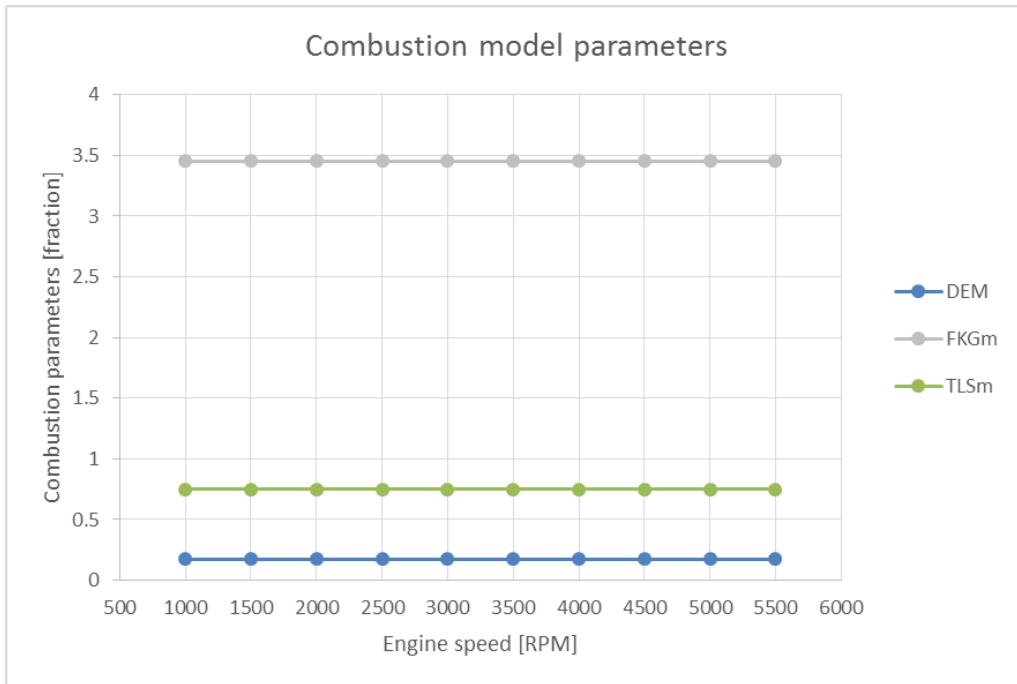


Figure 5.5: Fixed combustion parameters for Engine A

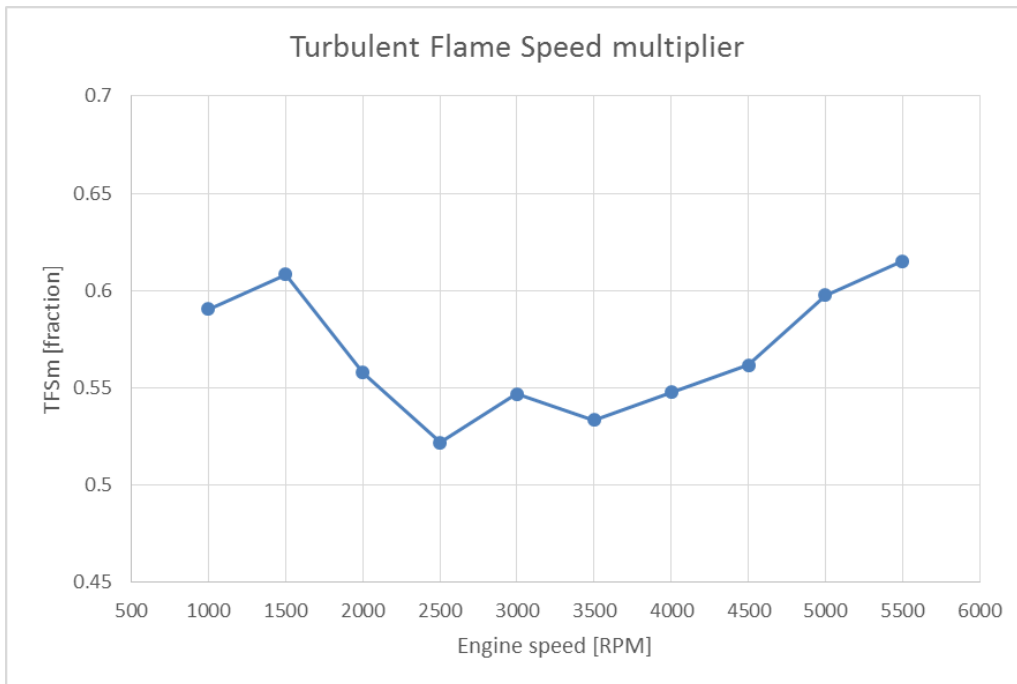


Figure 5.6: Variable combustion parameter for Engine A

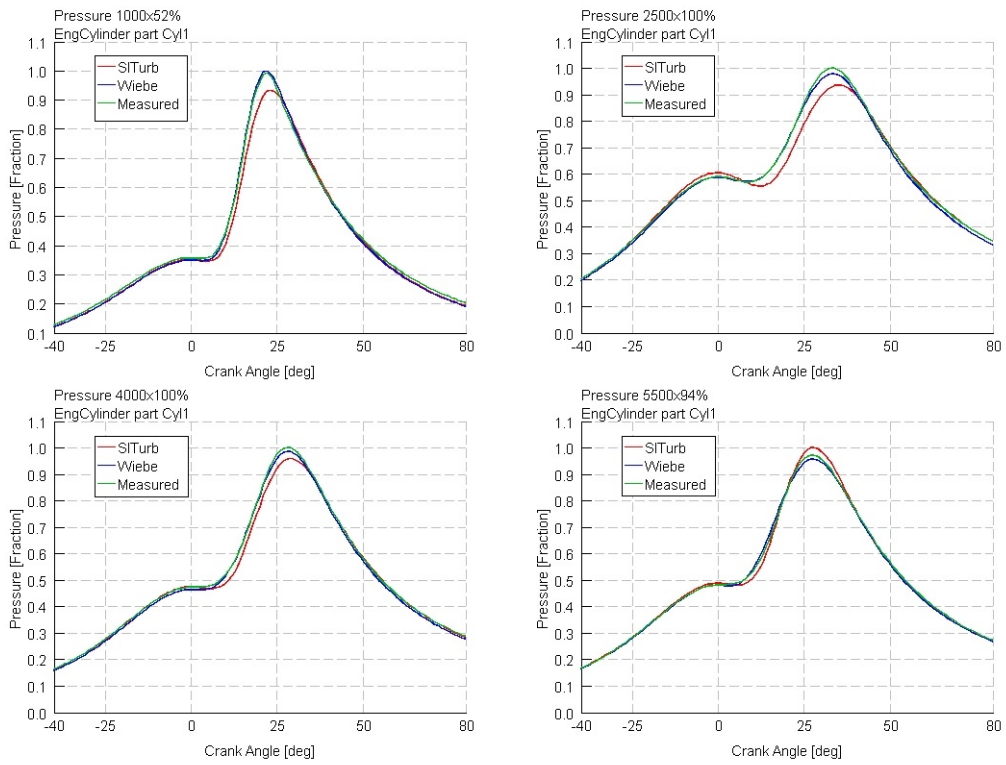


Figure 5.7: Engine A pressure trend comparison

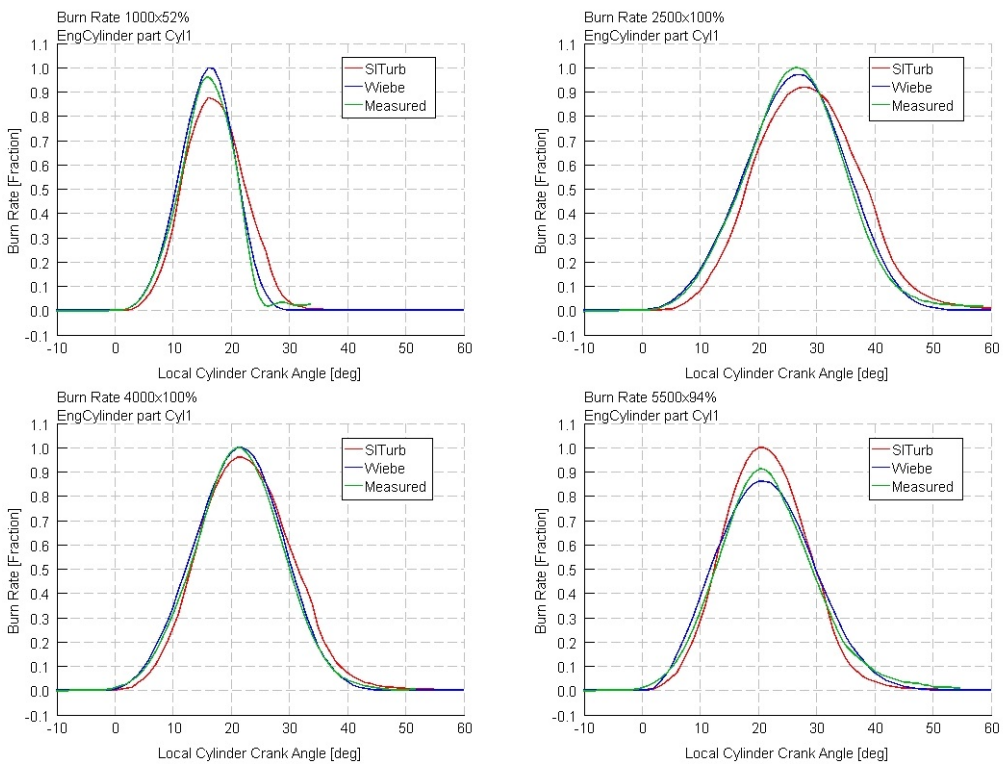


Figure 5.8: Engine A burn rate trend comparison

5.2 Engine B model

As already discussed, the starting point to achieve a good calibration of the predictive combustion model is to have an engine model which is able to replicate the measurements data (engine performance, combustion parameters, pressure at inlet and outlet of compressor and turbine etc.) with high fidelity. In order to achieve this results, the model should describe the gas path in the best possible way, while for what concerns the combustion, the non-predictive model can be chosen at this stage. However also in this case, a small calibration procedure is needed to impose the combustion, in such a way that it exactly corresponds to the experimental one.

The calibration procedure selected for this work is an iterative method: the Cylinder Pressure Only Analysis (CPOA) is used to compute the experimental burn rates from the in-cylinder measured pressure; then the calculated burn rates are imposed in the detailed engine model by means of Wiebe functions, defined by the Mass Burned Fraction anchor angle at 50% (MFB50), the combustion duration (MFB10-90%) and the combustion exponent. This iterative procedure has been selected to remove the unrealistic combustion tails due to thermal shock-induced transducer drift. Figure 5.9 summarises this approach.

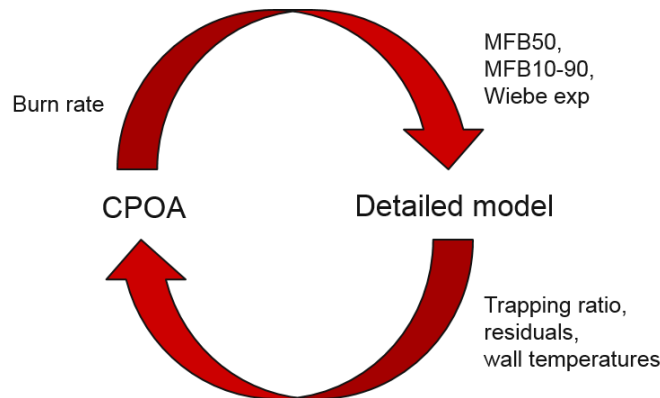


Figure 5.9: Non-Predictive combustion calibration

The engine model required to perform this step is the simple single cylinder, depicted in Figure 5.10. The inputs of this model are inserted in the cylinder object, as on the right side of the figure. Volumetric efficiency, trapping ratio, fuel mass trapped at IVC (Intake Valve Closing), fuel vapor fraction at IVC and residuals fraction at IVC are taken from the detailed engine model and inputted in the "Initial State Object"; the in-cylinder pressure from measurement instead is inserted in the "Measured Cylinder Pressure Analysis Object". Moreover, in order to calculate the burn rate, the "Cylinder Pressure Analysis Mode" should be set to "Measured_CylP_only". For what concerns the thermal side, the "EngCylTWallSoln" object is used to predict the structure temperatures, including the

surface temperatures that are used in the calculation of in-cylinder heat transfer, which is then performed thanks to the "EngCylHeatTr" used in the "Heat Transfer Object". The iterative procedure described so far has been applied for each cylinder (in this case four) in order to obtain as final result the values of MFB50, MFB10-90 and Wiebe exponent for each cylinder and for each case under study (in this case the four operating points described in Section 4.2).

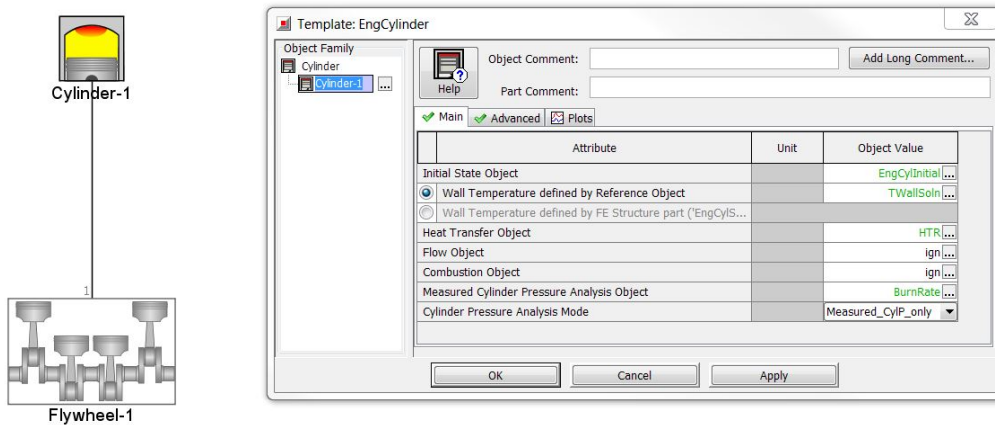


Figure 5.10: CPOA single cylinder model (left) and inputs (right)

Once the combustion has been imposed in order to replicate the experimental tests, the following step is to check the gas path: this means that the model should be able to draw the correct amount of fresh charge and then to expel the quantity of gases as in measurements. Gas path is extremely important because the trapped conditions at Intake Valve Closing (IVC) influence the combustion process and the exhaust gases affect turbocharger and engine performance. Therefore, one of the key steps in the engine model validation is to check that both intake and exhaust valves are matching the experimental tests, in terms of lift and timing.

For what concerns the intake side, the engine is equipped with Variable Valve Actuation (VVA), both in terms of lift and timing: they are referred to as Variable Valve Lift (VVL) and Variable Valve Timing (VVT). In order to model this in GT-Power software, measured data are needed, in particular the valve lift as function of the crank angle and the valve timing (for instance the Intake Valve Opening IVO or the Closing IVC). From the test bench, all these data have been recorded and therefore they can be inputted in the valve object of the engine model: the IVO (which is different for each operating point since the engine is equipped with VVT) is used as cam timing angle, with anchor reference equal to the gas exchange Top Dead Centre (TDC); the valve lift, which is variable according the case under study, is also inserted as input from TXT files. Since valve lifts have been recorded only for one intake valve, the same lift and timing are applied to all

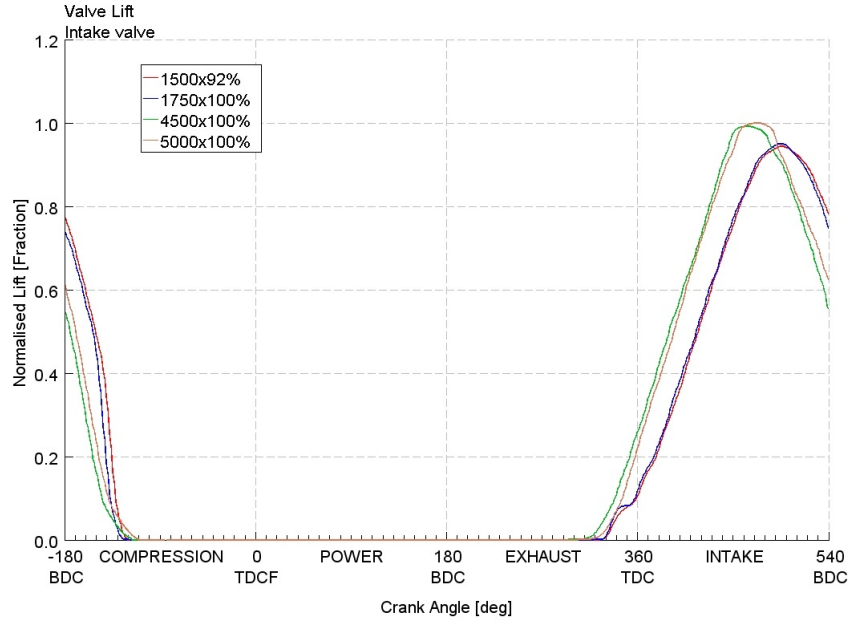


Figure 5.11: Intake valve lift

the eight intake valves of the engine, even if some differences between the valves is present in the actual engine. Figure 5.11 shows the valve lifts from test which are imposed in the engine model: the y-axis has been normalised to the overall maximum lift of the four cases while the x-axis shows the crank angle. Looking at the graph, it is possible to see that higher lift and early timing, i.e. IVO, are adopted for high engine speed cases. This solution allows more air to enter the cylinder at high rpm high load thus improving engine performance.

The same methodology has then been applied to the exhaust side of the engine. The measurement of the valve lift can be directly inserted in the engine model and since the exhaust camshaft is not equipped with VVL, a single lift is used for all the cases under study and then it is shifted according the variable timing. However a big issue had to be faced: due to lack of time, the instrumentation for the measure of exhaust valve timing used in the test bench was not properly setup. As a consequence, the output of this measurement was not to be trusted. The solution adopted to solve this problem is a manual parameter sweep: the Exhaust Valve Closing (EVC) is set as cam timing angle in the exhaust valve object of the engine map and then it has been varied in order to match the blowdown phenomenon. The blowdown is the escape of exhaust gases from the combustion chamber when the exhaust valve opens, thus leading to the drop visible in Figure 5.12. This drop corresponds to the moment when the pressure is lowered till the atmospheric value, as a consequence of the exhaust valve opening. In Figure 5.12, both y-axes have been normalised to the maximum pressure and maximum valve lift respectively. The green curve corresponds to the pressure trace obtained in the test bench, while the

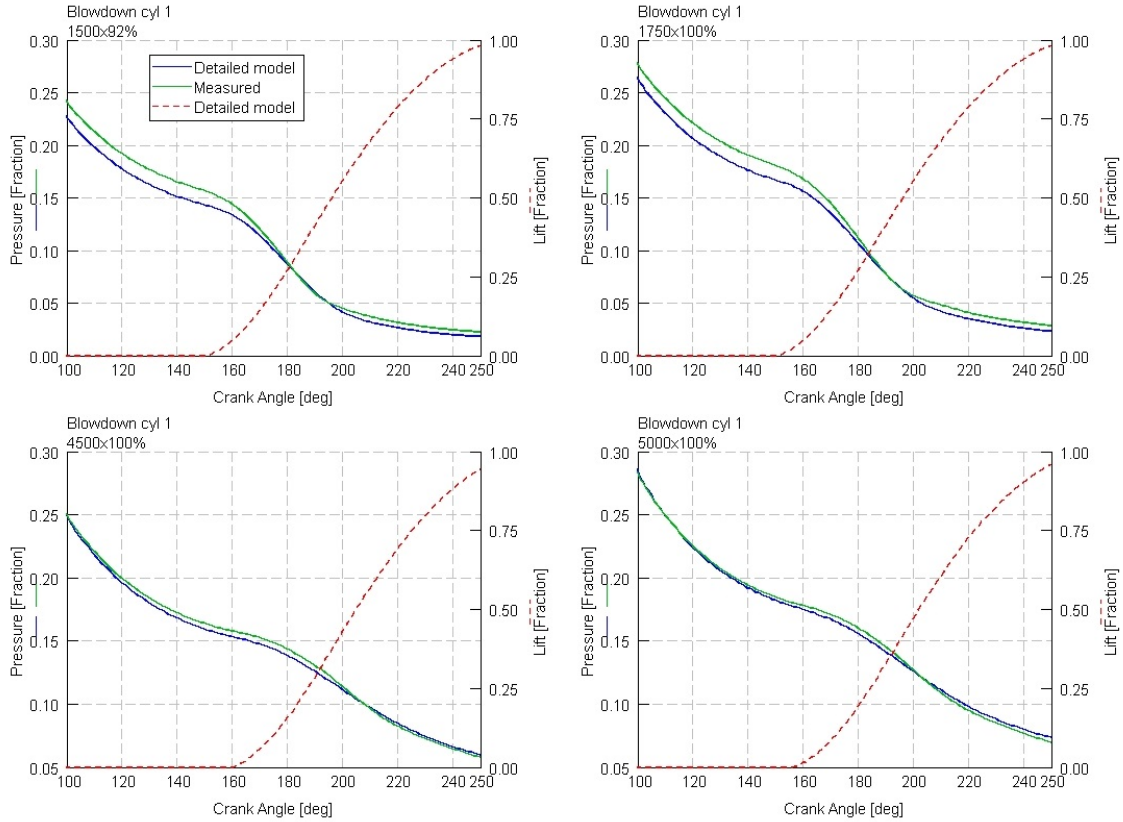


Figure 5.12: Blowdown and exhaust valve lift

blue one is the in-cylinder pressure output from the detailed engine model with imposed combustion. The red dashed line represents instead the exhaust valve lift. All four cases under study are represented in the same figure. As a conclusion, this manual EVC sweep has led to fairly good results, thus being confident that the exhaust valve are able to replicate the behaviour of the actual engine.

An other important check to properly describe the air path is the compressor performance. Inside the GT-Power software, the compressor is modelled with a template, in which predictions of mass flow rate, outlet temperature and consumed power are calculated by the use of a map. Therefore, it is crucial to match the experimental inlet compressor conditions, so that the calculated quantities are as close as possible to the ones recorded in the test bench. A big difference between the experimental and the simulated inlet compressor pressure was also found. In order to fix the issue, the decision was to act on the tuning orifice in the intake line, highlighted with the red circle in Figure 5.13. The goal is to find the optimal value for the diameter of the tuning orifice which guarantees the pressure at the compressor inlet, measured in the object AIS-03 highlighted with the green circle, to be equal to the experimental value. Since the analysis of the pressure drops in the intake line requires the information about pressure and flow rate, the air flow rate has been kept fixed by using the wastegate controller with the experimental flow rate

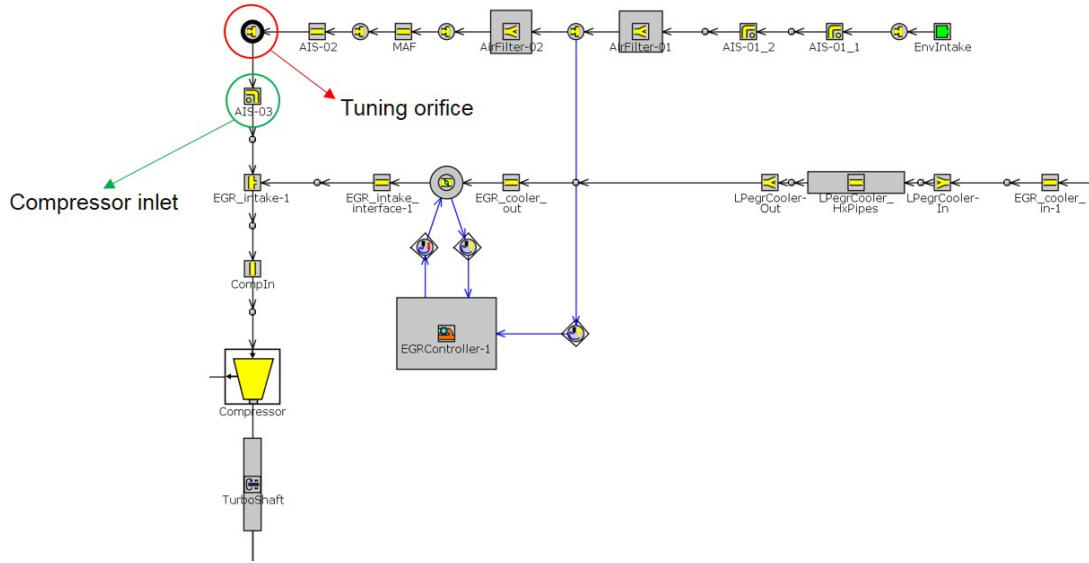


Figure 5.13: Engine B map

as target. Then an optimisation has been run for just the operating point at 4500 rpm and Wide Open Throttle (WOT), using the diameter of the tuning orifice as independent variable. The results of this optimisation are summarised in Figure 5.14. This graph shows the comparison between the experimental (green curve) and the simulated (blue curve) pressure in the object AIS-03: the optimised orifice diameter has been applied to all the four operating conditions and the normalised pressure with respect to the overall maximum value has been plotted versus the engine speed. As it is possible to see, the result is an almost perfect match with measured data, which corresponds to a satisfying outcome.

Despite all these adjustments and improvements, the GT-Power model of *Engine B* showed one remarkable issue more: a pressure mismatch at the end of the compression stroke, which corresponds to the crank angle at which the combustion has not started yet, because the spark timing for all the operating points is some degrees after the Top Dead Centre Firing (TDCf). Therefore, since it could be said that the combustion does not represent the problem in this case, the blowby has been investigated. This phenomenon corresponds to the leakage of combustion gases between the piston and the cylinder wall into the crankcase, which in turn could be responsible for a lowering of the effective compression ratio. In order to evaluate the quantity of flow rate which is wasted in blowby per cycle per cylinder, the measurement data for the volume flow rate into the crankcase has been converted into mass flow rate by multiplying this value by the density of the air, because it has been assumed that the blowby gases have the same composition of air. This is of course an assumption which does not corresponds to the reality but for sake of this analysis it is reasonable enough. Once the blowby mass flow rate is known,

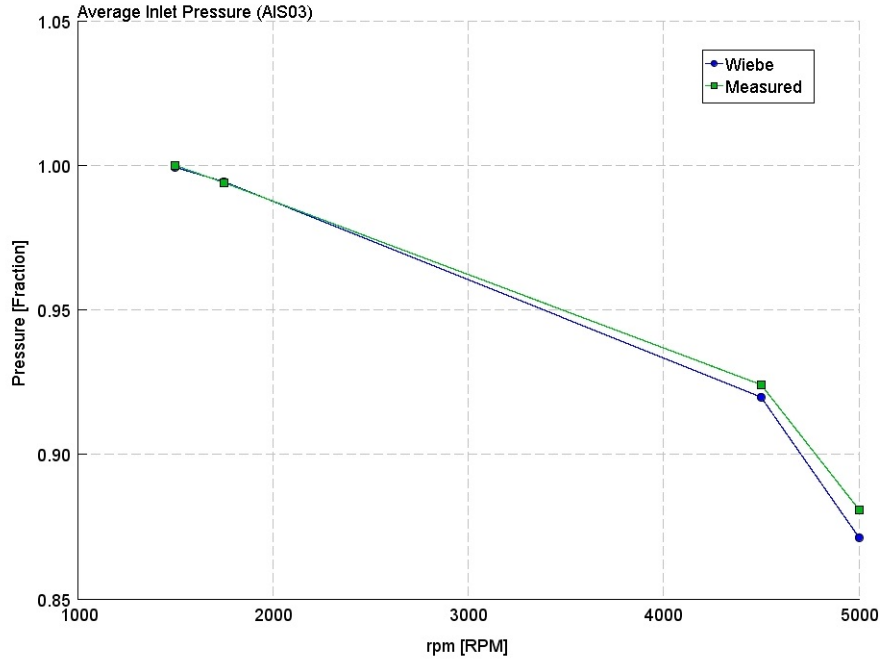


Figure 5.14: Compressor inlet pressure

a simple subtraction between the air flow rate recorded in the test bench and the blowby itself can be performed, thus leading to the actual flow rate which is then trapped in the cylinder. At this point the volumetric efficiency, considering the air minus the blowby mass flow rate $\dot{m}_{air-blowby}$, can be calculated with the formula:

$$\lambda_v = \frac{\dot{m}_{air-blowby}}{\rho_{air} i V_d \frac{n}{m}}$$

where ρ_{air} is the density of the air at ambient condition, i is the number of cylinders, V_d is the displaced volume, n is the engine speed (rpm) and m is the coefficient of engine type, equal to 1 for two stroke and equal to 2 for four stroke engines.

The volumetric efficiency trend as function of the engine speed is plotted in Figure 5.15. In the y-axis, the volumetric efficiency, which is usually expressed as a percentage, is represented as a fraction, because all the results have been normalised to the maximum value. The blue curve corresponds to the volumetric efficiency calculated from test, the orange one to the output of the detailed model with imposed combustion, while the grey one takes into account the blowby flow rate. For all the calculations, the reference condition was the air at ambient pressure and temperature. All the three curves are quite close to each other, showing a maximum error lower than 3%. As a consequence of this calculation, the volumetric efficiency can be then used as input in the Cylinder Pressure Only Analysis (CPOA) in order to run the model with the trapped quantities close to the ones measured in the test bench. The results obtained with this simulation are reported in Figure 5.16. In these graphs, which for sake of simplicity are only two (one for low

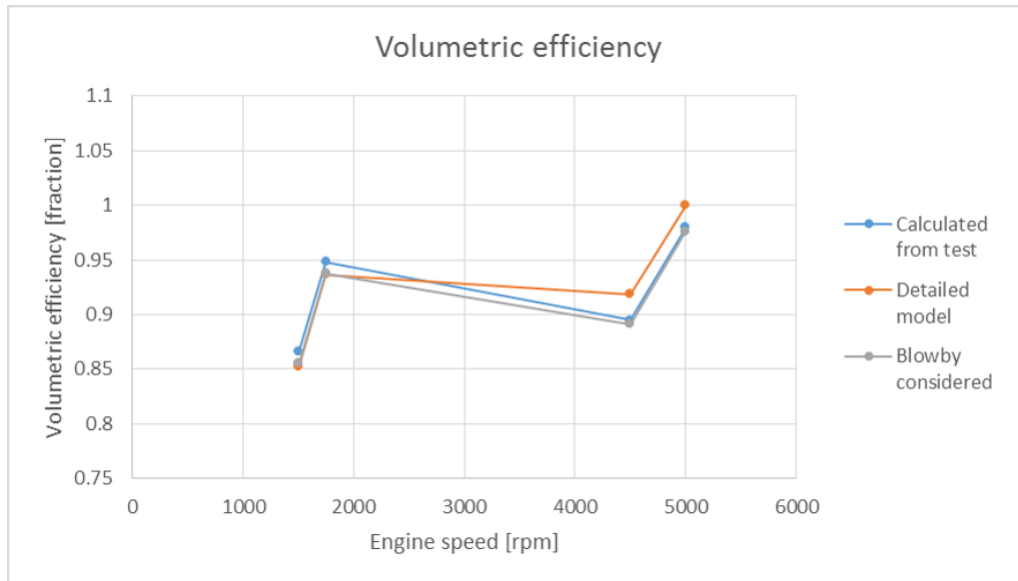


Figure 5.15: Volumetric efficiency comparison

rpm and one for high rpm case), the blue curve represents the in-cylinder pressure trace recorded in the test bench and the orange one corresponds to the pressure simulated by GT-Power. It is visible that the compression mismatch is still present: the blowby therefore can not be considered the responsible for the problem, as the small difference in volumetric efficiency already suggested (see Figure 5.15).

After having fixed all the issues about the airpath and having discarded the blowby hypothesis, the only remaining option is acting on the compression ratio (CR): in order to solve the compression mismatch the compression ratio in the GT-Power engine model had to be lowered by 1 point, compared to the design value. This might seem like a workaround but actually it has been proven by measurement in the test bench that the design CR could not be reached with the actual engine. The compression ratio from test was in fact 0.42 points lower than the design one: this probably could correspond to some issues during the design phase. However, since the mono-dimensional engine model requires a compression ratio 1 point lower, the most likely solution we can get is that in the actual engine something the 1D code is not able to capture is happening. This problem is still under investigation but, for the purpose of this thesis and to carry on the project, the lower CR has been assumed from this point on.

With this last modification, the detailed model with non-predictive combustion model can be considered ready. All the results obtained with this engine model, in terms of cylinder pressure, burn rates and engine performance, are summarised in Figures 5.17, 5.18 and 5.19 and 5.20 respectively. All these graphs have been normalised to the overall maximum value so the y-axis shows the fraction from 0 to 1. They represent a comparison between the engine model (blue curve, Wiebe in the legend) and the test data (green curve,

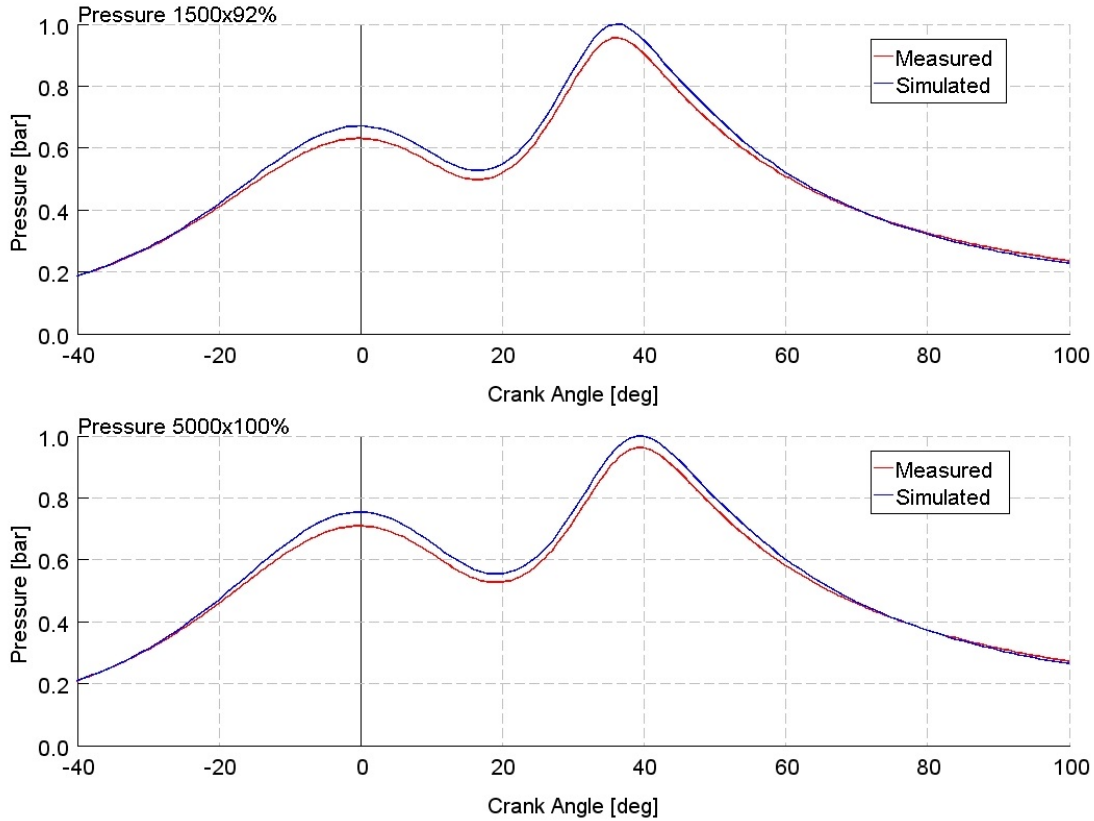


Figure 5.16: CPOA pressure when blowby is considered

measured in the legend). As it is possible to see from these plots, all the compression issues have been solved and so the pressure trace from test is almost perfectly replicated and the combustion process is well described by the burn rate curves. For what concerns the engine performance, the bmep and the air fuel ratio show perfect match with the test data because these two quantities are controlled in the model; for any other parameters the results are quite satisfying, because the error percentage never reaches high values (for example, the volumetric efficiency error with respect to the calculated one is within 5%). In the end the model can be considered as a good starting point for any predictive combustion modelling.

An other possible way to evaluate the detailed model is to represent the error plots of each operating point for some meaningful parameters related to combustion. These parameters are the Indicated Mean Effective Pressure (IMEP), the Mass Fraction Burned angle at 50% (MFB50), the combustion duration (MFB10-90), the Peak Firing Pressure (PFP) value and crank angle and they are listed in Figure 5.21. In each subfigure the error for each operating condition in term of percentage or crank angle (CA) is represented with blue and red dots: blue corresponds to a positive error while red to negative error; the bigger the dot the bigger the error. A summary of all these errors is shown in Table 5.1. As we might expect from an imposed combustion, the results show high level of accuracy,

especially for IMEP and PFP; the MFB50 error is anyway around $\pm 1.5^\circ$ crank angle which is a reasonable achievement; for what concerns the MFB10-90, the combustion duration is usually tricky to fully capture, because of the combustion tails which are difficult to model.

Parameter	Unit	Average error	Maximum error
IMEP	[%]	0.28	1.04
MFB50	[CA]	-1.17	-1.52
MFB10-90	[CA]	2.78	3.03
PFP angle	[CA]	0.38	0.59
PFP	[%]	0.01	0.02

Table 5.1: Detail model errors summary

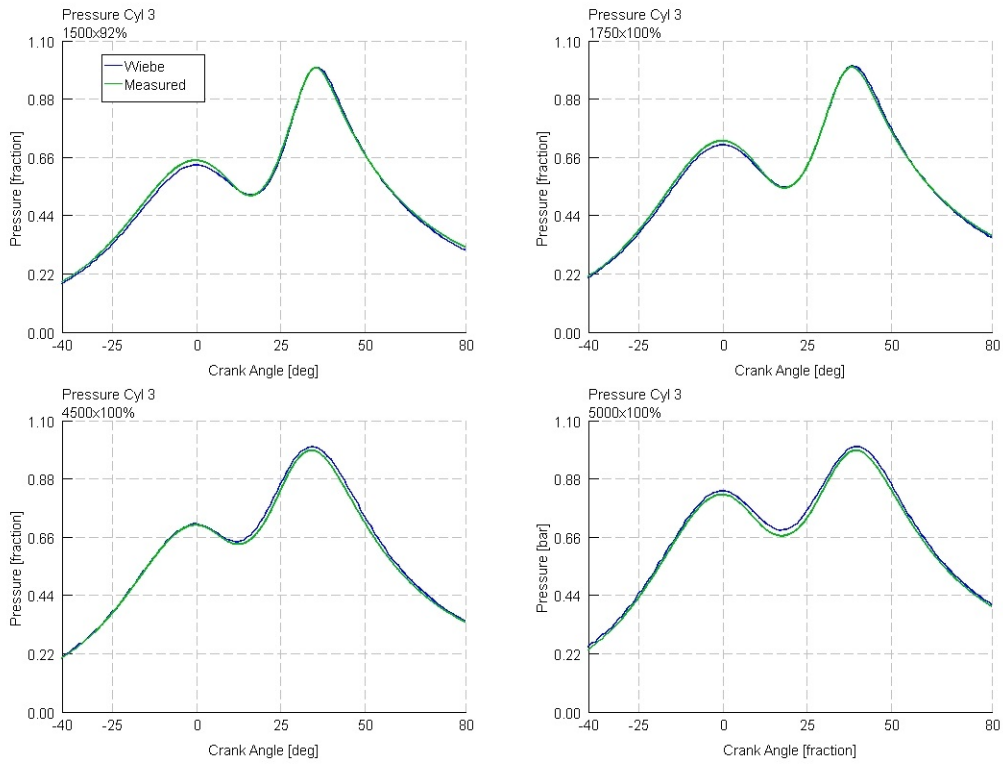


Figure 5.17: *Engine B* Detailed model cylinder pressure

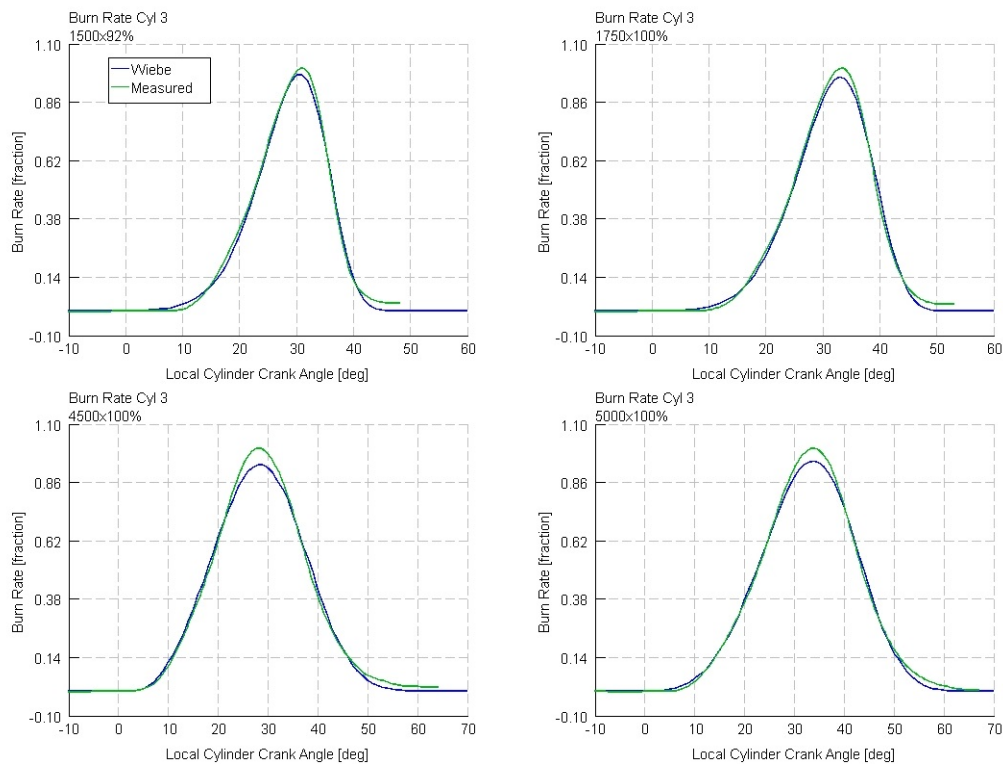


Figure 5.18: *Engine B* Detailed model burn rates

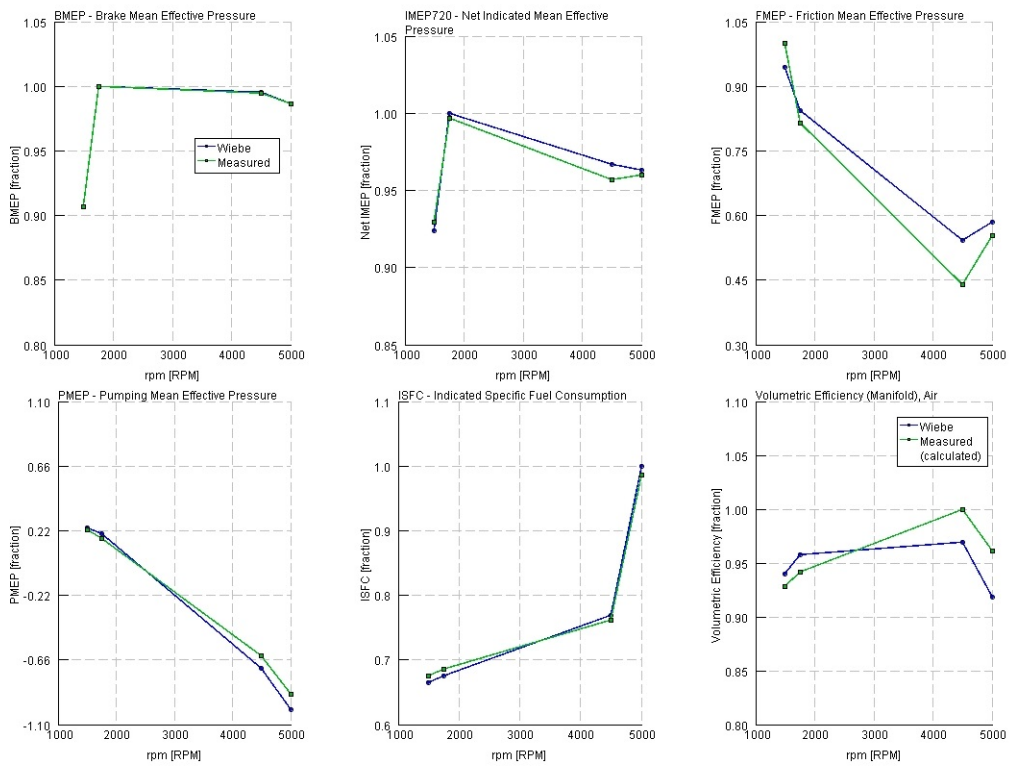


Figure 5.19: Engine B Detailed model performance (1)

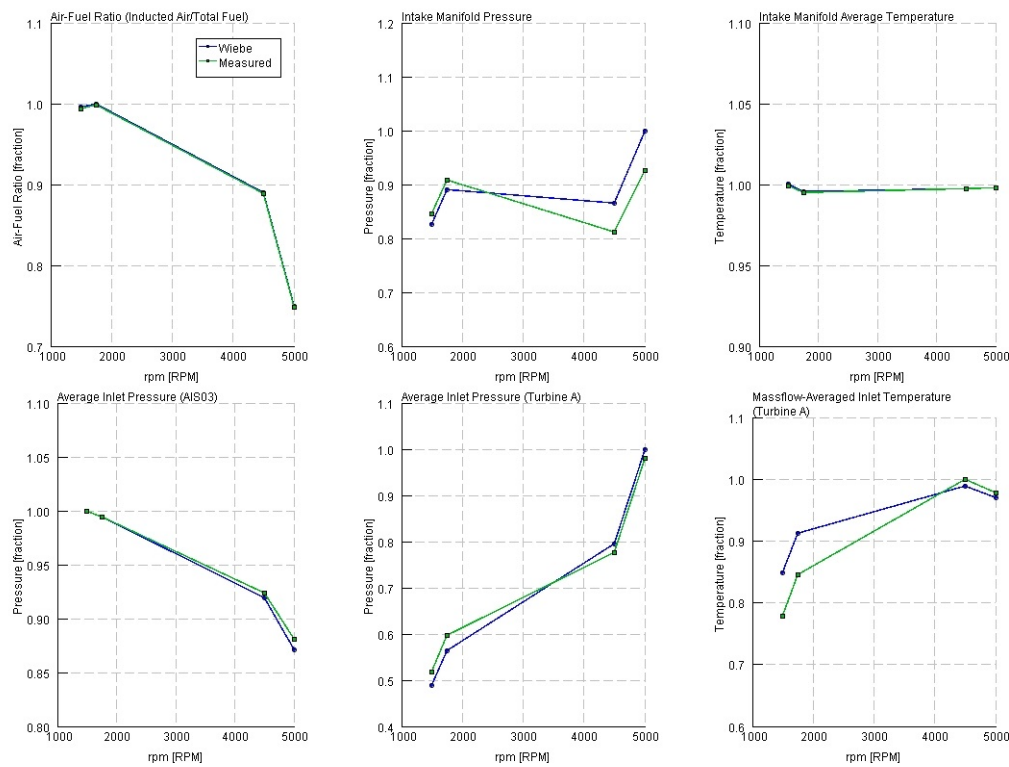


Figure 5.20: Engine B Detailed model performance (2)

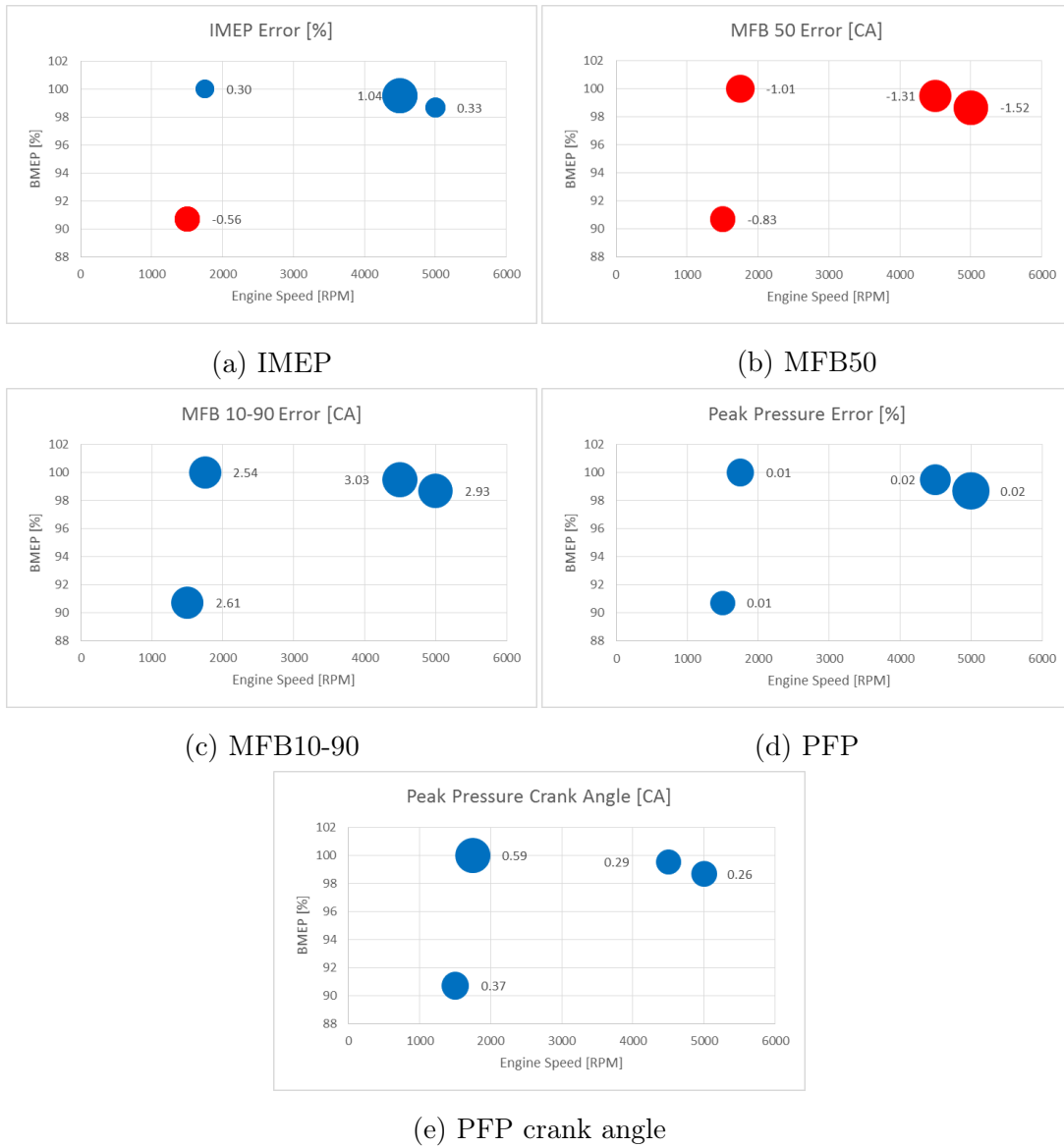


Figure 5.21: Errors of the detailed model compared to the experimental results

5.3 Calibration transplant

The third section of this chapter deals with the description of the "transplant" operation, as it will be named in this thesis. The operation corresponds to the application of the existing turbulence and combustion calibrations from the *Engine A* to the updated version, i.e. the *Engine B*. The potential benefit from the output of this analysis is relevant: the aim in fact is to understand if the predictive combustion model SI-Turb is able to cope with some hardware changes that are made when the engine build is updated. If the answer to this question is positive, SI-Turb will enable simulations during the design phase, without requiring the physical engine to be tested in the cell. This represents a huge advantage in terms of money and time in the development of a new engine build.

Since both the turbulence and the combustion calibration were already available, the setup of the predictive model is straightforward: the set of 4 turbulence terms described in Section 3.2 and the set of 4 combustion multipliers described in Section 3.3 have to be inputted in the Flow and Combustion Object of the cylinder template in the engine map, as shown by the red rectangles in Figure 5.22.

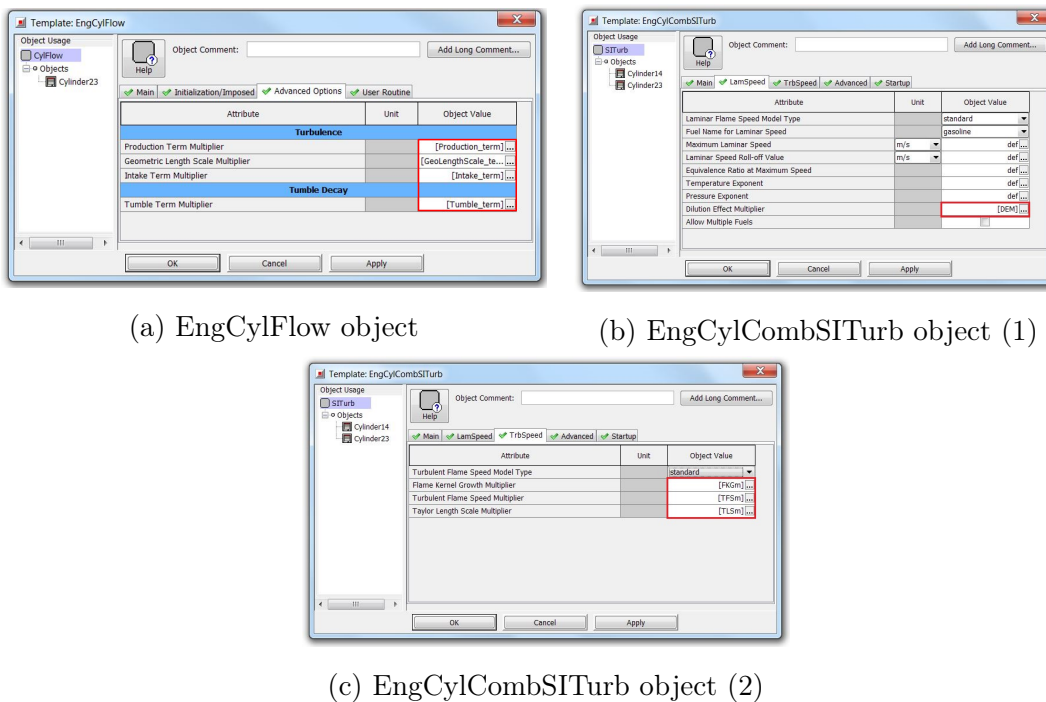


Figure 5.22: Flow and Combustion objects of the cylinder template

The next subsection will show all the results obtained with the calibration "transplant" operation, but before analysing that it is worth to discuss about the changes that have been applied to *Engine B*. This step is necessary to understand which parameters affecting the combustion have been modified, in order then to properly evaluate the outcomes of the transplant simulation. The main hardware differences between *Engine A* and *Engine*

B are summarised in the following list:

- The combustion chamber design has been extremely modified, since both piston surface and cylinder head have been changed. This has a relevant effect on the predictive combustion model itself since it specifically requires the CAD files of these components as inputs.
- As consequence of the combustion chamber update, the engine compression ratio has been increased by 3 points.
- The intake manifold design has been changed too, thus leading to a different charge motion of the air entering the cylinder; therefore the forward and reverse flow coefficients and the tumble coefficient of the intake valves had to be updated with the results from the 3D CFD simulation of the *Engine B*. This change shows particular interest since it translates into a different level of turbulence which in turn corresponds to additional work for the 0D turbulence model of SI-Turb.
- As already explained in Chapter 4, *Engine B* is equipped with a Low Pressure Exhaust Gas Recirculation system which picks up some of the exhaust gases downstream the turbine and the catalyst and recirculates it into the intake manifold, upstream the compressor. The operating points considered in this work are at full load only, which means that the percentage of EGR is very low. The reason behind this is the effect of the EGR which reduces the temperature inside the chamber leading to a reduction in NO_x but also to a slower combustion (with larger possibility for high cycle to cycle variations and misfiring), which clearly are not desirable conditions at full load. As a conclusion, when the combustion model is transplanted from *Engine A* to *Engine B*, it has to describe some dilution effects, even if just marginal, which in the original engine were not present.

5.3.1 Transplant results

Following the same approach used to show the results of the detailed model with imposed combustion as in Section 5.2, Figures 5.23, 5.24, 5.25 and 5.26 reproduce the pressure trends, the burn rates and the engine performance obtained with the transplanted predictive combustion model SI-Turb. All these plots have the y-axis normalised to the overall maximum value, so that the result is a fraction from 0 to 1 of each specific parameter. The graphical representation of the bubble charts concerning the error in terms of percentage or crank angle related to the combustion parameters can be adopted. This is what Figure 5.27 shows. The overall results seem to be quite promising. The IMEP percentage error is within 1% for all cases and the MFB50 crank angle error is within ± 1 degree except

for one case, the highest rpm one, which shows a large underestimation; these results represent a slight improvement compared to the detailed model. For what concerns the combustion duration MFB10-90 error, the result is of the same order of magnitude of the detailed model and it is anyway within ± 5 degree range. The peak firing pressure PFP parameter is the one that shows the highest error, both in terms of percentage and crank angle position of the peak value; the explanation of this outcome could be the fact that with the transplant operation the combustion model has not been calibrated according the proper spark timing but it has been just copied from an older engine with a different combustion phase. Table 5.2 summarises the analysis of the errors by showing the average and maximum values for all the parameters under investigation.

Parameter	Unit	Average error	Maximum error
IMEP	[%]	0.21	0.92
MFB50	[CA]	-0.63	-3.07
MFB10-90	[CA]	3.88	4.79
PFP angle	[CA]	0.91	2.59
PFP	[%]	-3.87	-7.68

Table 5.2: SI-Turb transplant model errors summary

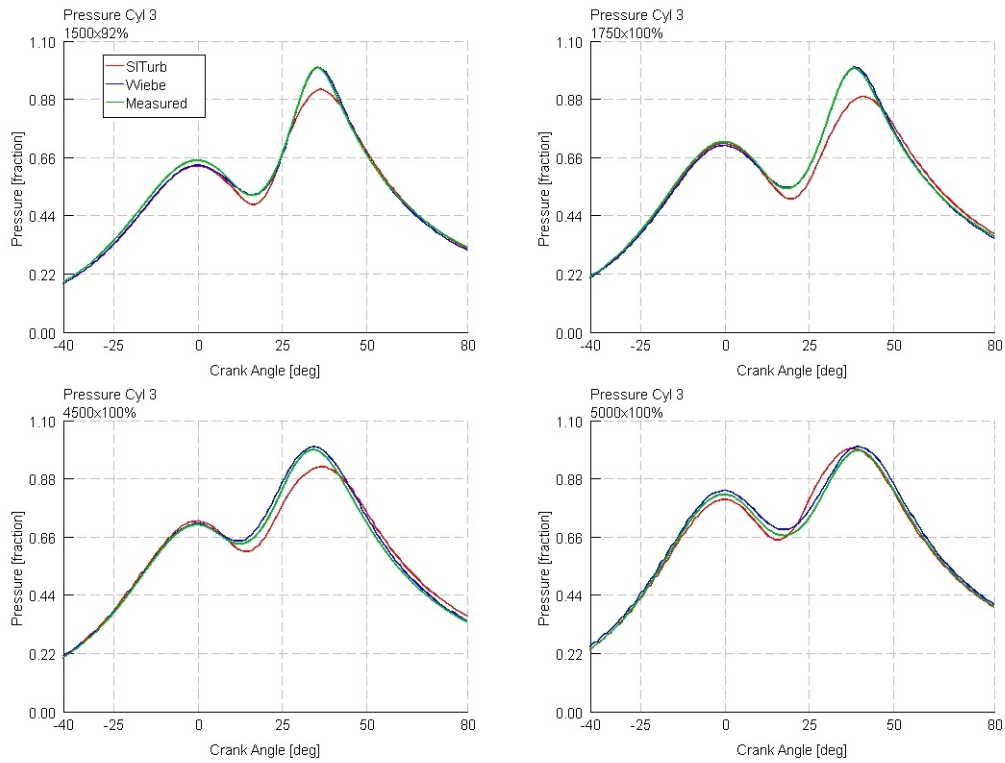


Figure 5.23: Engine B SI-Turb transplant model pressure

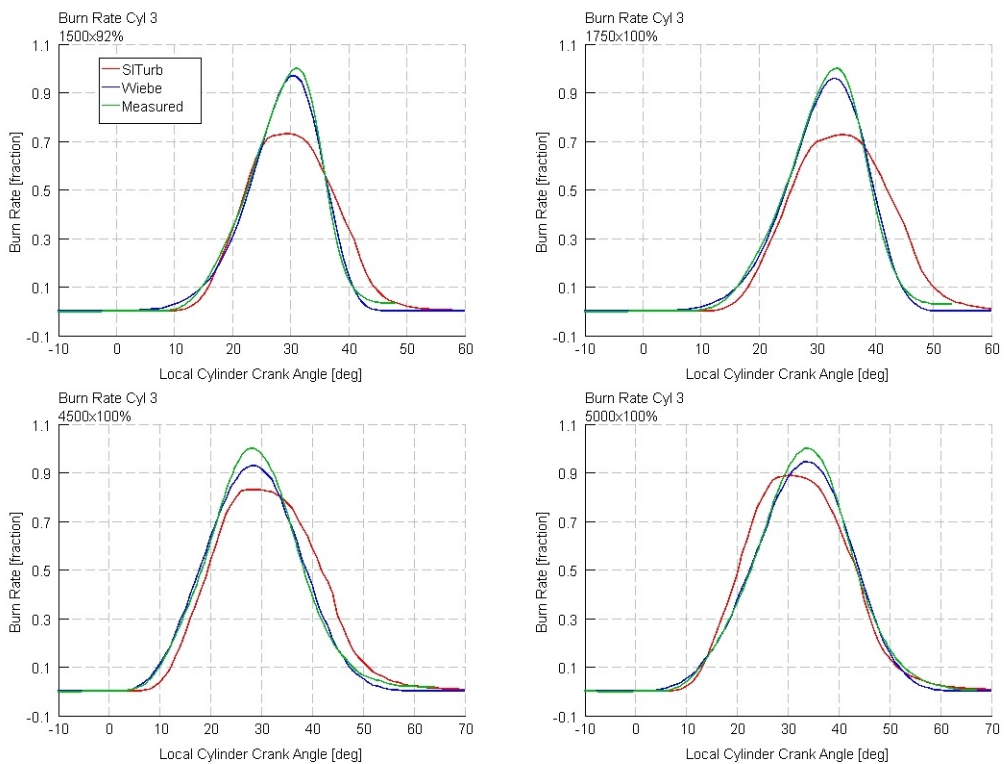


Figure 5.24: Engine B SI-Turb transplant model burn rates

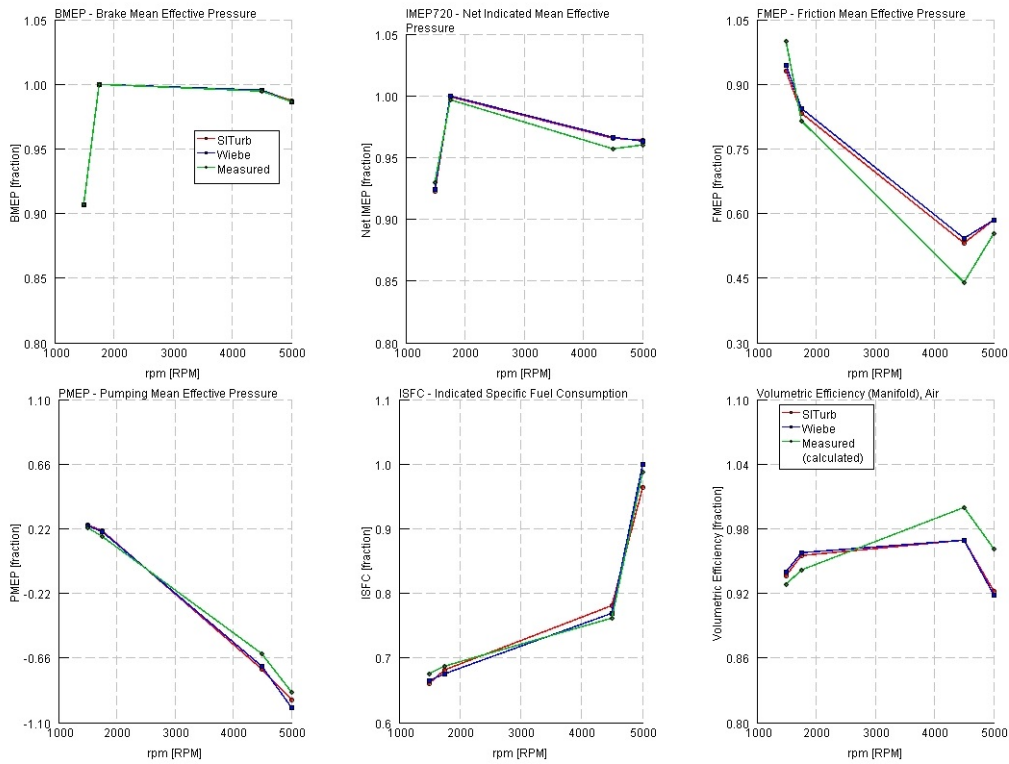


Figure 5.25: Engine B SI-Turb transplant model performance (1)

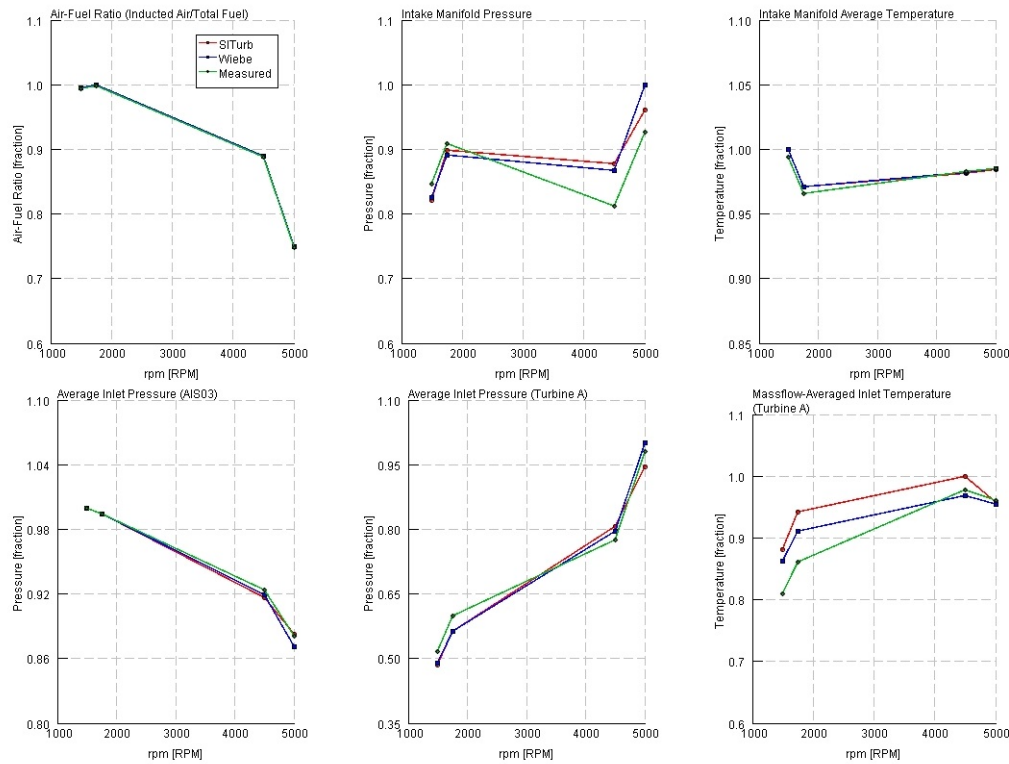


Figure 5.26: Engine B SI-Turb transplant model performance (2)

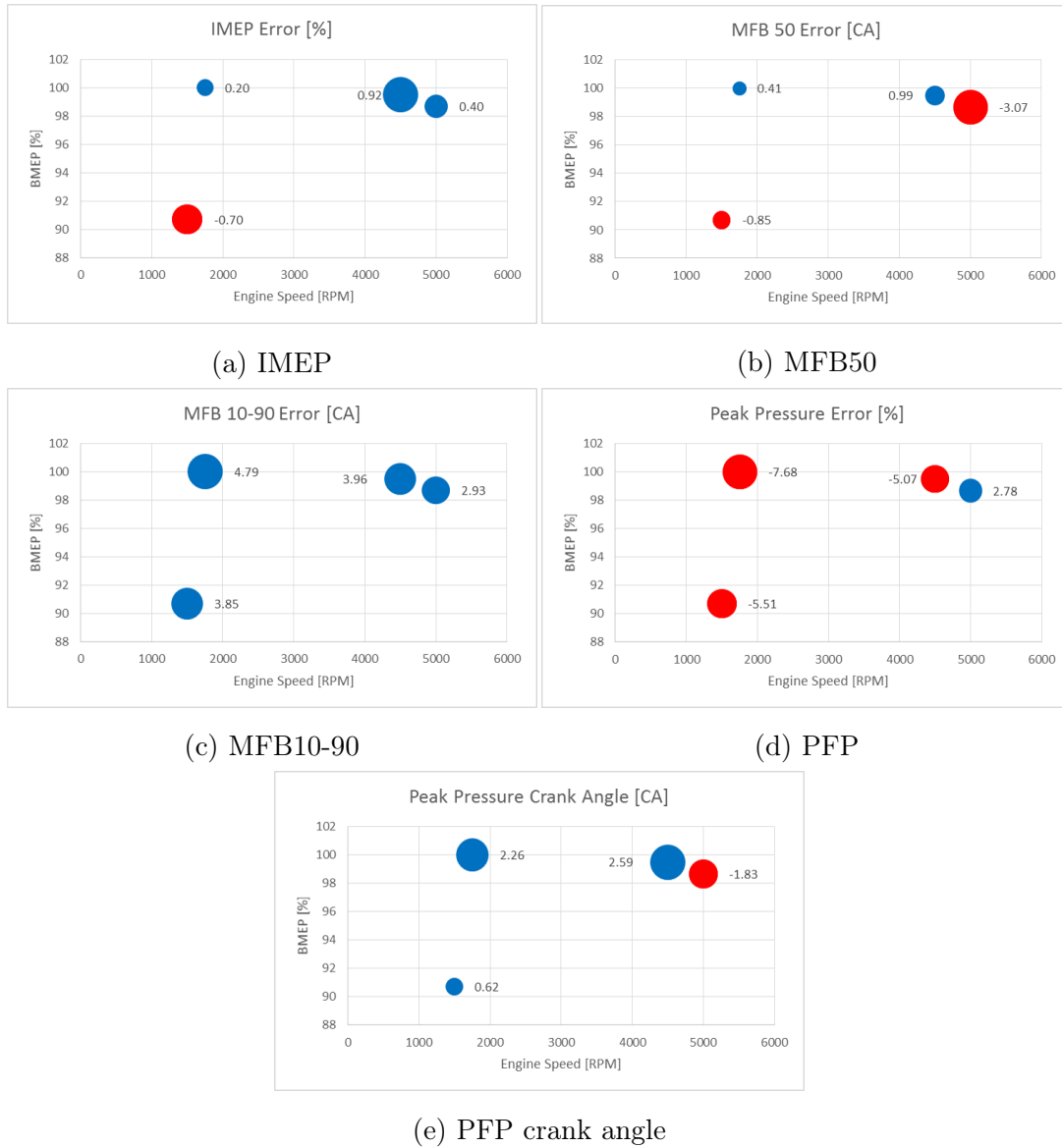


Figure 5.27: Errors of the SI-Turb transplant compared to the experimental results

5.4 Engine B calibration

This final section will focus on the core part of the whole project, i.e. the calibration of the predictive combustion model SI-Turb for *Engine B*. This time, the calibration will be performed starting from scratch, so the previous work for *Engine A* will not be considered or used: as a consequence, the outcome of this work package will be a full predictive model, calibrated specifically to match *Engine B* test data. The procedure that will be followed is the one already described at the beginning of this chapter, which corresponds to the recommended one by Gamma Technologies [3], but some small improvements will be made. For sake of organisation and clarity, the calibration procedure of the predictive combustion model can be split in two main steps: turbulence and combustion calibrations. In the former an automatic logic to obtain the four turbulence parameters will be implemented while the latter will follow exactly the recommendations from Gamma Technologies.

5.4.1 Automatic turbulence calibration

The main goal of this step is to find the optimal set of turbulence parameters (intake, production, geometric length scale and tumble terms) able to repeat the turbulence level inside the cylinder for a wide variety of operating conditions. In order to do this, the in-cylinder turbulence should be evaluated through 3D CFD simulations, because the 0D K-k- ϵ turbulence model inside GT-Power needs be compared with the outputs of the three-dimensional analysis. The approach to model the turbulence is quite different between 3D and 1D codes: in 3D CFD all the combustion chamber plus intake and exhaust ports and valves are modelled and the turbulence is generated by the ports, the opening valve and the piston movement; the turbulence model in GT-Power instead is valid inside the cylinder only and it is used just to define the initial conditions of the combustion process. Therefore, since the simplified 1D approach does not take into account the charge motion in the same way as 3D CFD, the zero dimensional model has to be tuned against the results coming from CFD, to obtain the highest fidelity as possible.

In order to start with the CFD simulations, boundary conditions are needed. They are represented by geometrical parameters of the engine (bore, stroke, compression ratio etc.), injection characteristics (start of injection, pulse width etc), operating conditions variables (speed, load, air and fuel flows etc) and parameters depending on crank angle (valve lifts, intake, in-cylinder and exhaust pressures, heat release rate and trapped mass). Not all these information are available from test data, because some parameters are not always recorded or some of them can not even be measured (like the trapped conditions inside the cylinder), so the engine model with imposed combustion built in Section 5.2 is now used to provide the boundary conditions of the CFD simulation. To perform this task,

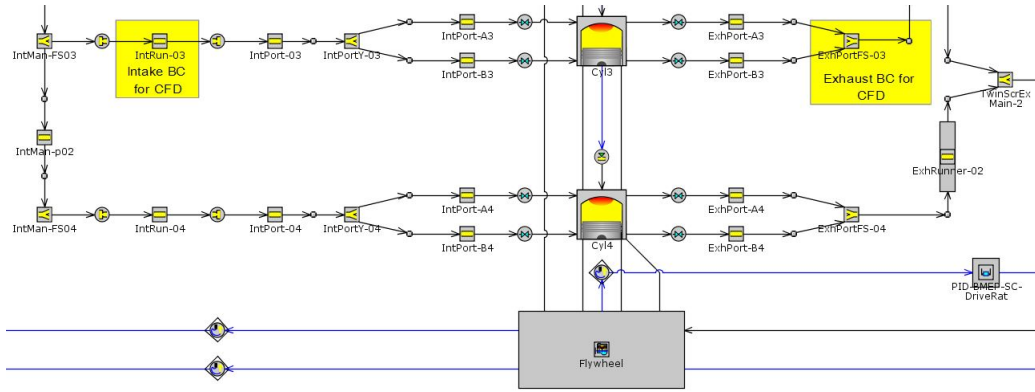


Figure 5.28: Boundary conditions location in 1D model of *Engine B*

the position where to take the boundary conditions has to be carefully evaluated: in the CFD software the simulation is run considering the cylinder plus intake and exhaust ports and therefore it is critical to gather from the 1D model the information of intake and exhaust instantaneous pressure at the proper location. After a rapid check of the geometry and the evaluation of the distances of intake and exhaust from the centre of the cylinder, the location in the 1D engine map has been chosen. The yellow labels in Figure 5.28 shows exactly these positions. The cylinder number 3 has been selected because, considering the cylinder to cylinder variation, it is the one that better matches with experimental tests. For what concerns the operating conditions, two out of the four experimental points available have been selected: one low and one high engine speed case. Usually one low speed low load and one high speed high load points are chosen, in order to tune the turbulence model considering a wide variety of conditions but, as explained in Section 4.2, only the full load curve was available. This does not represent the ideal scenario, which in the end it will correspond to a decreased level of predictive capability.

The software used to run these simulations is STAR-CD by Siemens. The Reynolds-Averaged Navier–Stokes approach (or RANS) is used: the RANS equations are time-averaged equations of motion for fluid flow. The idea behind is the Reynolds decomposition, whereby an instantaneous quantity is decomposed into its time-averaged and fluctuating quantities. The RANS equations are primarily used to describe turbulent flows and can be used with approximations based on knowledge of the properties of flow turbulence to give approximate time-averaged solutions to the Navier–Stokes equations. The turbulence instead is handled by the $k-\epsilon$ RNG model: using Re-Normalisation Group (RNG) methods it is possible to renormalise the Navier-Stokes equations, to account for the effects of smaller scales of motion [6]. In the standard $k-\epsilon$ model the eddy viscosity is determined from a single turbulence length scale, so the calculated turbulent diffusion is that which occurs only at the specified scale, whereas in reality all scales of motion will contribute to the turbulent diffusion. The RNG approach results in a modified form

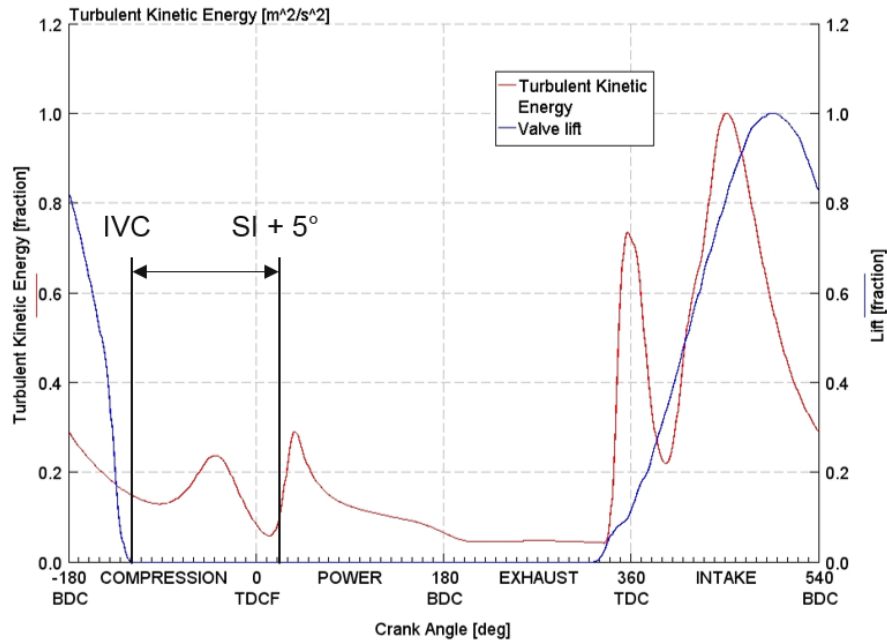


Figure 5.29: Crank angle interval for turbulence calibration

of the ϵ equation which attempts to account for the different scales of motion through changes to the production term. Moreover, a Lagrangian multiphase model for the direct injection of liquid in the cylinder and break up models for the evaporation are used.

Some more clarifications about the CFD simulation are now needed, before moving to the description of the calibration step itself. Since the goal is to obtain the turbulence level during the closed cycle until the Spark Ignition, the CFD simulation has been run in motored condition, i.e. the combustion has not been considered. Also in the case of the CFD model some adjustment have been applied: in fact, the experimental pressure trace was not matching if the design compression ratio was used. As a consequence, it was lowered as in the case of the 1D model by the same amount, showing a perfect pressure match and thus maintaining consistency with 1D.

Once the CFD simulation have been run and the results have been post-processed, the outcomes obtained can be used to tune the 0D turbulence model inside GT-Power, described by the four terms which have to be inserted in the Flow Object of the cylinder template in the engine map. The possible strategies to perform the tuning of the turbulence model are essentially two: a manual trial and error procedure or an automatic process which has to be implemented in the engine model. The manual procedure works in an iterative way: one simulation with baseline turbulence parameters (equal to 1) is run, the turbulent kinetic energy of the in-cylinder flow is compared with the one from CFD and then each turbulence term is varied in the next simulations, in order to obtain a satisfying match with CFD outcome. This procedure relies on a sensitivity study on the

turbulence parameters in order to understand the influence they have on the results, so that the user is able to properly tweak them. The automatic process is similar but it does not require any manual adjustment since an error function is calculated and then minimised. The output of the simulation with the automatic logic built in is represented by the optimal set of turbulence terms, which then can be directly used. This second approach is the one adopted in this thesis and it will be described in the following. An important remark has to be done at this point: the target to be achieved with the turbulence calibration is a good match with CFD outputs in terms of Turbulent Kinetic Energy (TKE), not considering all the crank angle interval but a smaller portion close to the end of the compression stroke. In particular, it has been chosen to vary this interval from the Intake Valve Closing (IVC) to some degrees after the Spark Ignition (SI). The cause of this choice is that the simplified 0D turbulence model gives a more qualitative description than CFD, so it is impossible to be as precise as CFD across all crank angle range. The goal is therefore to reproduce the correct level of turbulence just before the combustion start, because it is the moment in which the charge motion influences the most the combustion evolution. This is what is shown in Figure 5.29, where on the left y-axis the normalised TKE to the maximum value is plotted, while on the right y-axis the normalised valve lift is present. As it is possible to see, the crank angle of interest ranges from the IVC value to 5° after SI.

After the definition of the interval, the automatic logic can be built. Basically, the idea behind is to calculate in that interval an error function between CFD and 1D and then use it as target variable for an optimisation process, where the four turbulence parameters represent the independent variables. The error function can be expressed with the formula:

$$Err_{CFD} = \int_{IVC}^{SI+5^\circ} \frac{\sqrt{(TKE_{CFD} - TKE_{1D})^2}}{\overline{TKE}_{CFD}} d\theta.$$

The root mean square error of the turbulent kinetic energy from CFD and 1D is calculated and then divided by the mean value of the turbulent kinetic energy from CFD (\overline{TKE}_{CFD}). This normalisation to the mean value is required because without it the optimisation process would give more weight to the high speed case, since the order of magnitude of the turbulent kinetic energy increases with rpm. In the end, the error function is integrated in the crank angle θ of interest in order to obtain the cumulative value. This logic is applied to the full detailed engine model in the 1D environment by using the mathematical operation templates available in the software. After this, the optimisation is setup using the Direct Optimiser tool built in GT-Power, which allows the user to choose the objective function and the input variables. For the turbulence optimisation, the two cases from CFD (one low and one high speed, both at full load) have to be run and a set of optimal values of the turbulence parameters valid for all the operating conditions

n	Population size
3	10
4	16
5	20
6	27

Table 5.3: Population size typical values

should be identified, in order to increase the level of predictivity of the model. This sweep optimisation problem is fully supported in the Advanced Direct Optimiser (ADO) of GT-Power software. In case of interest in a set of parameters for each single case, an independent optimisation should be performed instead, which is possible in the ADO as well. The search method algorithm selected for this step is the Genetic algorithm because it is the recommended choice for problems with medium to high complexity, with 3 or more independent variables. The main parameter to setup this algorithm is the population size, which can be identified with the formula behind and then from the knowledge of n , the final value is retrieved from the Table 5.3.

$$n = (\text{Independent variables}) * (\text{Active cases}) + (\text{Sweep variables})$$

Since this is a sweep optimisation with four variables (the four turbulence terms), the final population size was set to 16. The other important parameter is the number of generations to run, which is set to 20. Multiplying these two inputs yields the total number of iterations that the optimiser will run. There is no automatic stopping criteria when using the genetic algorithm; the optimiser will stop after completing all iterations according to the number of generations. The dependent variable to be optimised is set to the cumulative error between CFD and 1D and the goal to minimise this function; the parameters to be varied are the four turbulence terms, the range where they vary is defined by the upper and the lower limit while the initialisation of each parameter (inserted in the EngCylFlow object) is the value in the middle of the range. The simulation is finally launched and after approximately 30 hours the optimal set of turbulence terms is obtained. Sometimes it can happen that the limits of the ranges coincide with the final optimised parameters: in this case a second iteration of the optimisation has to be re-run with larger ranges. For sake of confidentiality, the actual values of the parameters can not be shown but the trends of the normalised turbulent kinetic energy compared to the CFD outputs are represented in Figures 5.30 and 5.32. A more clear representation is present in Figures 5.31 and 5.33, where a zoom in the crank angle interval of interest from IVC to some degrees after SI is performed. In these two graphs, the TDC firing (TDCf) is at

0 degree and the compression stroke goes from -180 degrees to TDCf.

From the knowledge of the four turbulence parameters, it is possible to perform a validation of the calibration, by simply running the turbulence model in the operating conditions not previously used in the automatic process. In this case, the validation points correspond to 1750 rpm and 4500 rpm, both of them at full load. The turbulent kinetic energy, normalised to the maximum value, for the two operating conditions selected is shown in Figures 5.34 and 5.36. As for the calibration step, a more detailed look at the crank angle interval under study is visible in Figures 5.35 and 5.37. Even if the available validation points are quite close to the calibration one, both in terms of engine speed and load, the interesting result out of this validation process is the demonstration of the turbulence model capability to adapt in a satisfying way to changes in operating conditions: in the most relevant crank angle interval, i.e. from the intake valve closing to the spark ignition, the turbulence level matches in fact the CFD output, almost mirroring the results obtained in the calibration process.

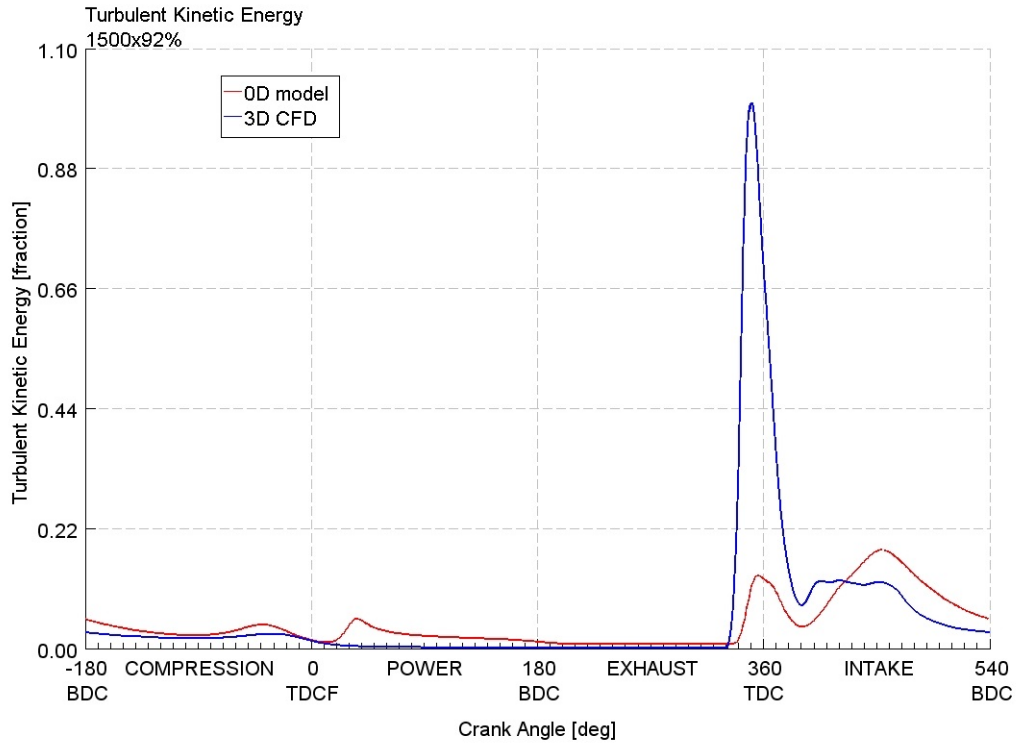


Figure 5.30: *Engine B* Turbulent Kinetic Energy 1500 rpm 92% load

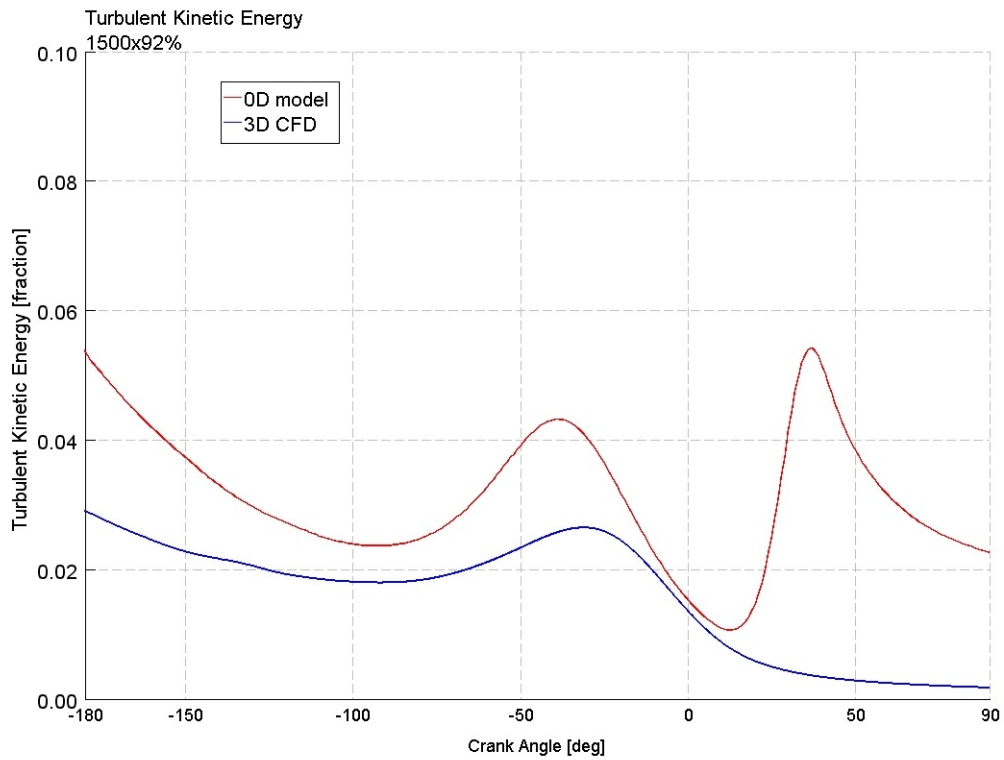


Figure 5.31: *Engine B* Turbulent Kinetic Energy 1500 rpm 92% load, zoom in the crank angle of interest

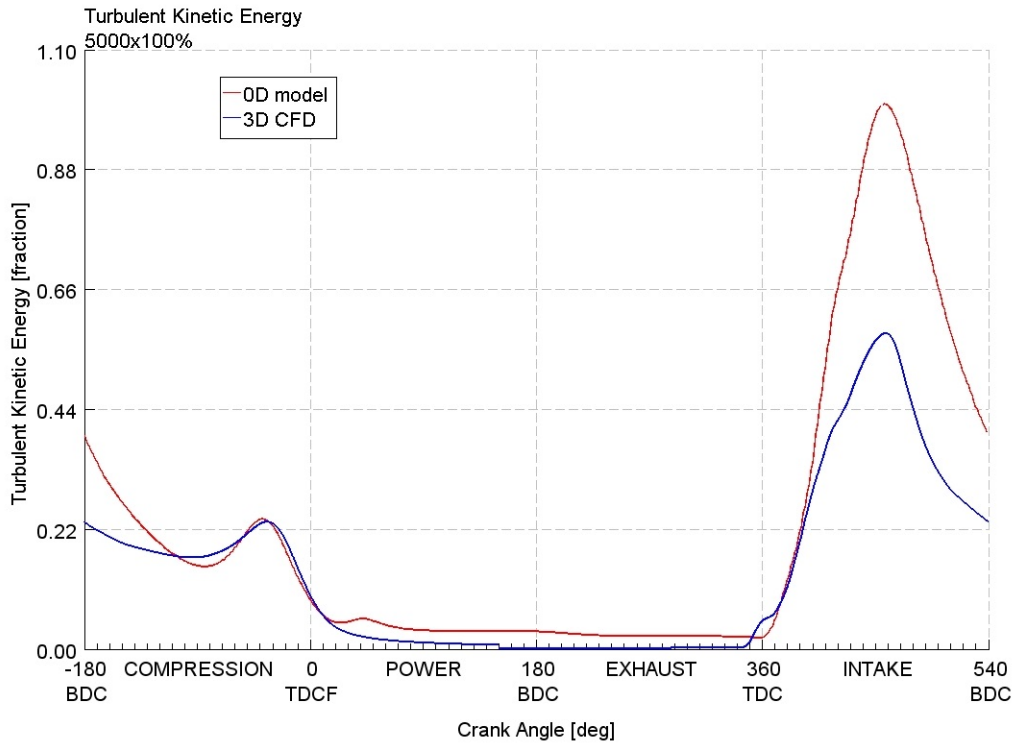


Figure 5.32: Engine B Turbulent Kinetic Energy 5000 rpm 100% load

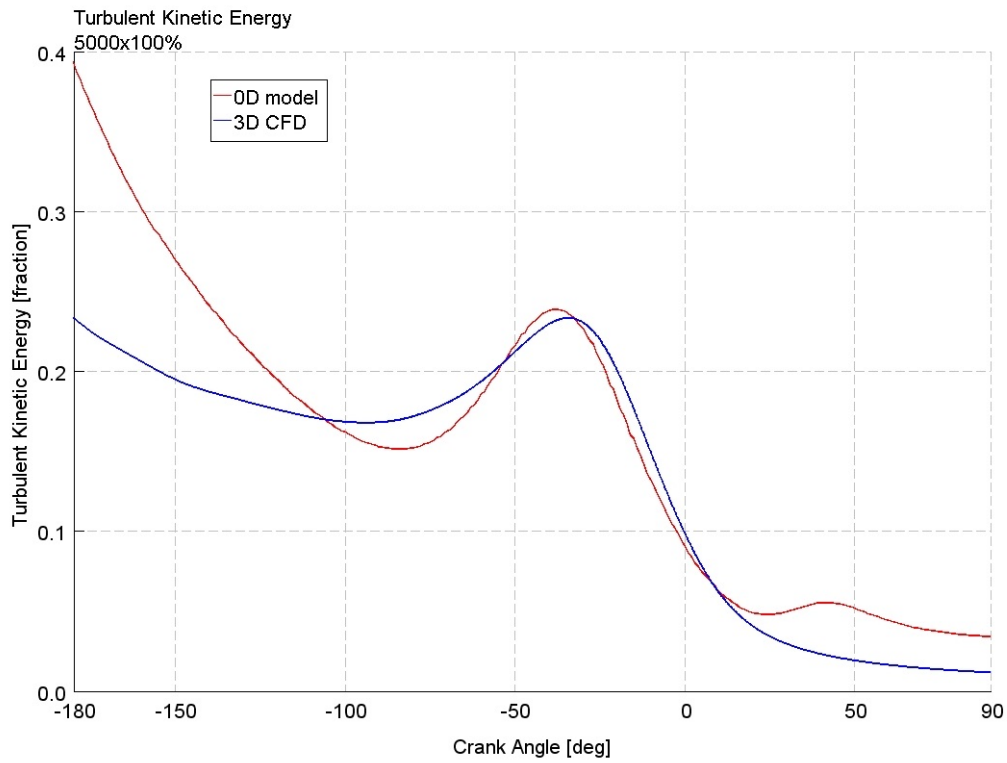
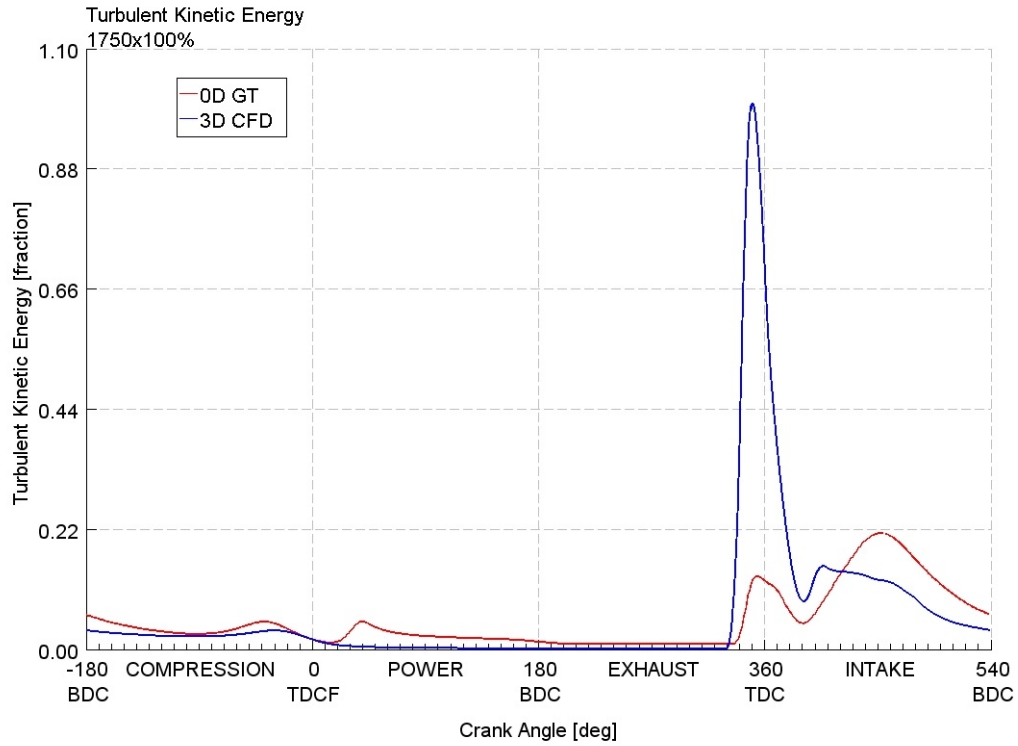
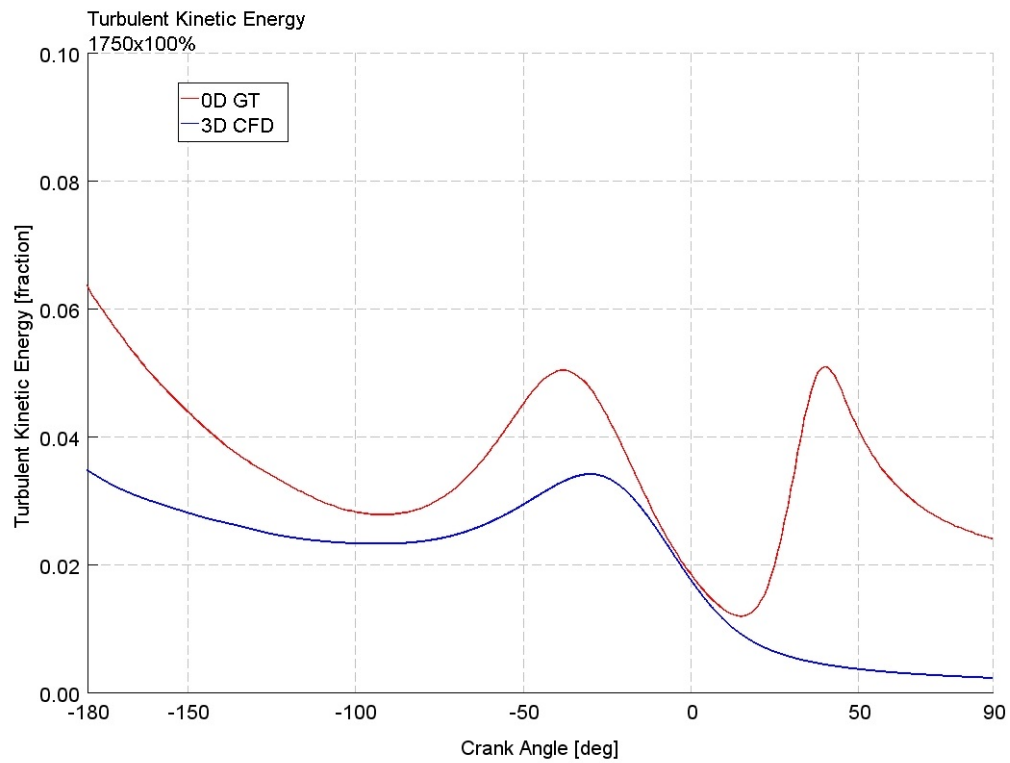
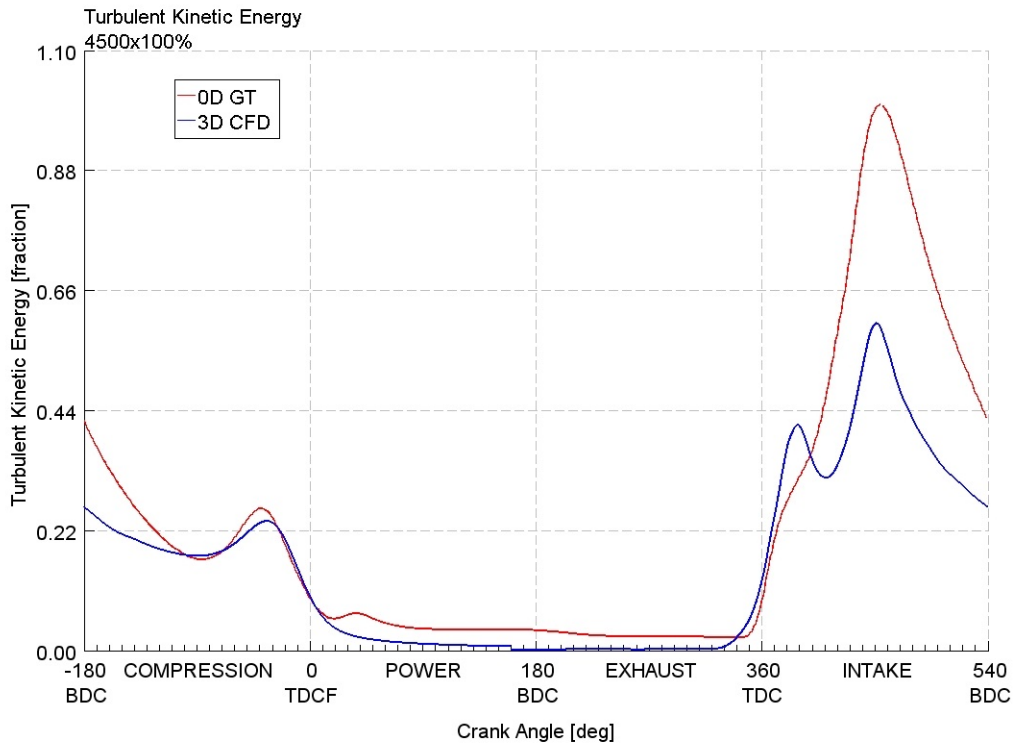
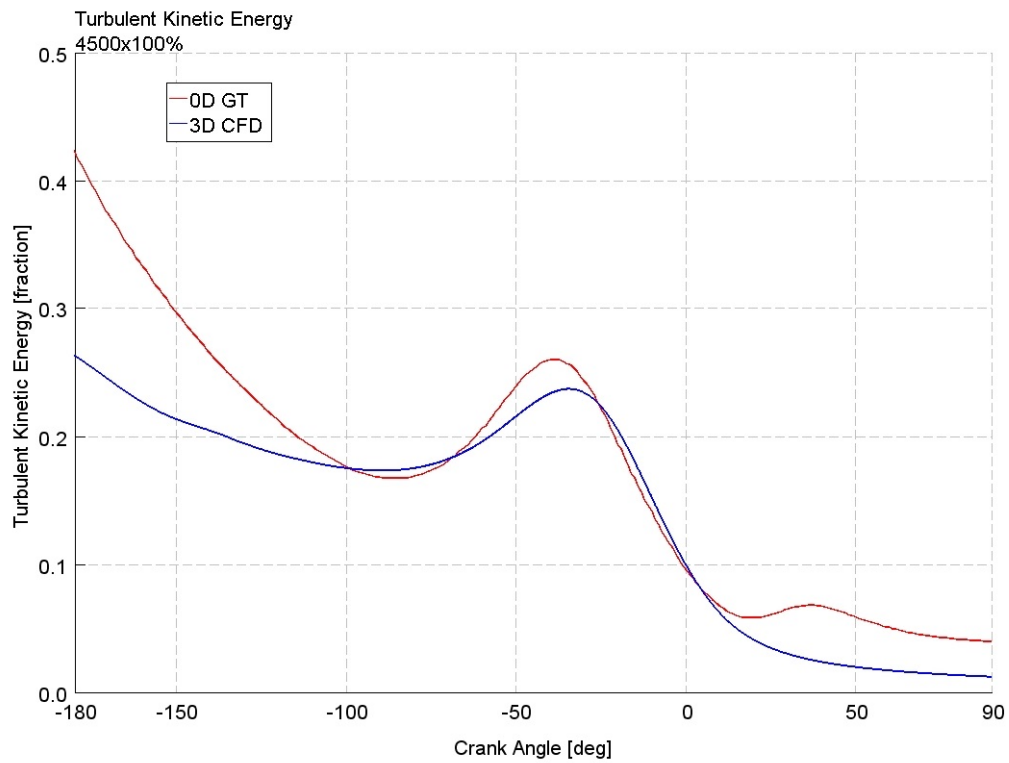


Figure 5.33: Engine B Turbulent Kinetic Energy 5000 rpm 100% load, zoom in the crank angle of interest

Figure 5.34: *Engine B* Turbulent Kinetic Energy 1750 rpm 100% loadFigure 5.35: *Engine B* Turbulent Kinetic Energy 1750 rpm 100% load, zoom in the crank angle of interest

Figure 5.36: *Engine B* Turbulent Kinetic Energy 4500 rpm 100% loadFigure 5.37: *Engine B* Turbulent Kinetic Energy 4500 rpm 100% load, zoom in the crank angle of interest

5.4.2 Combustion calibration

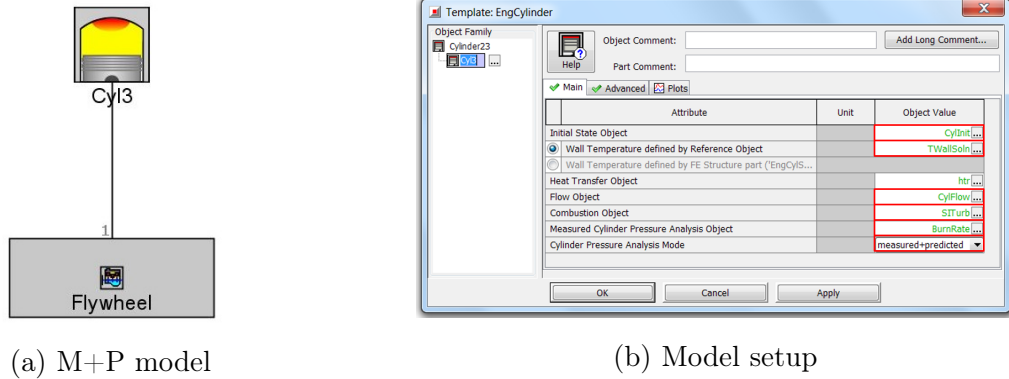


Figure 5.38: Measured + Predicted model and initialisation

The final step of the process is represented by the combustion calibration, which will lead to the definition of the four combustion multipliers of SI-Turb model. To perform this, a Measured + Predicted (M+P) Analysis model has to be setup. It will only perform a closed volume pressure analysis, i.e. no gas-exchange is included, therefore the model used is a simple single-cylinder, made up of cylinder and cranktrain objects only as shown in Figure 5.38a. The model will provide a comparison of cylinder pressure and burn rate between the measurement and the predictive combustion model SI-Turb. In the cylinder, the Cylinder Pressure Analysis Mode has to be set to measured+predicted: the measurement burn rate is calculated from the cylinder pressure which is inputted in the Measured Cylinder Pressure Analysis object, while the Combustion object is set to the predictive model SI-Turb, as reported in Figure 5.38b. Moreover to perform this calibration, the model has to be initialised carefully with conditions at cycle start. The initialisation is done at three different locations in the cylinder:

- An EngCylInit object has to be specified as the Initial State Object in EngCylinder. It initialises the cylinder using Volumetric Efficiency, Trapping Ratio, Fuel at IVC and Residual Fraction, from the detailed model previously described.
- The cylinder wall temperatures in EngCylITWallSoln have to be set using the results from the detailed model. As the measured+predicted model is only running one cycle, the wall temperature solver will not be active, and will be using the initial values specified.
- The turbulence in the cylinder has to be specified in the EngCylIFlow object. In the Initialisation/Imposed folder, all quantities have to be specified using results from the detailed model with the Flow object active as in the turbulence calibration

step. These quantities are taken at cycle start and they are the swirls and tumble numbers, the turbulent strength and length scale and the mean flow strength.

Going more into the details, the EngCylCombSITurb model, specified as Combustion Object, requires the definition of the EngCylFlame object, using the head and piston STL files for the combustion chamber geometry description. Also, the spark plug location is specified here. The Combustion Anchoring Option has to be set to SparkTiming and its value is inserted as input. In the end, the four combustion parameters are inserted in Laminar and Turbulent Speed tabs of the EngCylCombSITurb template; during the combustion calibration step, these combustion multipliers are created as parameters but their value is set to the default one (equal to 1) in order to perform the optimisation. This model setup is shown in the Figures 5.39, 5.40 and 5.41.

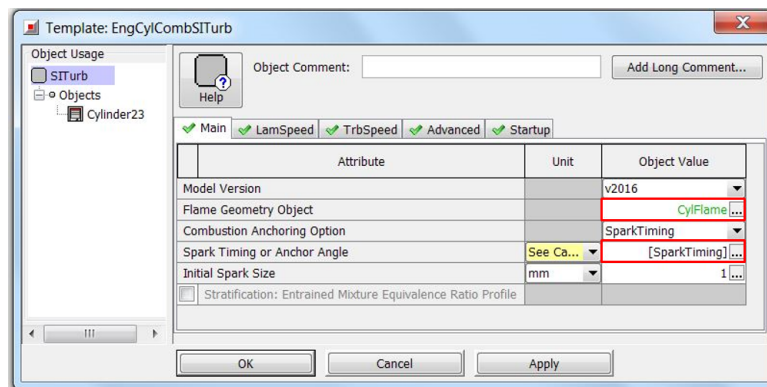


Figure 5.39: EngCylCombSITurb setup: Main tab

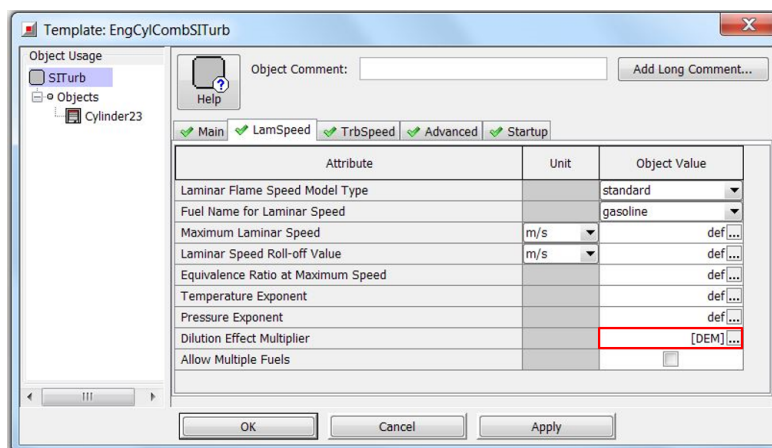


Figure 5.40: EngCylCombSITurb setup: LamSpeed tab

The goal of a predictive combustion model calibration process is to find the single set of model constants that will provide the best possible match to a wide variety of operating points. This best match may be defined in terms of matching measured and predicted

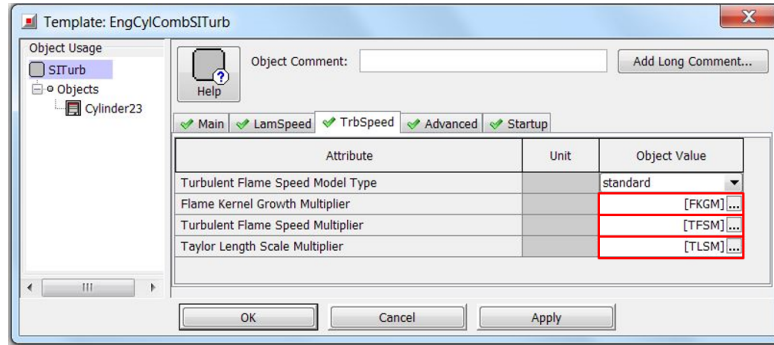


Figure 5.41: EngCylCombSITurb setup: TrbSpeed tab

burn rate, cylinder pressure, IMEP, emissions, etc. and it can be evaluated using the Advanced Direct Optimiser (ADO), which is provided by GT-SUITE. The Objective in the optimizer should be set to Minimize. As optimization target, a special RLT is available in the EngCylinder part for the calibration task: Improved Burn Rate RMS Error (Meas vs Pred) in the Pressure Analysis, Predicted folder. It should be set as the Dependent Variable RLT. For the search algorithm, the Genetic Algorithm option is recommended with the settings in Table 5.4. Figure 5.42 instead shows how the optimisation setup is performed in GT-Power.

Setting	Recommended value
Population size	30
Number of generations	34
Mutation rate	0.5
Mutation rate distribution index	15

Table 5.4: Genetic algorithm settings

The independent variables to be set are the four calibration parameters defined in EngCylCombSITurb in the previous step: Dilution Exponent Multiplier, Flame Kernel Growth Multiplier, Turbulent Flame Speed Multiplier and Taylor Length Scale Multiplier. The Case Handling attribute is set to Sweep for each of the independent variables. This option will find a single optimised value with respect to all cases since the target is the prediction in all operating conditions; on the other hand, the Independent option will look for a separate optimised value for each case, thus improving the overall result but jeopardising the predictive capability. The recommended range of the parameters is shown in Table 5.5. All these settings are inserted in the Independent Variables folder in the ADO window, as reported in Figure 5.43.

Once this stage has been reached, the Optimisation itself could be run and after it is

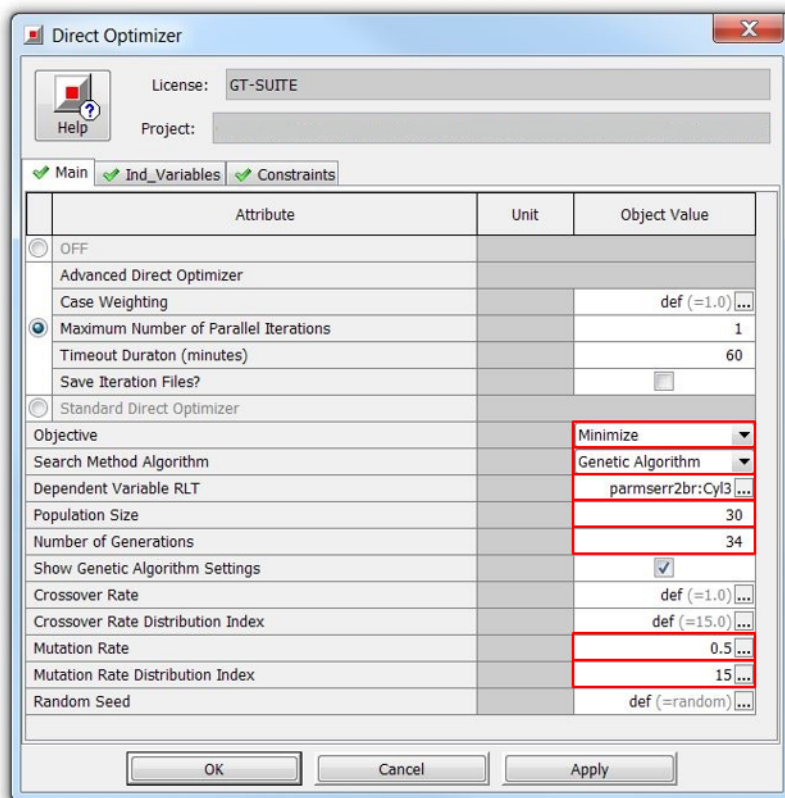


Figure 5.42: Advanced Direct Optimiser setup

finished the optimised values of the four combustion parameters could be inserted in the EngCylCombSITurb template as already shown in Figures 5.39, 5.40 and 5.41. Sometimes one or more combustion parameters reaches the limit of optimisation range and therefore a second iteration of the optimisation with wider ranges has to be performed. Once the final values are obtained, the cylinder pressure and burn rates from the measurement and prediction of SITurb should be compared in GT-POST, to make sure the calibration achieved satisfactory results. This will be shown in the next section.

Parameter	Minimum	Maximum
Dilution Effect multiplier	0.5	2
Flame Kernel Growth multiplier	0.5	2
Turbulent Flame Speed multiplier	0.5	2
Taylor Length Scale multiplier	1	3

Table 5.5: Typical ranges of the combustion multipliers

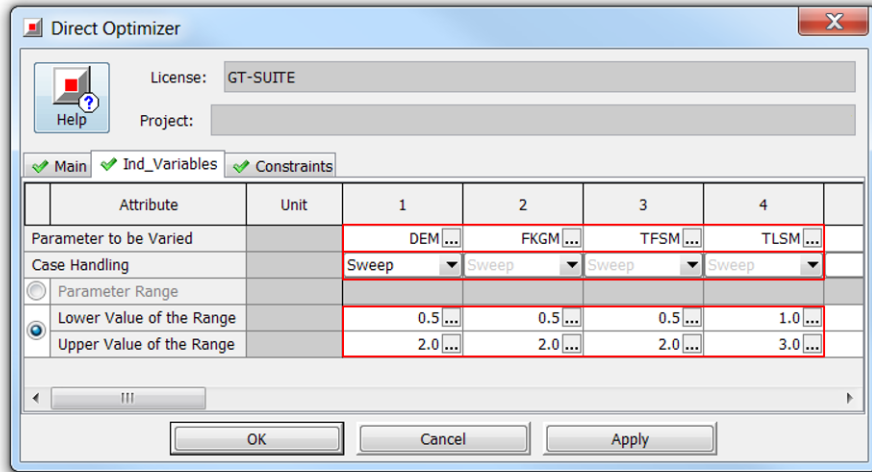


Figure 5.43: Optimisation parameters setup

5.4.3 Engine B results

This section will summarise the results from the calibration process and then the final SI-Turb build will be assessed. In particular for what concerns the outputs of the optimisation, the simulation has been re-run because at the end of the first iteration two out of the four parameters reached their limit. This meant that a second iteration was required with a wider range for those combustion multipliers: the results obtained are normalised with respect to the the typical value of each parameter inside the recommended range and they are listed in Table 5.6.

Parameter	Value
Dilution Effect multiplier	0.512
Flame Kernel Growth multiplier	3.277
Turbulent Flame Speed multiplier	0.594
Taylor Length Scale multiplier	0.702

Table 5.6: Combustion multipliers results from ADO

Once the sets of turbulence and combustion parameters are known, the final SI-Turb model can be built following the procedure previously described. The only objects which have to be modified compared to the detailed model with imposed combustion are the flow and the combustion object: the flow object has to be active and filled in with the results from the automatic turbulence calibration, whereas the combustion object is changed from EngCylCombSIWiebe to EngCylCombSITurb and is set with the outputs from the ADO as explained in Section 5.4.2. At this point the final model is ready to be run and all the results already shown for the detailed model and the transplant can be obtained. Figures

5.44, 5.45, 5.46 and 5.47 show the comparison between the predictive model SI-Turb (red curve), the imposed combustion model Wiebe (blue curve) and the measurement data (green curve) in terms of pressure trace, burn rate and engine performances. All these graphs once again have been normalised to the overall maximum value so the y-axis always shows the fraction from 0 to 1. Looking at the pressure trends and comparing them to the results in Figure 5.23 obtained with the transplant operation, it is possible to see how the error about the Peak Firing Pressure has been significantly reduced, even if the same results as the imposed combustion can not be achieved. The same comparison between transplant and final predictive build can be made for the burn rate plots: analysing Figures 5.24 and 5.45, one can easily see that the calibration process has led to a better description of the combustion process, especially for the two cases at low engine speed. At high rpm instead, the combustion predicted by the SI-Turb model is faster than the measured one, as it is possible to see from the steeper slope of the ascending part of the burn rate curve. If the engine performances are considered as in Figures 5.46 and 5.47, the predictive model achieves basically the same results as the detailed Wiebe model, thus showing to be a useful tool for a general description of the engine behaviour.

As a final graphical representation, the bubble charts can be used again: the error in terms of percentage or crank angle of IMEP, MFB50, MFB10-90, PFP and PFP CA are listed in Figure 5.48. The same logic applies: red dots correspond to an underestimation of the parameter compared to the experimental value, while blue dots represent an overestimation; obviously, the bigger the dot the bigger the error. Table 5.7 summarises the errors described so far and shows the average and the maximum values for each combustion parameters. If one compares these results with the one obtained for the transplant operation (listed in Table 5.2), the following conclusion can be made:

- The combustion process is overall better described with the final SI-Turb model, since the Peak Firing Pressure angle and particularly the combustion duration MFB10-90 show lower error.
- The Peak Firing Pressure value moved from an underestimation in the case of the transplant to an overestimation for the final SI-Turb model. The order of magnitude of the error remains the same for both cases.
- The IMEP error of the final SI-Turb model shows a slight deterioration but it represents anyway a satisfying result since it is lower than 0.5%.
- The MFB50 error exhibits generally a significant worsening, more than 1 crank angle degree. The final SI-Turb model is predicting a faster combustion than what the transplant operation is doing. This is clearly visible in Figure 5.48a.

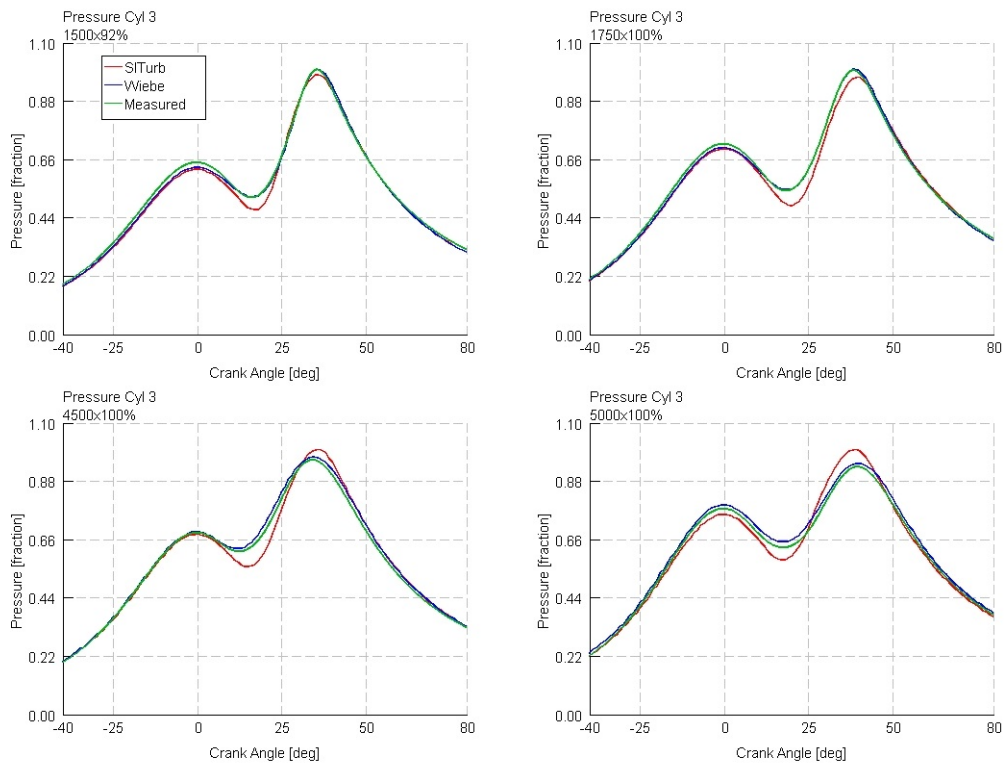


Figure 5.44: Engine B SI-Turb final model pressure

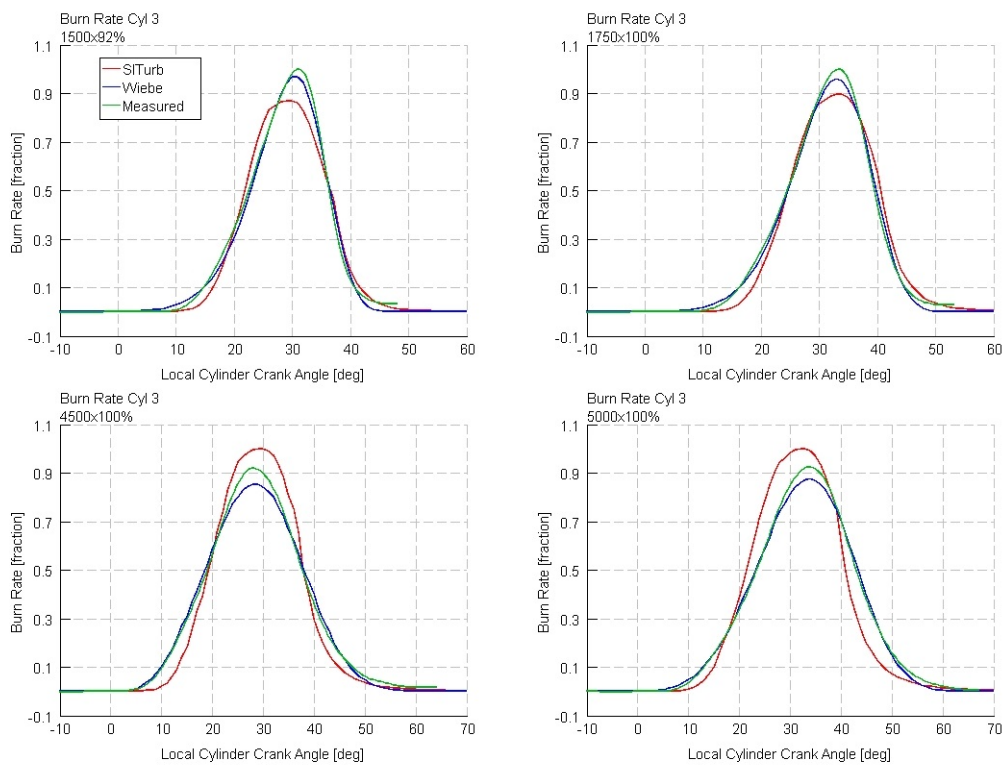


Figure 5.45: Engine B SI-Turb final model burn rates

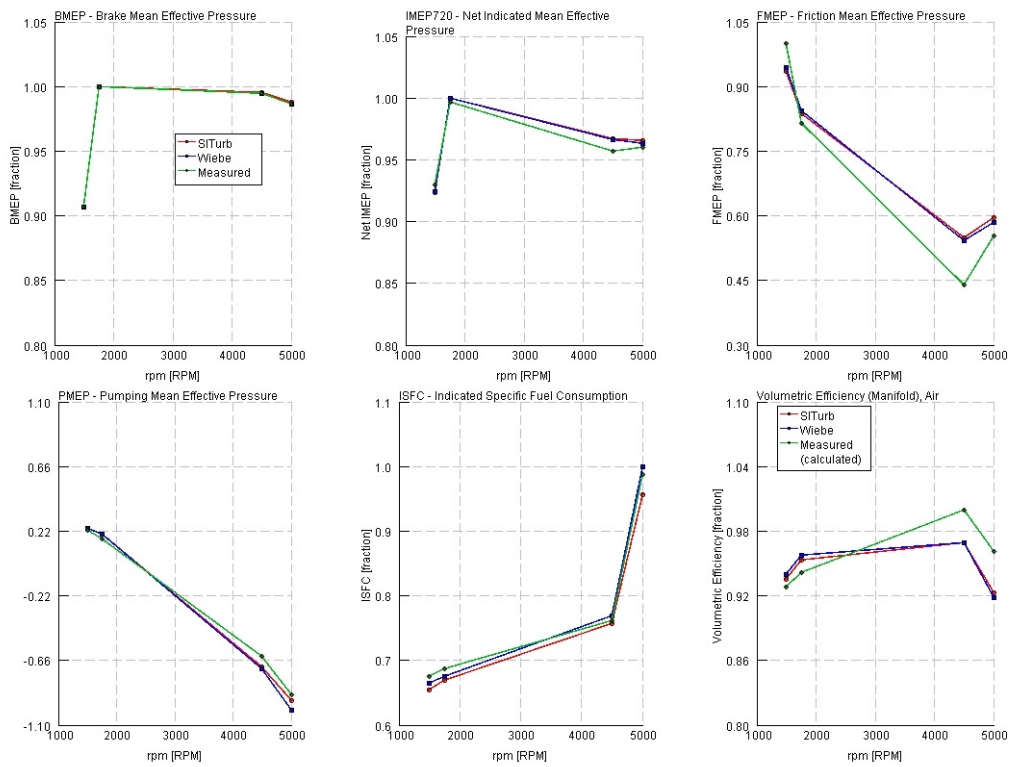


Figure 5.46: Engine B SI-Turb final model performance (1)

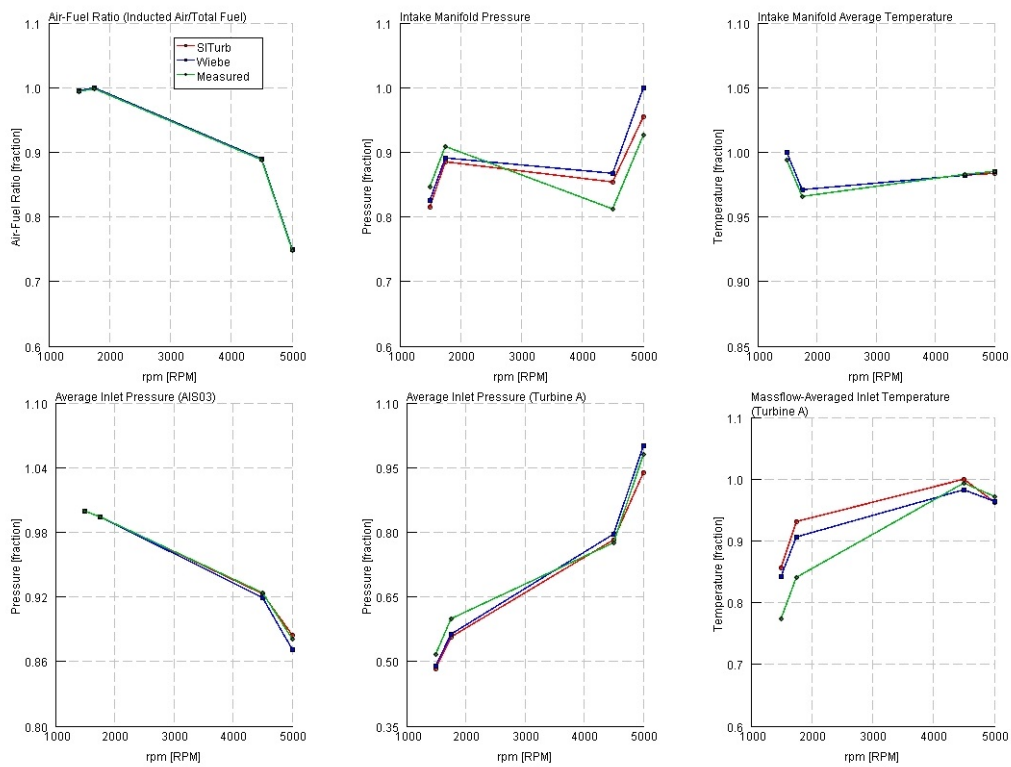


Figure 5.47: Engine B SI-Turb final model performance (2)

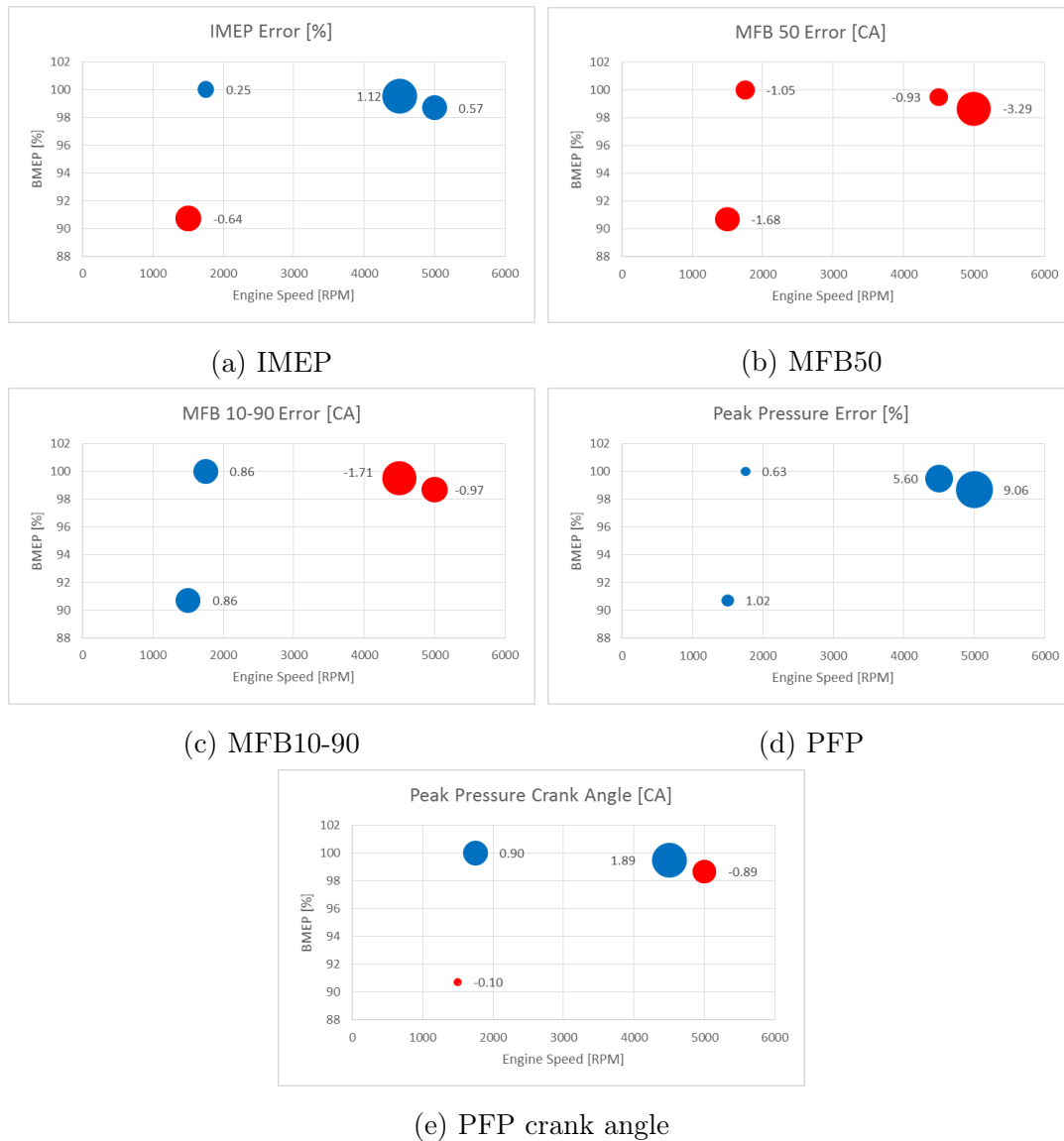


Figure 5.48: Errors of the SI-Turb final model compared to the experimental results

Parameter	Unit	Average error	Maximum error
IMEP	[%]	0.32	1.12
MFB50	[CA]	-1.74	-3.29
MFB10-90	[CA]	-0.24	-1.71
PFP angle	[CA]	0.45	1.89
PFP	[%]	4.08	9.06

Table 5.7: SI-Turb final model errors summary

Among all these conclusions, the most interesting and surprising is the outcome of the error on the combustion hub: despite the burn rate trend obtained from the calibration of the model shows a better match with experimental data than the transplant operation, the consequent MFB50 results translates into a faster combustion when compared to the one of the transplant. In order to explain this behaviour, the Root Mean Square Error (RMSE) between the measured and the predicted burn rate is calculated, using both the combustion calibration of *Engine A* and the one obtained for *Engine B*. Figure 5.49 represents the RMSE of each operating condition for the transplant (blue curve) and the final SI-Turb model (orange curve). As it is possible to see from the graph, the error obtained with the calibration of the SI-Turb model achieves better results for two out of the four operating conditions under study, while in the other two cases the results match the one obtained with the transplant operation. Thanks to this analysis, one can confidentially say that the final model is able to describe the combustion process with higher fidelity overall, but jeopardising the MFB50 value. However, sometimes specific targets for the combustion hub parameter are required, for instance in the case of coupling the predictive combustion and a knock model. In order to meet these requirements, the solution could be to force the combustion calibration to target the experimental values of the MFB50: this is possible during the optimisation step by imposing as objectives to minimise the Burn Rate RMSE and to target the desired values for MFB50. The procedure will not be described in this thesis due to the lack of time and because it represents a consequent step of this project that will be analysed in the future.

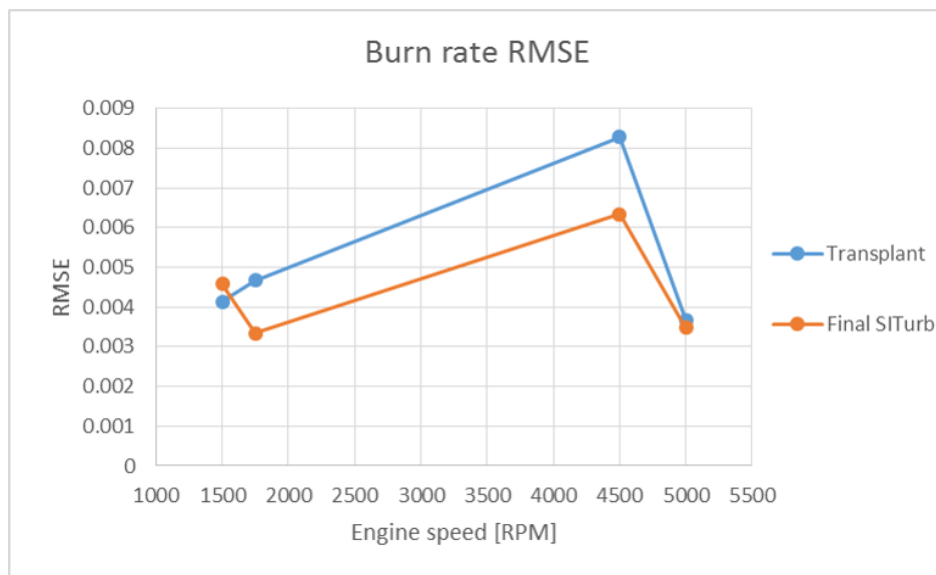


Figure 5.49: Burn rate RMSE comparison

Chapter 6

Conclusions

The work developed in this thesis focused on the assessment of the predictive capability of the combustion model SI-Turb, in the commercial 1D software GT-Power. The baseline of this project was the available calibration of the model for an existing engine build. The first analysis was therefore the evaluation of the model capability to adapt to a new engine version, with some significant hardware changes, without performing any calibration or adjustment. The combustion tool showed to be effective in the definition of the engine performance, achieving in fact almost the same results as the detailed model with imposed combustion. When describing the combustion process in details, the most important parameters achieved acceptable results, which thus allow to have a general overview on the engine behaviour without requiring any calibration effort at all. This ability of the combustion model to adapt to some hardware changes could be exploited to investigate the effect of new solutions in the early stages of development.

The next obvious step was then to calibrate the combustion model specifically for the engine under study. This step led to an improved overall description of the combustion phenomenon. The calibration process was also perfected in some areas, in order to allow any future user to have the guidelines to succeed. Some key factors were highlighted: first of all, the availability of a 1D engine model with high fidelity when compared to experimental data, then the need for good quality test data and for time to run the CFD analysis required for the turbulence calibration showed their relevant importance.

The possible future developments of the predictive combustion model could be many. SI-Turb enables for example enhanced predictive capability when knock is considered, by coupling the predictive combustion with a knock model. An other interesting field of research it is represented by the possibility to calibrate the SI-Turb model using results from CFD instead of experimental data; this will allow to build a predictive engine model even before the physical engine has been manufactured and tested, which in turns translates into a savings in money and time.

Bibliography

- [1] J. B. Heywood, *Internal Combustion Engine Fundamentals*. McGraw Hill International edition, 1988.
- [2] G. Ferrari, *Motori a Combustione Interna*. Il Capitello, 1992.
- [3] GT-SUITE, *Engine Performance Application Manual*. Gamma Technologies, 2016.
- [4] N. Fogla, M. Bybee, M. Mirzaeian, F. Millo, and S. Wahiduzzaman, “Development of a k-k- ϵ phenomenological model to predict in-cylinder turbulence,” *SAE International Journal of Engines*, vol. 10, pp. 562–575, mar 2017.
- [5] M. Mirzaeian, F. Millo, and L. Rolando, “Assessment of the predictive capabilities of a combustion model for a modern downsized turbocharged si engine,” in *SAE 2016 World Congress and Exhibition*, SAE International, apr 2016.
- [6] O. S. T. S. G. T. . S. C. Yakhot, V., “Development of turbulence models for shear flows by a double expansion technique,” *Physics of Fluids A*, vol. 4, no. 7, pp. 1510–1520, 1992.